Downloaded from orbit.dtu.dk on: May 05, 2023

DTU Library

Yield conditions for cracked reinforced concrete disks

Hoang, Cao Linh

Publication date:
2000

Document Version
Publisher's PDF, also known as Version of record

Link back to DTU Orbit

Citation (APA):
Hoang, C. L. (2000). *Yield conditions for cracked reinforced concrete disks*. Technical University of Denmark. BYG-Rapport No. R-66

General rights
Copyright and moral rights for the publications made accessible in the public portal are retained by the authors and/or other copyright owners and it is a condition of accessing publications that users recognise and abide by the legal requirements associated with these rights.

- Users may download and print one copy of any publication from the public portal for the purpose of private study or research.
- You may not further distribute the material or use it for any profit-making activity or commercial gain
- You may freely distribute the URL identifying the publication in the public portal

If you believe that this document breaches copyright please contact us providing details, and we will remove access to the work immediately and investigate your claim.

R 66

INSTITUT FOR BÆRENDE KONSTRUKTIONER OG MATERIALER

DTU

Yield Conditions for Cracked Reinforced Concrete Disks

LINH CAO HOANG

DEPARTMENT OF STRUCTURAL ENGINEERING AND MATERIALS
TECHNICAL UNIVERSITY OF DENMARK Series R No 66 2000

Institut for Bærende Konstruktioner og Materialer
Danmarks Tekniske Universitet

Yield Conditions for Cracked Reinforced Concrete Disks

Linh Cao Hoang

Yield Conditions for Cracked Reinforced Concrete Disks
Danmarks Tekniske Universitet
Tryk: DTU-tryk
Kgs. Lyngby
ISBN 87-7740-271-5
ISSN 1396-2167
Bogbinder:
H. Meyer

Preface

This report is prepared as a partial fulfillment of the requirements for obtaining the Ph.D. degree at the Technical University of Denmark.

The work has been carried out at the Department of Structural Engineering and Materials, Technical University of Denmark, under the supervision of Professor, Dr. techn. M.P. Nielsen.

I would like to thank my supervisor for giving valuable advice and inspiration as well as valuable criticism to the report.

Thanks are also due to my co-supervisors Assoc. Prof., Ph.D. Henrik Stang and Ph.D. Bent Feddersen.

Lyngby, February 2000.

Linh Cao Hoang

Summary

This report deals with the strength of cracked reinforced concrete disks determined by means of the theory of plasticity.

The basic assumption is that the sliding resistance in cracks is lower than the sliding resistance for uncracked concrete.

To treat disks suffering from cracking in many directions, the state of *isotropical cracking* is introduced. This idealized state implies that in any section perpendicular to the plane of the disk, a crack may be found. An isotropic failure criterion is formulated for the idealized material. Based on this failure criterion, a yield condition is developed for isotropicly cracked disks reinforced in two directions at right angles to each other. The case of pure shear is treated in detail, both by the lower bound and the upper bound method. Comparison of the obtained results with the plastic solutions for uncracked concrete is carried out.

The strength of disks cracked in only one direction or in two directions at right angles to each other has also been studied. Such disks are termed *anisotropicly cracked disks.*

A lower bound solution for the shear strength of disks cracked only along the so-called initial crack direction is derived. The results show that the maximum allowable uniaxial concrete stress may decrease, depending on the direction of the principal concrete stresses, to half of the original web crushing strength. Comparison of the predicted maximum concrete stress with test measurements shows good agreement.

Finally, for anisotropicly cracked disks subjected to arbitrary in-plane loading, a yield condition is formulated. The yield condition is a modification of the yield condition developed by Nielsen [69.1].

Resumé

Denne rapport behandler styrken af revnede, armerede betonskiver bestemt ved hjælp af plasticitetsteorien.

Den grundlæggende antagelse er, at modstanden mod glidningsbrud i revner er mindre end den er for urevnet beton.

For at behandle skiver revnet i mange retninger introduceres den såkaldte *isotropt revnede tilstand.* Denne idealiserede tilstand af revnedannelse indebærer, at man vil støde på en revne i ethvert tværsnit vinkelret på skivens plan. For det revnede betonmateriale er der formuleret en isotrop brudbetingelse. Med udgangspunkt i denne brudbetingelse udledes en flydebetingelse for isotropt revnede skiver armeret i to på hinanden vinkelrette retninger. Ved hjælp af nedre- og øvreværdimetoden gives en detailleret behandling af isotropt revnede skiver udsat for ren forskydning. Resultaterne sammenlignes med løsninger for urevnet beton.

Styrken af skiver, der enten er revnet i én retning eller i to på hinanden vinkelrette retninger, er også studeret. Sådanne skiver betegnes som *anisotropt revnede skiver.*

En nedreværdiløsning for forskydningsstyrken af skiver revnet i den såkaldte initiale revneretning er udledt. Resultatet viser, at den maksimalt tilladelige enaksede betonspænding kan, afhængigt af retningen for hovedspændingerne i betonen, aftage til halvdelen af betonens effektive trykstyrke. Sammenligning af den beregnede maksimale betonspænding med forsøgsresultater viser god overensstemmelse.

Endelig formuleres en flydebetingelse for anisotropt revnede skiver udsat for vilkårlig belastning. Flydebetingelsen er en modifikation af flydebetingelsen udviklet af Nielsen [69.1].

Table of Contents

Notation

a : Shear span

b : Web width of beam

c : Cohesion of concrete

c' : Cohesion in a crack

D : Dissipation

f_c : Uniaxial compressive strength of concrete

f_t : Tensile strength of concrete

f_y : Yield strength of reinforcement

h : Depth of beam

P : Concentrated load

$\mathbf{Q}$: General stress vector

$\mathbf{q}$: General strain vector

u : Relative displacement in yield line

V_{sx} : Volume of the reinforcement bars parallel to the x-axis

V_{sy} : Volume of the reinforcement bars parallel to the y-axis

W_E : External work at failure

W_I : Internal work at failure

W_{Ic} : Internal work done in the concrete

W_{Is} : Internal work done in the reinforcement

W_l : Internal work per unit length of the yield line

x : Horizontal projection of yield line in beam subjected to shear

x_o : Length of loading plate/support plate

α : Angle between yield line and displacement direction

β : Angle defining the orientation of the initial crack system

ε_{c1}, ε_{c2}, ε_{c3} : Principal concrete strains

Φ : Degree of reinforcement

Φ_x : = $\rho_x f_y / f_c$

Φ_y : = $\rho_y f_y / f_c$

γ : Shear strain

φ : Angle of friction

ν : Effectiveness factor

θ : Angle defining the direction of the principal concrete stresses

ρ_x : Reinforcement ratio (for bars parallel to the x-axis)

ρ_y : Reinforcement ratio (for bars parallel to the y-axis)

σ_1, σ_2, σ_3 : Principal stresses

σ_c : Concrete stress

σ_{c1}, σ_{c2} : Principal concrete stresses

σ_{cn}, σ_{ct} : Normal stresses in concrete in the (n,t)- system

σ_{con} : Confining stress in concrete

σ_{cx}, σ_{cy} : Normal stresses in concrete in the (x,y)- system

σ_n, σ_t : Normal stresses in the (n,t)- system

σ_{sx}, σ_{sy} : Stresses in reinforcement bars

σ_x, σ_y : Normal stresses in the (x,y)- system

τ : Shear stress

τ_{cnt}, τ_{nt} : Shear stress in the (n,t)- system

τ_{cxy}, τ_{xy} : Shear stress in the (x,y)- system

τ_o : Shear strength of non shear reinforced beams (original solution)

Chapter 1
Introduction

Comprehensive rehabilitation or total replacement are awaiting an increasing number of existing reinforced concrete structures.

The reasons for this are that the mechanisms of chemical subversion of reinforced concrete have taken place much faster than expected and that many structures are designed to sustain smaller loads than those appearing today. Further, the structures may have been designed according to antiquated standards, which in some cases may be encumbered with erroneous design principles.

Rehabilitation of structures is an expensive affair, especially in view of the fact that it is a solution often chosen when there are uncertainties concerning the actual load-carrying capacity of the structure suffering from different kinds of damages.

Rehabilitation is often in question when a structure is observed to suffer from cracking which was unpredictable in the design phase. It could be concrete cracked in all directions, for example due to chemical reactions, or severe cracking in certain directions due to overloading, creep and shrinkage, temperature differences, etc. .

When examining such structures, one always faces the problem :

" What is the strength of the cracked concrete and how does it influence the load-carrying capacity of the structure ? ".

If these questions could be replied with reasonable accuracy, then it may turn out that rehabilitation, with respect to the load-carrying capacity, in many cases would be unnecessary[1].

As a step toward a more rational decision basis for rehabilitation of concrete structures, this thesis deals with the determination of the (remaining) load-carrying capacity of cracked reinforced concrete disks subjected to in-plane loading. The results presented here have been obtained by means of the theory of plasticity.

To obtain manageable solutions/models, some drastic simplifications about the crack patterns will be made. Thus, in this thesis we shall deal with two states of cracking : the reinforced disks may suffer from cracking in one or two directions, or it may suffer from cracking in all directions. The latter case is called isotropical cracking and represents an idealized state which, as revealed later, allows us to treat the cracked concrete as a completely new material with isotropic material properties. This idealized state of cracking may be taken as a model for concrete structures with unsystematic crack patterns or structures suffering from cyclic loads giving rise to many crack directions.

All though cracking of concrete often increases the danger of exposing the reinforcement material to corrosion, the present study only focus on the strength reduction of concrete. The influence of cracking on the properties of the reinforcement will not be touched upon.

The thesis is built up as follows:

Chapter 2 summarizes the basic concepts and assumptions of the theory of perfectly rigid-plastic bodies. As a new contribution to the field of concrete plasticity, a yield condition for plain and isotropicly cracked concrete in plane stress is proposed. The corresponding dissipation formulas will be derived.

In chapter 3, the yield condition presented forms the point of departure for the derivation of a yield condition for isotropicly cracked reinforced concrete disks. The case of disks subjected to pure shear will be treated in details.

---

[1] Naturally, rehabilitation concerns other aspect than just a strengthening.

Chapter 4 deals with reinforced disks which suffer from cracking in one or two directions. Solutions for the case of disks subjected to pure shear are derived and a yield condition for isotropicly reinforced disks with low reinforcement degrees is formulated.

Chapter 5 summarizes the results presented.

Chapter 2
Basic Assumptions

In this chapter we shall describe the theory and the assumptions which form the basis of the results presented in the thesis.

2.1 Theory of plasticity

We begin with a short description of some basic concepts from the theory of perfectly rigid-plastic bodies. To study the theory and it's applications in detail, the reader is referred to [98.4], in which further references can be found.

2.1.1 Yield condition and flow rule. A perfectly rigid-plastic material is defined as a material which is able to sustain stresses up till a certain level, the so-called yield point, without undergoing deformations. Once the yield point has been reached arbitrarily large deformations/yielding may take place under constant stresses.

The yield point is determined by a *yield condition* or a *failure criterion*[2] which in general takes the form

$$f(Q_1, Q_2, \ldots, Q_n) = 0 \tag{2.1}$$

where $(Q_1, Q_2, \ldots, Q_n) = \mathbf{Q}$ are the generalized stresses. Any stress combination satisfying $f(Q_1, Q_2, \ldots, Q_n) = 0$ is said to be lying on the *yield surface* and may

---

[2] The terms yield condition and failure criterion will be used synonymously herea fter.

result in yielding. The yield surface is assumed to be a *convex* and *closed surface*[3] containing the point $\mathbf{Q} = (0,0,...,0)$. When $f<0$ we have stresses which can be sustained by the body whereas $f>0$ represents stress combinations that can not occur. The generalized stresses are chosen in such a way, that they together with the generalized strains $\mathbf{q}=(q_1, q_2,...,q_n)$ define the virtual work W per unit length, area or volume as follows

$$W = Q_1 \cdot q_1 + Q_2 \cdot q_2 + ... + Q_n \cdot q_n \tag{2.2}$$

The work D, necessary to produce a given strain field $(q_1, q_2,...,q_n)$ in the body, thus becomes

$$D = \int_V (Q_1 q_1 + Q_2 q_2 + ... + Q_n q_n) dV = \int_V W \, dV \tag{2.3}$$

where the notation dV may represent a length-, area- or volume element. D is called the *dissipation* and (2.3) is interpreted as the total energy absorbed by the body during deformation.

The stress field corresponding to a given strain field is determined by the *associated flow rule*, which states

$$q_i = \lambda \frac{\partial f}{\partial Q_i}, \qquad i = 1,2,...,n \tag{2.4}$$

where λ is an indeterminate non negative factor. The associated flow rule (2.4) may be taken as a basic assumption or as a result of assuming the *von Mises' hypothesis on maximum work*, which states that for a given strain field the stresses will assume such values that the work W becomes as large as possible, see e.g. [98.4]. Depicting in the same coordinate system as the yield surface, the generalized strain vector will become an outward normal to the yield surface. Hence, the associated flow rule is also called the *normality condition.*

Along planes or at apexes on the yield surface, there is no unique relation between $(Q_1, Q_2,...,Q_n)$ and $(q_1, q_2,...,q_n)$. Any stress combination on a plane is

---

[3] Not all yield conditions used in concrete mechanics are closed. For instance the Coulomb yield condition is open in the negative principal stress space. Then modifications to the general theory must be considered.

capable of producing the strain vector normal to the plane. The strain vector at an apex can, as stated in [84.1], be assumed "to lie arbitrarily in the angle determined by the limit positions of **q** when the point (apex) is approached in all possible ways".

Figure 2.1 illustrates for a two dimensional case the consequences of the assumed normality condition.

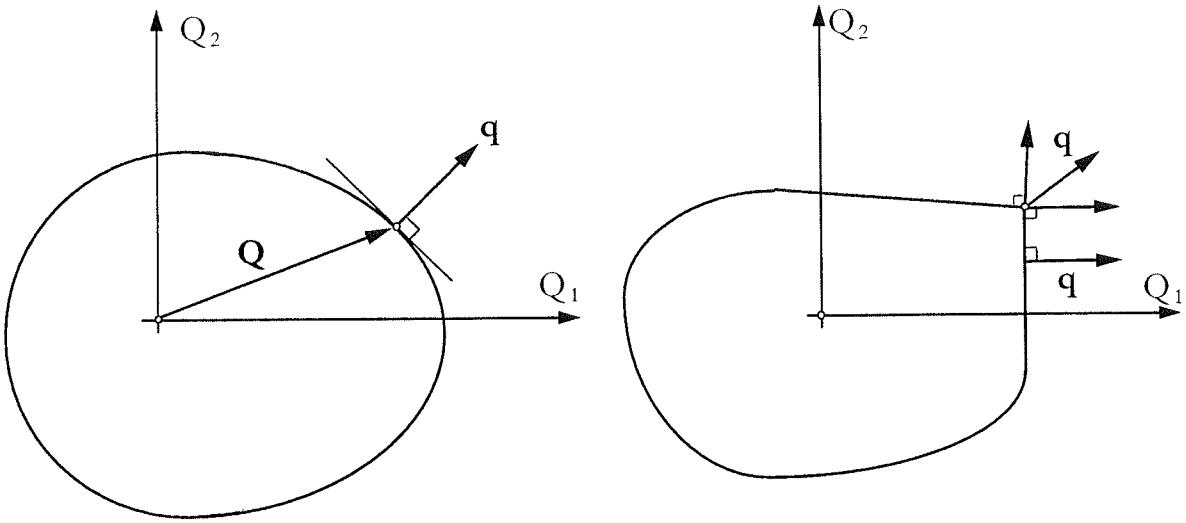

Figure 2.1 *Yield surfaces and normality condition.*

2.1.2 Principles of extremum. By means of the convexity condition of the yield surface and the normality condition, a set of extremum principles, useful for the determination of the load-carrying capacity of structures, may be formulated:

- **Lower bound theorem**

  A load for which a safe and statically admissible stress field can be found will be less or equal to the collapse load of the structure.

  The stress field is safe when it corresponds to stresses within or on the yield surface, i.e. $f(\mathbf{Q}) \leqslant 0$. The stress field is statically admissible if it satisfies the equilibrium conditions and the statical boundary conditions.

- **Upper bound theorem**

  A load found by the work equation for a geometrically admissible failure mechanism will be higher or equal to the collapse load of the structure.

- **Uniqueness theorem**

  An exact solution has been found if the highest lower bound solution equals the lowest upper bound solution.

2.1.3 Combined yield condition. For a composite material consisting of two rigid-plastic materials which obey the normality condition and have convex yield surfaces, the resulting yield surface for the composite material may be shown to possess these properties as well, see e.g. Bræstrup [70.1].

The resulting yield surface can in principle be found as the *envelope surface* when the origin of one yield surface is translated without rotation on the other yield surface, see e.g. Müller [78.2]. This is visualized in figure 2.2 for a two dimensional case, where $f(Q_{cs1},Q_{cs2})$ is the yield condition of the composite material and $f(Q_{c1},Q_{c2})$ and $f(Q_{s1},Q_{s2})$ are the yield conditions of the two basic materials. This principle is useful in that sense, that it, from the appearances of the separate yield surfaces, gives an idea of how the resulting yield surface will appear. The principle is, however, mathematically speaking not easy to handle. More simple is an ad hoc method of constructing the resulting yield surface by considering different states of safe stress fields and afterward using the normality condition to show that geometrically possible strain fields exist for each particular stress field.

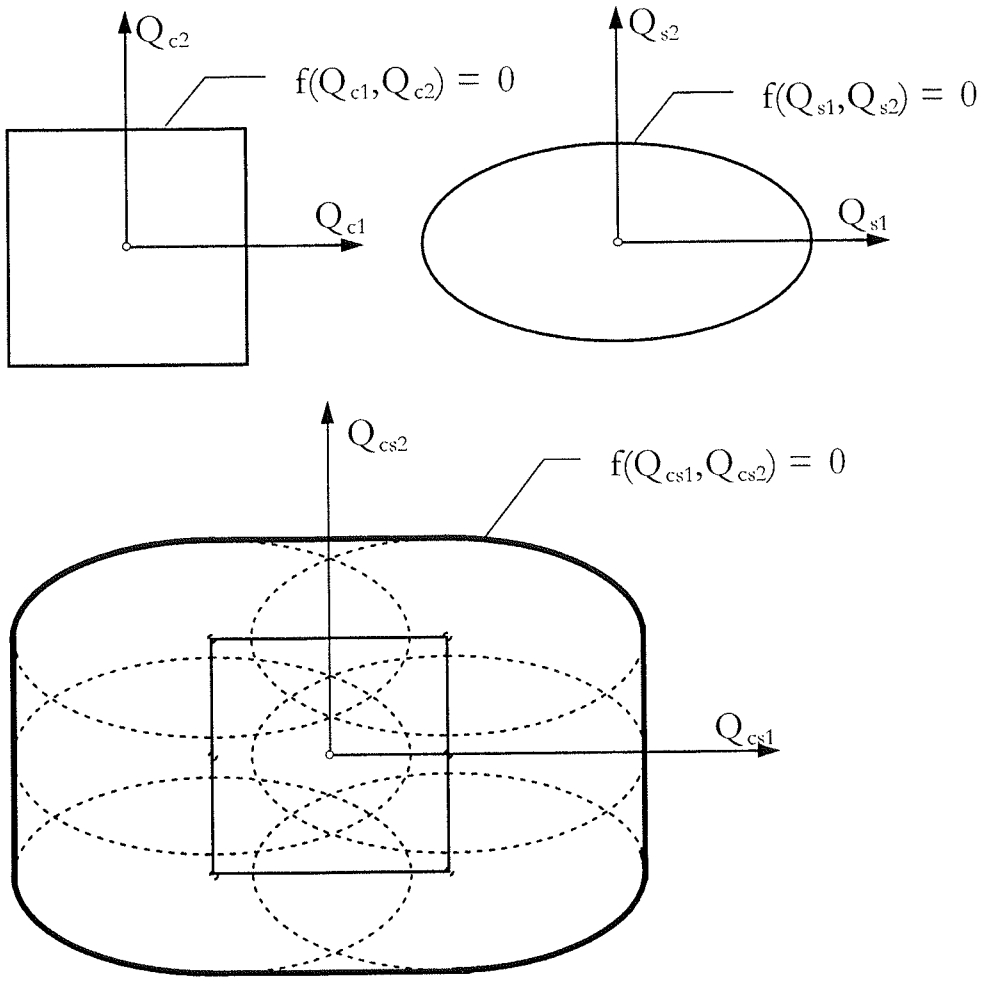

Figure 2.2 *The yield surface of the composite material $f(Q_{cs1},Q_{cs2})=0$ appears as the surface of envelope when the origin of $f(Q_{s1},Q_{s2})=0$ is translated without rotation on $f(Q_{c1},Q_{c2})=0$.*

2.2 Yield conditions for concrete and reinforc e-ment

To develop theories for structural elements of reinforced concrete within the framework of the theory of rigid-plastic bodies, we must consider/assume concrete and the reinforcement material as being rigid-plastic materials.

2.2.1 Uncracked concrete[4]**.** As yield condition for uncracked concrete, we will adopt the *modified Coulomb failure criterion* which consists of a *sliding criterion* and a *separation criterion.*

Sliding failure may take place when the shear stress τ reaches the sliding resistance given as

$$\tau = c - \sigma \tan \varphi \tag{2.5}$$

where c is the internal cohesion, φ is the angle of friction and σ is the normal stress, positive as tensile stress, in the section considered. Expressing the sliding criterion by means of the principle stresses, (2.5) turns into

$$\tfrac{1}{2}\sigma_1(1+\sin\varphi) - \tfrac{1}{2}\sigma_3(1-\sin\varphi) - c\cos\varphi = 0 \tag{2.6}$$

Here σ_1 and σ_3 are the major and the minor principal stress, respectively. Notice that the intermediate principle stress does not influence the failure criterion. From (2.6) it may be shown that the cohesion c is determined by the following equation

$$f_c = \frac{2c \cdot \cos\varphi}{1-\sin\varphi} \tag{2.7}$$

where f_c is the uniaxial compressive strength of concrete.

Experiments have shown, see [84.1], that the angle of friction may be taken as $\varphi \approx 37°$, which means

$$\tan\varphi = 0.75 \tag{2.8}$$

By inserting this value in (2.7), the cohesion thus becomes

$$c = \frac{1}{4} f_c \tag{2.9}$$

---

[4] In the context of this thesis *uncracked concrete* means concrete without visible macrocracks. Microcracks are almost unavoidable and are in many cases formed even before loading, [97.1]. These cracks will not be the subject of study here and we shall therefore consider concrete with microcracks as being "uncracked".

Separation failure takes place when the normal stress in a section reaches the uniaxial tensile strength f_t, i.e.

$$\sigma = f_t \tag{2.10}$$

Usually the tensile strength is assumed to be $f_t = 0$. This would designate the failure criterion as being modified with a zero tension cut-off.

The described modified Coulomb failure criterion has been applied successfully to a number of problems in concrete mechanics, see [78.1] and [98.4].

2.2.2 Cracked concrete. In almost any structural element the concrete is cracked. If sliding failure takes place along a crack (macrocrack) we would expect that a certain amount of sliding resistance must be overcome due to the roughness of the crack (the so-called aggregate-interlock effect). Hence, it seems reasonable to adopt a modified Coulomb failure criterion with zero tension cut-off as a yield condition along cracks :

$$|\tau| = c' - \sigma \tan\varphi' \tag{2.11}$$

Here *c'* and φ' are the cohesion and the angle of friction of the crack, respectively. By means of a micromechanical model, J.P. Zhang [97.1] has proposed the following relation :

$$c' = \frac{1}{2} c \tag{2.12}$$

It was further, on the basis of experiments, assumed that

$$\varphi' = \varphi \tag{2.13}$$

which proved to yield quite good agreement with results of Push-Off tests on pre-cracked specimens, see [97.1]. The maximum crack width and the maximum concrete strength in the tests were about 0.7 mm and 45 MPa, respectively. The criteria (2.12) - (2.13) have also been successfully applied to plastic analysis of non-shear reinforced beams and slabs, see [94.2] and [97.4]. Application of the criteria to lightly shear reinforced beams is explored in [98.5].

2.2.3 Reinforcement. Regarding the reinforcement bars, we will assume that only longitudinal tensile and compressive stresses can be carried.

The corresponding rigid-plastic stress-strain relationship is shown in figure 2.3 where f_y as usual denotes the yield stress.

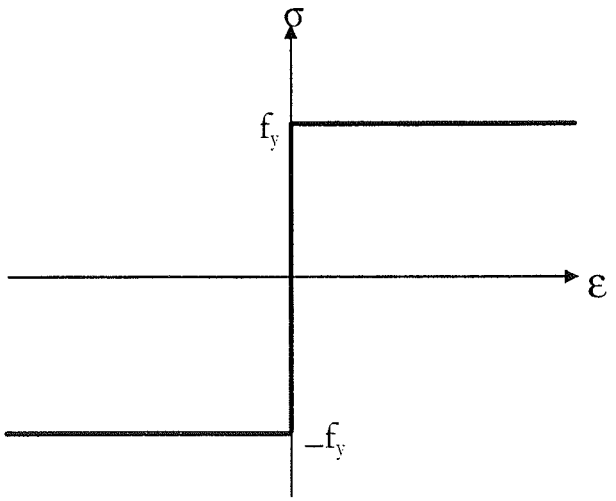

Figure 2.3 *Assumed stress-strain relationship for the reinforcement.*

2.3 Yield condition for isotropicly cracked co n-crete in plane stress

Consider now a plain concrete element, the thickness of which is assumed to be much smaller than it's height and width. The element is placed in a state of plane stress as visualized in figure 2.4 where the applied principal stresses are assumed to be ranged as $0 \geq \sigma_{c1} \geq \sigma_{c2}$. In term of geometry and loading type, we are dealing with a concrete disk.

The element is assumed to be suffering from cracking in a countless number of planes, which all are perpendicular to the plane of the disk. This idealized state of cracking may be called *isotropical cracking* and implies that in any sections perpendicular to the plane of the disk, we may find a crack surface. Thus, *crack sliding failure* may take place if the shear stress τ in any arbitrary sections perpendicular to plane of the disk satisfies, see (2. 9) and (2.12)-(2.13),

$$|\tau| = \frac{1}{8} f_c - 0.75\sigma \qquad (2.14)$$

where σ as before is the normal stress, positive as tension, in the section considered.

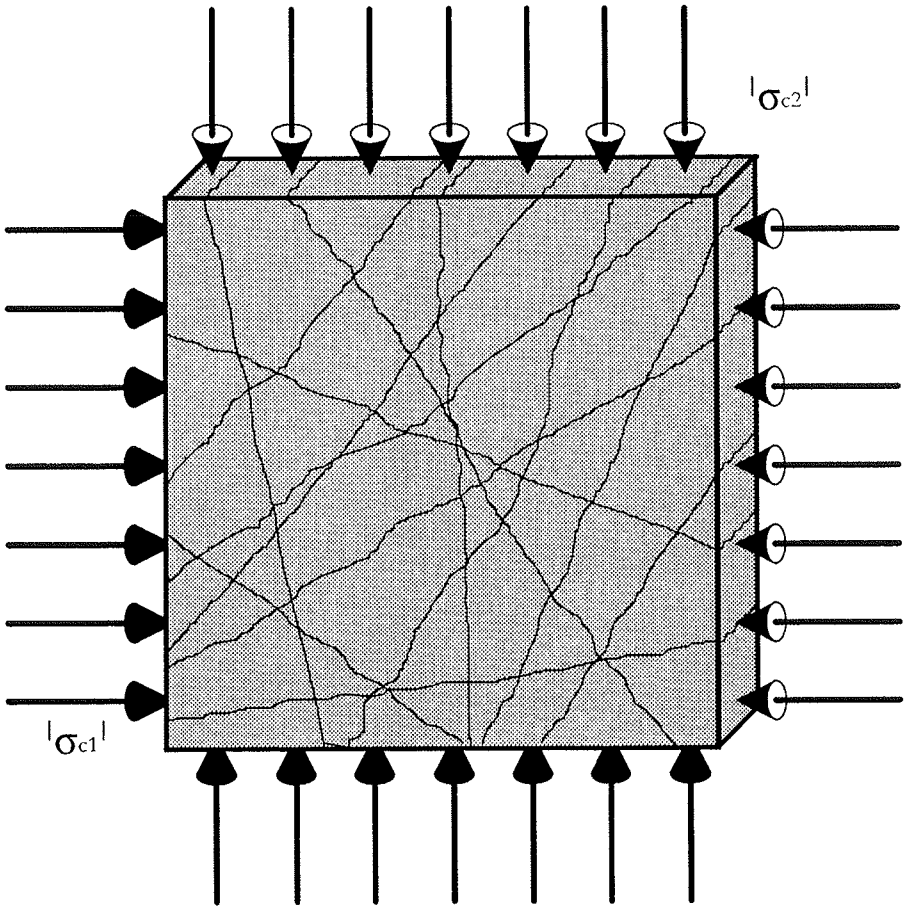

Figure 2.4 *Isotropicly cracked concrete element placed in plane stress field.*

Besides the criterion (2.14), sliding failure may also take place when (2.5) is satisfied in any arbitrary sections, i.e.

$$|\tau| = \frac{1}{4} f_c - 0.75\sigma \tag{2.15}$$

Here the failure takes place as an out of plane failure through uncracked concrete, see figure 2.5.

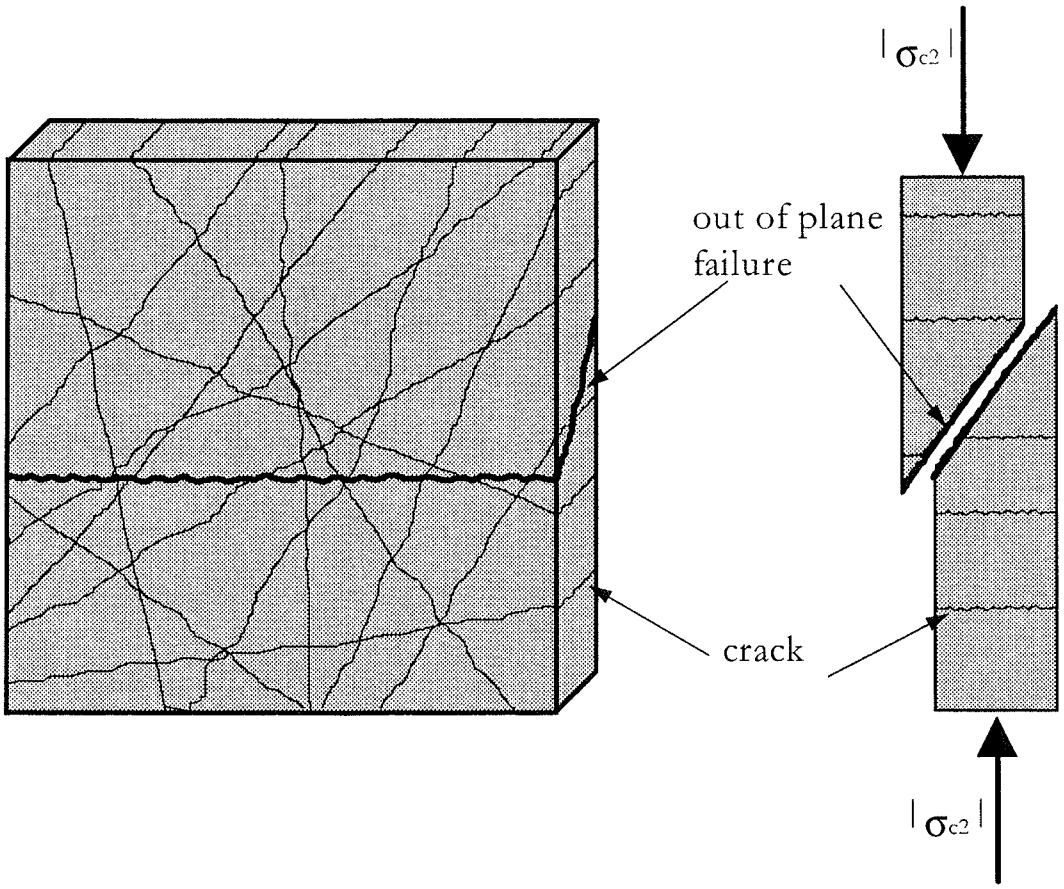

Figure 2.5 *Sliding failure through uncracked concrete.*

Lastly, a separation failure requires

$$\sigma = 0 \tag{2.16}$$

The graphical representations of the conditions (2.14) - (2.16) are shown in figure 2.6 where the Mohr's circles for the stress fields $(0, \sigma_{c1}, \sigma_{c2})$ which may cause failure also have been drawn. Notice that when examining the crack sliding criterion (2.14), the Mohr's circle to be drawn is the one corresponding to the diameter $|\sigma_{c1} - \sigma_{c2}|$ as the criterion only applies to sections perpendicular to the plane of the disk.

By some geometrical considerations of the Mohr's circles shown in figure 2.6, the criteria (2.14) - (2.16) may be transformed into principal stresses as follows

$$4\sigma_{c1} - \sigma_{c2} = \frac{1}{2} f_c \tag{2.17}$$

$$-\sigma_{c2} = f_c \tag{2.18}$$

$$\sigma_{c1} = 0 \tag{2.19}$$

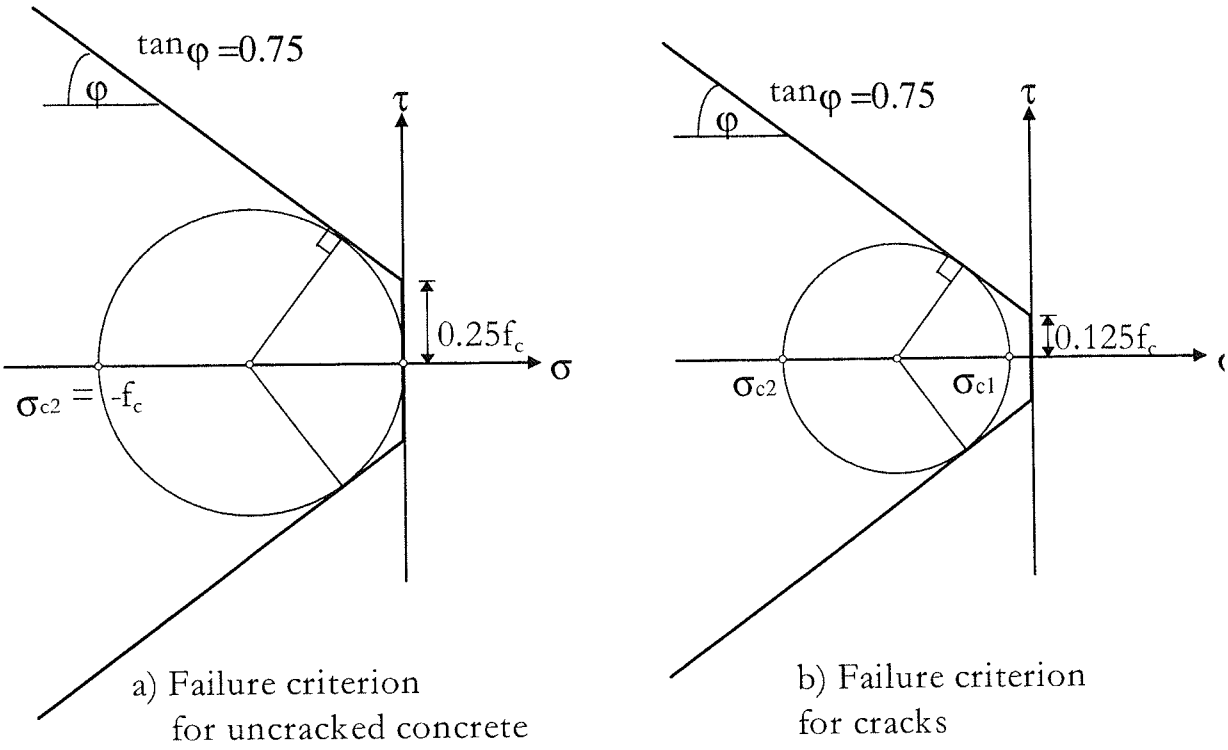

Figure 2.6 *Modified Coulomb failure criteria for isotropicly cracked concrete with Mohr's circles representing stress fields that cause sliding failure.*

The criteria (2.17) - (2.19) are depicted in figure 2.7. By reflection in the line $\sigma_{c2} = \sigma_{c1}$, the case $\sigma_{c2} \geq \sigma_{c1}$ will be covered as well. The closed area in figure 2.7 thus represents the yield condition for isotropicly cracked concrete in plane stress. The corresponding strain vectors obeying the normality condition are also shown.

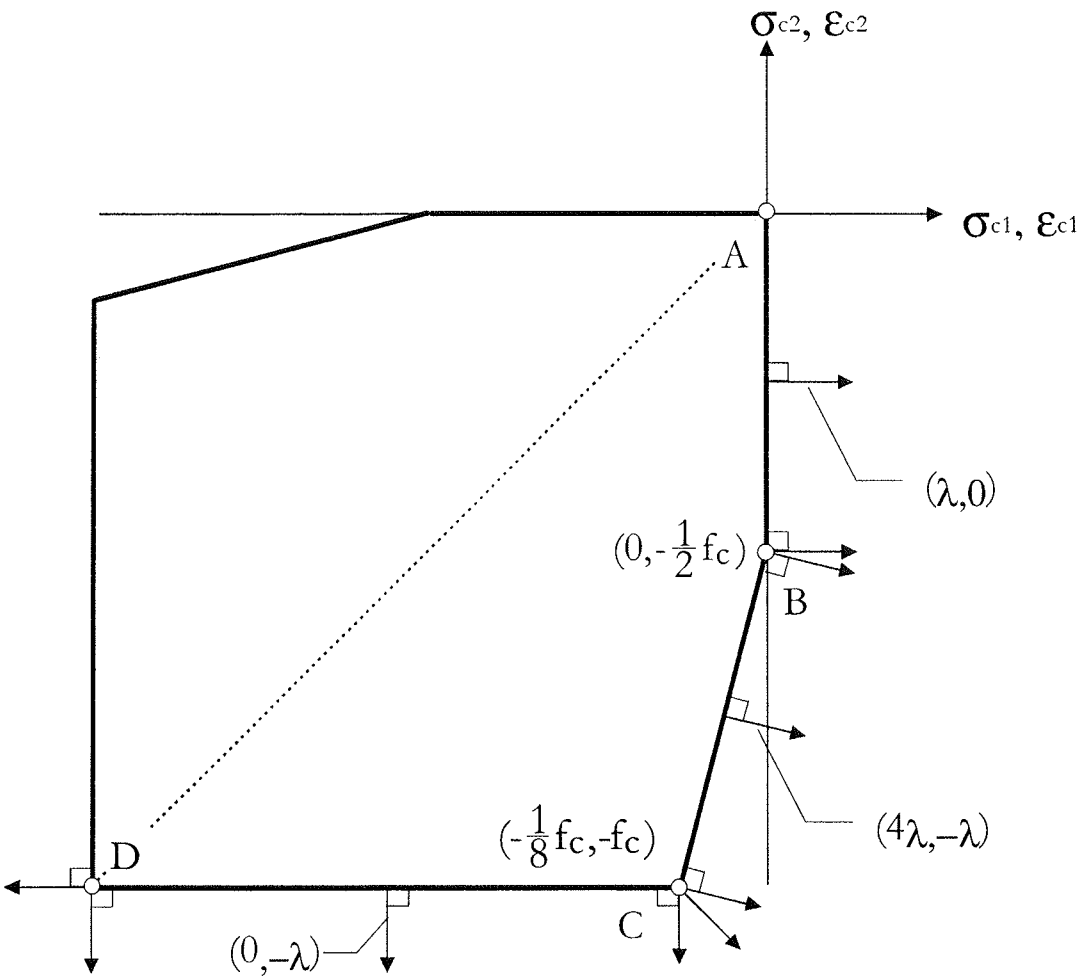

Figure 2.7 *Yield condition and flow rule in the principal stress system for isotropicly cracked concrete in plane stress.*

It should be noticed that there are also strains (ε_{c3}) perpendicular to the stress plane. These strains are, however, with respect to the internal work not interesting. In fact, we may even consider them being non-existing as we are dealing with a two-dimensional theory which, according to [84.1], may be considered as being "self-contained with it's individual two-dimensional yield condition and so on".

By establishing this yield condition, we are now able to treat the cracked concrete material as an isotropic material. This will be done in the next chapter. It appears from the above that we do not need to distinguish between cracked and uncracked sections when we investigate the strength of reinforced and isotropicly cracked concrete in plane stress.

It can be seen from the yield condition that the uniaxial compressive strength of an isotropicly cracked concrete is drastically reduced to $0.5f_c$[5]. To reach a compression stress equal to f_c, the concrete must be in biaxial compression with a confining stress of the at least $0.125f_c$.

Lastly, we mention that when the yield condition is transformed back into a (σ,τ)-system, it will appear as shown in figure 2.8.

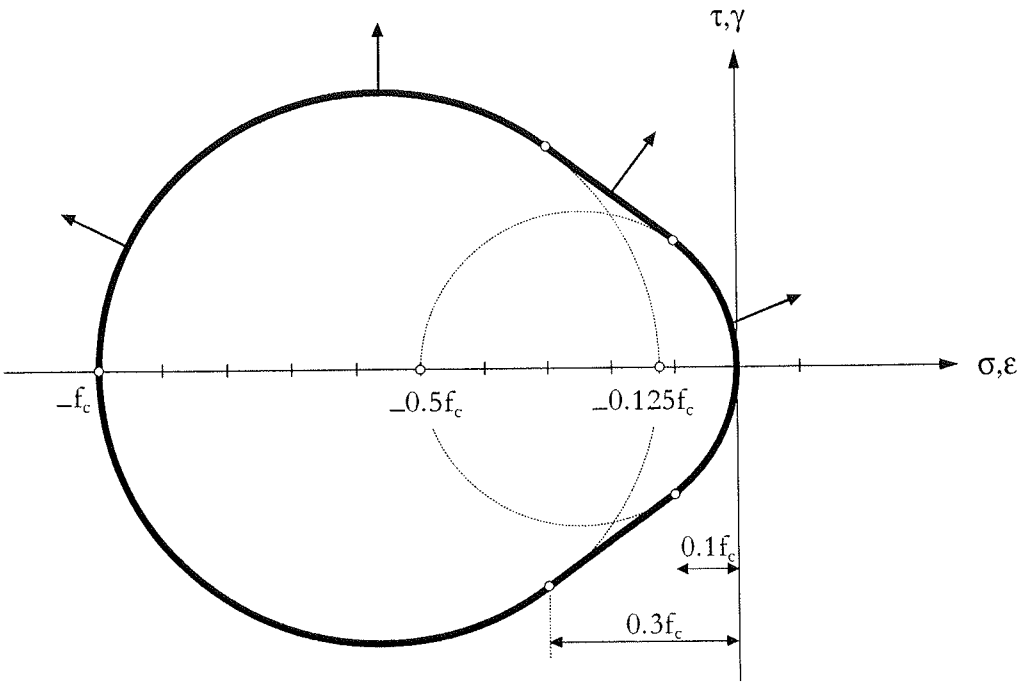

Figure 2.8 *Yield condition and flow rule in (σ,τ)-system for isotropicly cracked concrete in plane stress.*

2.4 Dissipation formulas for isotropicly cracked concrete in plane stress

As well-known to users of plastic theories, the concept of yield lines is of great practical importance when examining upper bounds to the load-carrying capacity of a structure, see e.g. [98.4]. What is needed in this context, besides

---

[5] A uniaxial compressive strength of this order has in fact been proposed in different refe r-ences for concrete members designed by strut-and-tie models, where the strut is crossing skew cracks. The different propo sals have been summarized in [91.3].

of finding geometrically admissible failure mechanisms, are the formulas for the dissipation in yield lines.

By following the concepts introduced in [75.1]&[76.1], we will now derive the dissipation formulas for yield lines in isotropicly cracked concrete in plane stress.

Figure 2.9 shows a narrow zone with the width δ (the yield line) separating two rigid parts I and II. The narrow zone is placed in a homogeneous strain field, which results in a displacement u of part I relative to part II. When the angle between the yield line and the direction of displacement is α the principal strains may be found to be

$$\left.\begin{matrix}\varepsilon_{c1}\\ \varepsilon_{c2}\end{matrix}\right\} = \frac{u}{2\delta}(\sin\alpha \pm 1) \tag{2.20}$$

It appears that we always have $\varepsilon_{c1} \geq 0$ and $\varepsilon_{c2} \leq 0$.

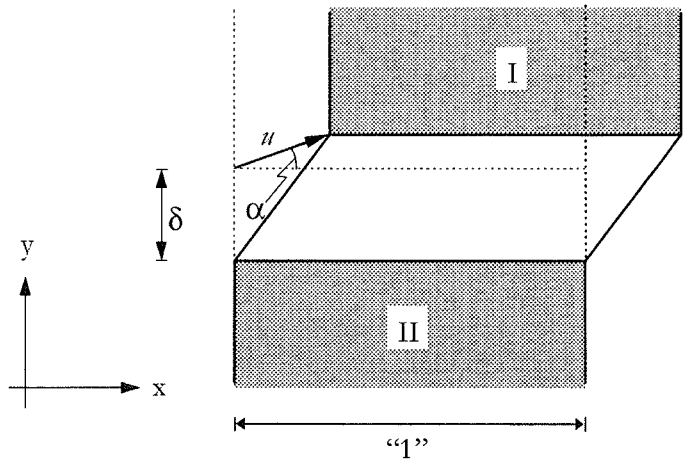

Figure 2.9 *Plastic deformations in a yield line.*

From (2.20) we may write the dissipation W_l per unit length of the yield line as, see also (2.2),

$$\begin{aligned} W_l &= \delta(\sigma_{c1}\varepsilon_{c1} + \sigma_{c2}\varepsilon_{c2}) \\ &= \frac{1}{2}\left(\sigma_{c1}(\sin\alpha + 1) + \sigma_{c2}(\sin\alpha - 1)\right)u \end{aligned} \tag{2.21}$$

where the thickness normal to the stress plane is assumed to be unity.

Now, due to the normality condition, we find from the yield condition in figure 2.7 and from (2.20) that the angle α must satisfy the following requirements:

$\alpha = 90^\circ$	for stresses along A-B
$\varphi \le \alpha \le 90^\circ$	at B
$\alpha = \varphi$	for stresses along B-C
$-90^\circ \le \alpha \le \varphi$	at C

At point B, where α is allowed to vary, we have $(\sigma_{c1},\sigma_{c2}) = (0,-1/2f_c)$ which inserted into (2.21) gives

$$W_l = \frac{1}{2}\left(-\frac{1}{2}f_c(\sin\alpha - 1)\right)u \quad \Rightarrow$$

$$\boxed{W_l = \frac{1}{4}f_c(1-\sin\alpha)\cdot u \qquad , \text{ for } \varphi \le \alpha \le 90^\circ} \tag{2.22}$$

At point C we have $(\sigma_{c1},\sigma_{c2}) = (-0{,}125f_c, -f_c)$. Thus:

$$W_l = \frac{1}{2}\left(-\frac{1}{8}f_c(\sin\alpha + 1) - f_c(\sin\alpha - 1)\right)u \quad \Rightarrow$$

$$\boxed{W_l = \frac{1}{16}f_c(7-9\sin\alpha)\cdot u \qquad , \text{ for } -90^\circ \le \alpha \le \varphi} \tag{2.23}$$

Chapter 3
Isotropicly Cracked Disks

3.1 Introductory remarks

The natural step that follows the introduction of a yield condition for plain and isotropicly cracked concrete in plane stress is to derive the corresponding yield condition for reinforced disks, which are cracked as assumed. Such a yield condition allows us to make comparison with the original yield condition based on uncracked concrete and thus enable us to determine the strength reduction due to cracking.

The original yield condition for reinforced concrete disks was given in 1963 by Nielsen, see [63.1], [69.1] and [98.4]. It was derived by use of the concept of admissible stress fields under the assumption that the uniaxial as well as the biaxial compressive strength of concrete is f_c and the tensile strength is zero.

A special case of the original yield condition has been obtained by Müller [78.2] who neglected the compressive strength of the reinforcement material and derived the yield condition by determining the surface of envelope as described in chapter 2.

Yield conditions taking into account the tensile strength of concrete have been developed by Thürlimann and Marti [77.1], see also Marti [80.1].

In principle, yield conditions for disks with arbitrary reinforcement layout may be developed. In the present study however, we will restrict ourselves

only to examine disks reinforced in two directions at right angle to each other, i.e. disks with orthogonal reinforcement. As shown in figure 3.1, the directions of the reinforcement are taken to be coinciding with the coordinate system (x,y). The state of stress in the concrete material may either be described by principal stresses (σ_{c1}, σ_{c2}) or according to the (x,y) system by (σ_{cx},σ_{cy},τ_{cxy}).

The stresses in the reinforcement bars are termed σ_{sx} and σ_{sy}. Assuming the reinforcement to be closely spaced, the actions in the reinforcement bars may be transformed into equivalent stresses $\rho_x\sigma_{sx}$ and $\rho_y\sigma_{sy}$, ρ_x and ρ_y being the reinforcement ratios.

The total stresses, which are carried by the reinforced disk are thus, see figure 3.1,

$$\begin{aligned} \sigma_x &= \sigma_{cx} + \rho_x\sigma_{sx} \\ \sigma_y &= \sigma_{cy} + \rho_y\sigma_{sy} \\ \tau_{xy} &= \tau_{cxy} \end{aligned} \tag{3.1}$$

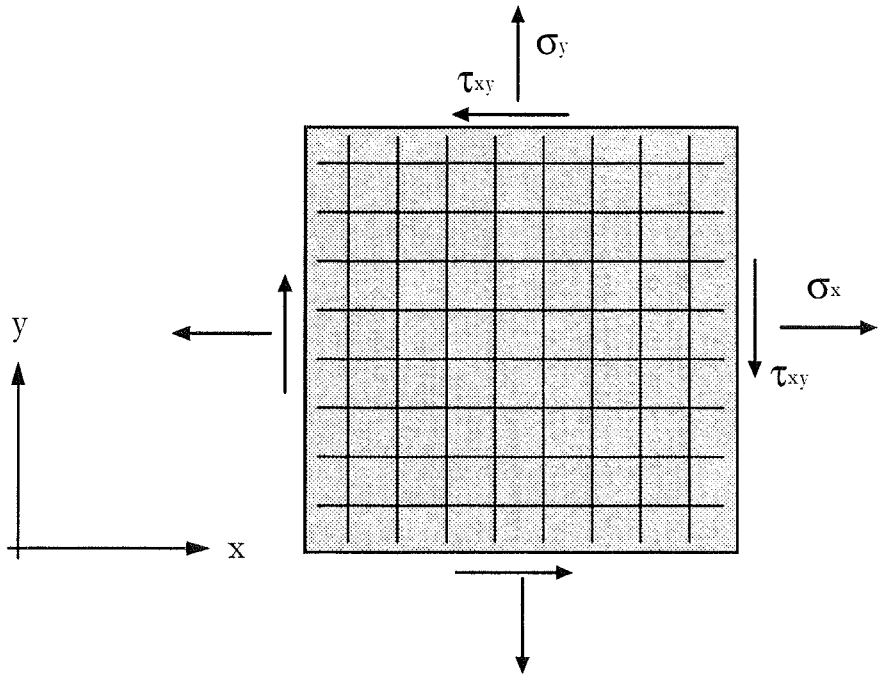

Figure 3.1 *Disk reinforced in orthogonal directions.*

3.2 Concrete and reinforcement

Before proceeding on to the task of determining which stress combinations $(\sigma_x,\sigma_y,\tau_{xy})$ an isotropicly cracked reinforced disk is able to carry, the yield conditions for the concrete and the reinforcement material will first be transformed into stresses referred to the rectangular (x,y)-system.

3.2.1 Yield condition for concrete. The yield condition for plain and isotropicly cracked concrete, as it appears in the principal stress plane in figure 2.7, may be transformed into the $(\sigma_{cx},\sigma_{cy},\tau_{cxy})$-space according to the transformation formulas :

$$\left.\begin{matrix}\sigma_{c1}\\ \sigma_{c2}\end{matrix}\right\} = \frac{1}{2}\left[\left(\sigma_{cx}+\sigma_{cy}\right) \pm \sqrt{\left(\sigma_{cx}-\sigma_{cy}\right)^2 + 4\tau_{cxy}^2}\right] \tag{3.2}$$

The angle θ between the directions of σ_{c1} and σ_{cx} is given by, see figure 3.2,

$$\tan 2\theta = \frac{2\tau_{cxy}}{\sigma_{cx}-\sigma_{cy}} \tag{3.3}$$

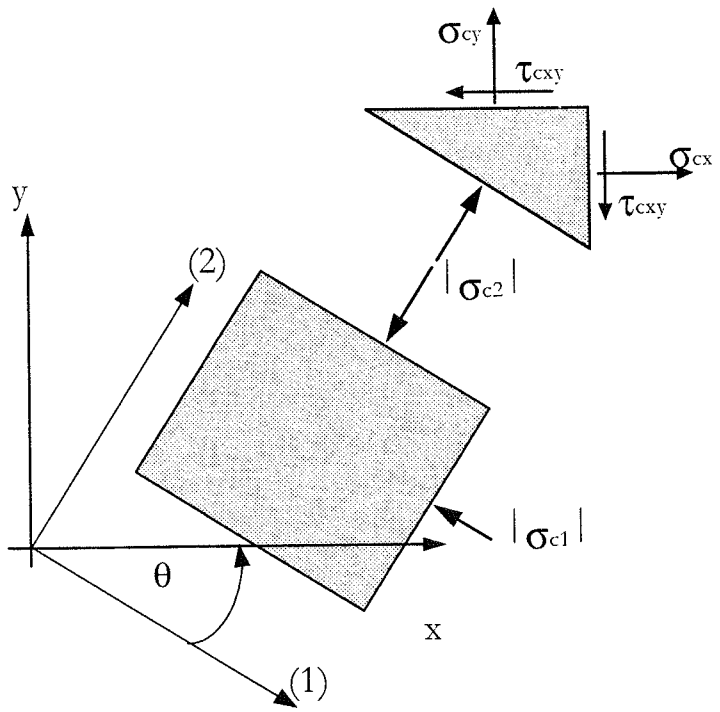

Figure 3.2 *Transformation of principal stresses into the* $(\sigma_{cx}, \sigma_{cy}, \tau_{cxy})$*-space.*

In the positive half space of τ_{cxy} the angle θ will lie within the interval $[0; \pi/2]$ and may be found by

$$\theta = \begin{cases} \frac{1}{2}\,\mathrm{Arc\,tan}\left(\frac{2\tau_{cxy}}{\sigma_{cx}-\sigma_{cy}}\right) & ,\text{for } \sigma_{cx}-\sigma_{cy}>0 \\ \frac{\pi}{4} & ,\text{for } \sigma_{cx}-\sigma_{cy}=0 \\ \frac{1}{2}\,\mathrm{Arc\,tan}\left[\left(\frac{2\tau_{cxy}}{\sigma_{cx}-\sigma_{cy}}\right)+\pi\right] & ,\text{for } \sigma_{cx}-\sigma_{cy}<0 \end{cases} \tag{3.4}$$

When the principal concrete stresses, expressed by means of (3.2), are subjected to the constraint of lying within the area circumscribed by the lines AB, BC, CD and DA in figure 2.7, we will arrive at the following conditions in the $(\sigma_{cx},\sigma_{cy},\tau_{cxy})$-space :

$$① : \tau_{cxy}^2 - \sigma_{cx}\sigma_{cy} \le 0 \tag{3.5}$$

$$② : \tau_{cxy}^2 - (f_c+\sigma_{cx})(f_c+\sigma_{cy}) \le 0 \tag{3.6}$$

$$③ : \tau_{cxy}^2 - \frac{1}{100}\left[(f_c+2\sigma_{cx})-8\sigma_{cy}\right]\left[(f_c+2\sigma_{cy})-8\sigma_{cx}\right] \le 0 \tag{3.7}$$

Figure 3.3a shows the regions ①, ② and ③ in which each of the conditions (3.5) - (3.7) applies. The different regions are bounded as follows:

$$① : \begin{cases} \sigma_{cx} \le 0 \ , \ \sigma_{cy} \le 0 \\ \sigma_{cx}+\sigma_{cy} \ge -\frac{1}{2}f_c \end{cases} \tag{3.8}$$

$$② : \begin{cases} \sigma_{cx} \ge -f_c \ , \ \sigma_{cy} \ge -f_c \\ \sigma_{cx}+\sigma_{cy} \le -\frac{9}{8}f_c \end{cases} \tag{3.9}$$

$$③ : \begin{cases} \sigma_{cx} \ge 4\sigma_{cy} - \frac{1}{2}f_c \\ \sigma_{cy} \ge 4\sigma_{cx} - \frac{1}{2}f_c \\ -\frac{9}{8}f_c \le \sigma_{cx}+\sigma_{cy} \le -\frac{1}{2}f_c \end{cases} \tag{3.10}$$

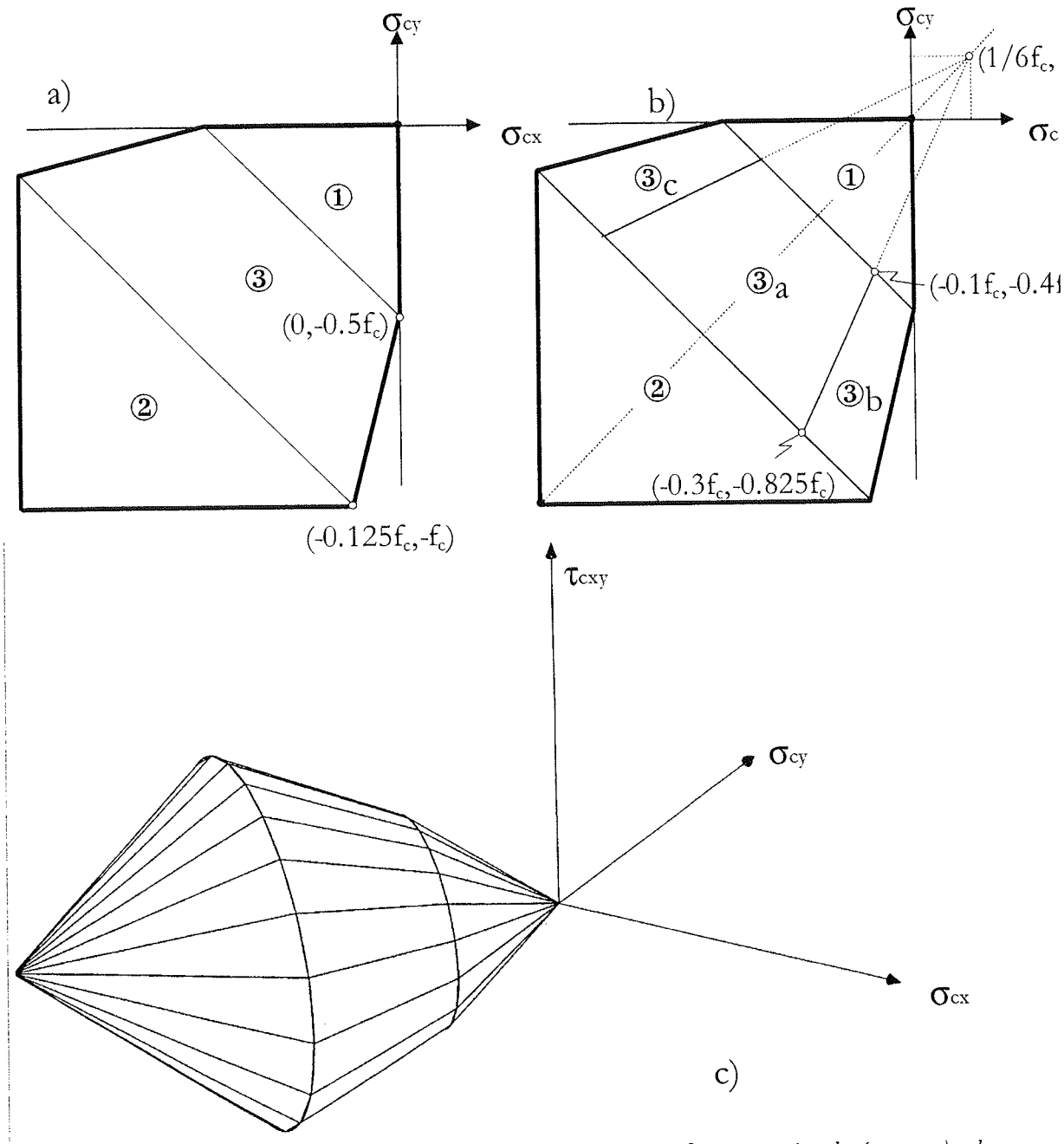

Figure 3.3 *a) and b): yield condition for isotropicly cracked concrete in the* $(\sigma_{cx},\sigma_{cy})$ *plane. c): yield surface for isotropicly cracked concrete in the* $(\sigma_{cx},\sigma_{cy},\tau_{xy})$*-space.*

If the inequality signs are replaced by equality signs, (3.5) - (3.7) will represent the *yield surface*, see figure 3.3c. The yield surface is composed of three cones, all with axis lying on the line $\sigma_{cx} = \sigma_{cy}$ in the $(\sigma_{cx}, \sigma_{cy})$-plane. The curves of intersection between the cones and planes with $\sigma_{cx} + \sigma_{cy} = \text{const.}$ are ellipses with the principal axes ratio $\sqrt{2} / 1$.

In order to anticipate the coming events we will as shown in figure 3.3b sub-divide the region ③ into three parts, namely ③a, ③b and ③c. The boundaries of these regions are :

$$③a: \begin{cases} \sigma_{cx} \geq \frac{1}{16}(34\sigma_{cy} - 3f_c) \\ \sigma_{cy} \geq \frac{1}{16}(34\sigma_{cx} - 3f_c) \\ -\frac{9}{8}f_c \leq \sigma_{cx} + \sigma_{cy} \leq -\frac{1}{2}f_c \end{cases} \tag{3.11}$$

$$③b: \begin{cases} \sigma_{cx} \geq +\frac{1}{34}(16\sigma_{cy} + 3f_c) \\ \sigma_{cy} \geq 4\sigma_{cx} - \frac{1}{2}f_c \\ -\frac{9}{8}f_c \leq \sigma_{cx} + \sigma_{cy} \leq -\frac{1}{2}f_c \end{cases} \tag{3.12}$$

$$③c: \begin{cases} \sigma_{cx} \geq 4\sigma_{cy} - \frac{1}{2}f_c \\ \sigma_{cy} \geq +\frac{1}{34}(16\sigma_{cx} + 3f_c) \\ -\frac{9}{8}f_c \leq \sigma_{cx} + \sigma_{cy} \leq -\frac{1}{2}f_c \end{cases} \tag{3.13}$$

3.2.2 Yield condition for the reinforcement. The yield condition for the reinforcement material is, according to our assumptions in section 2.2.3, obvious. In terms of equivalent reinforcement stresses ($\rho_x\sigma_{sx}, \rho_y\sigma_{sx}$) we have:

$$\begin{aligned} -\Phi_x f_c \leq \rho_x\sigma_{sx} \leq \Phi_x f_c \\ -\Phi_y f_c \leq \rho_y\sigma_{sy} \leq \Phi_y f_c \end{aligned} \tag{3.14}$$

where Φ_x and Φ_y are the *degrees of reinforcement* defined as

$$\begin{aligned} \Phi_x &= \rho_x \frac{f_y}{f_c} \\ \Phi_y &= \rho_y \frac{f_y}{f_c} \end{aligned} \tag{3.15}$$

The rectangular plane described by the condition (3.14) is illustrated in figure 3.4. Notice that in the case of skew reinforcement or in the case of orthogonal reinforcement orientated at an angle with the x- and y-direction, there will also be an equivalent reinforcement shear stress τ_{sxy}.

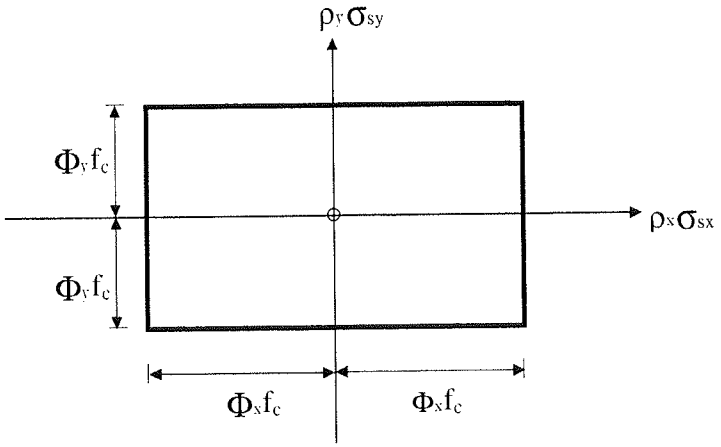

Figure 3.4 *Yield condition for orthogonal reinforcement.*

3.3 Yield condition for isotropicly reinforced disks

We shall begin with the derivation of the yield condition for an isotropicly reinforced disks, i.e. $\rho_x = \rho_y = \rho$ and $\Phi_x = \Phi_y = \Phi$. The corresponding yield condition for the reinforcement material is shown in figure 3.5.

According to the statements in section 2.1.3, any of the following linear combinations

$$\sigma_x = \sigma_{cx} + \rho\sigma_{sx} \tag{3.16}$$

$$\sigma_y = \sigma_{cy} + \rho\sigma_{sy} \tag{3.17}$$

$$\tau_{xy} = \tau_{cxy} \tag{3.18}$$

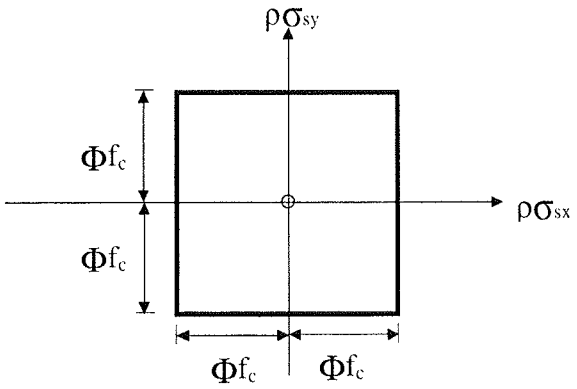

Figure 3.5 *Yield condition for orthogonal, isotropic reinforcement.*

will represent a safe stress field if the yield conditions (3.5) - (3.7) and (3.14) are not violated. Our task is now to determine the maximum shear stress τ_{xy} that can be carried when an admissible set of (σ_x, σ_y) is given.

Thus, before proceeding further, all the admissible sets of (σ_x, σ_y) must be determined, which naturally corresponds to determining the appearance of the yield condition in the (σ_x, σ_y) - plane. The admissible sets of (σ_x, σ_y) are, according to the discussion in section 2.1.3, circumscribed by the envelope obtained when the origin of the yield condition shown in figure 3.3a is translated along the boundary of the yield condition for the reinforcement. The result is shown in figure 3.6.

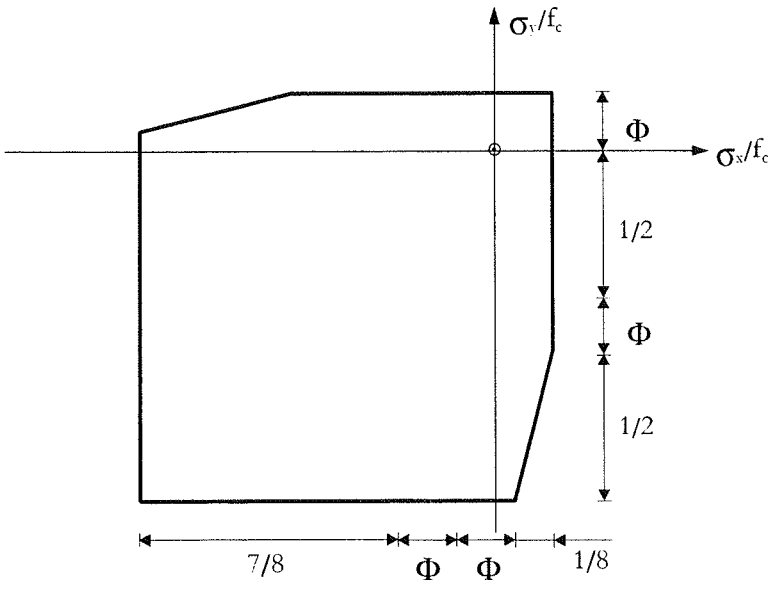

Figure 3.6 *Appearance of the yield condition in the (σ_x,σ_y)-plane, isotropic reinforcement.*

Now, knowing the admissible sets of (σ_x, σ_y), we rewrite (3.16) and (3.17) as follows:

$$\sigma_{cx} = \sigma_x - \rho\sigma_{sx} \tag{3.19}$$

$$\sigma_{cy} = \sigma_y - \rho\sigma_{sy} \tag{3.20}$$

By inserting the right-hand side of (3.19) and (3.20) into (3.5) - (3.7) we arrive at the following conditions

$$\tau_{xy}^2 - (\sigma_x - \rho\sigma_{sx})(\sigma_y - \rho\sigma_{sy}) \le 0 \tag{3.21}$$

$$\tau_{xy}^2 - (f_c + (\sigma_x - \rho\sigma_{sx}))(f_c + (\sigma_y - \rho\sigma_{sy})) \le 0 \tag{3.22}$$

$$\begin{aligned} &\tau_{xy}^2 - \frac{1}{100}\left[(f_c + 2(\sigma_x - \rho\sigma_{sx})) - 8(\sigma_y - \rho\sigma_{sy})\right] \cdot \\ &\left[(f_c + 2(\sigma_y - \rho\sigma_{sy})) - 8(\sigma_x - \rho\sigma_{sx})\right] \le 0 \end{aligned} \tag{3.23}$$

which, geometrically speaking, simply correspond to a pure translation of the cones ①, ② and ③, see figure 3.3a, with the translation vector $(\rho\sigma_{sx}, \rho\sigma_{sy})$.

Now, we begin to construct the yield condition by considering the reinforcement stresses $(\rho\sigma_{sx}, \rho\sigma_{sy}) = (\Phi f_c, \Phi f_c)$ and $(\rho\sigma_{sx}, \rho\sigma_{sy}) = (-\Phi f_c, -\Phi f_c)$, i.e. tensile yielding and compression yielding in both reinforcement directions. According to Nielsen [63.1], tensile yielding in both reinforcement directions should, in order to obtain as large τ_{xy} as possible, be combined with concrete stresses corresponding to uniaxial compression, whereas compression yielding in both reinforcement directions should go along with a biaxial compression stress field with σ_{c2} equals to $-f_c$. Thus, $(\rho\sigma_{sx}, \rho\sigma_{sy}) = (\Phi f_c, \Phi f_c)$ is inserted into (3.21) and $(\rho\sigma_{sx}, \rho\sigma_{sy}) = (-\Phi f_c, -\Phi f_c)$ into (3.22), which results in a shift of the cones ① and ② as shown in figure 3.7.

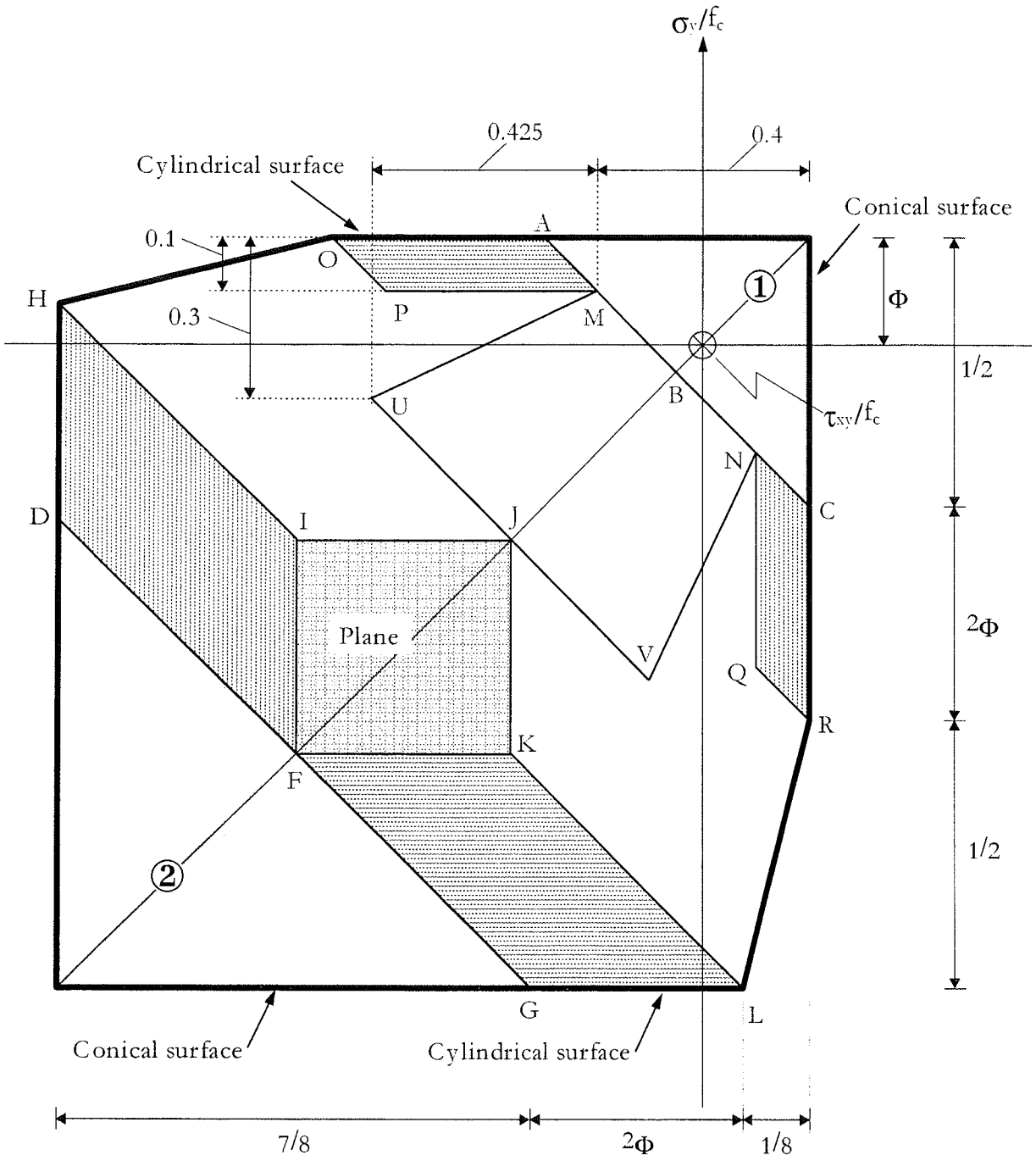

Figure 3.7 *Construction of the yield condition, isotropic reinforcement.*

Proceeding further, the yield condition in the areas *FKLG*, *FDHI* and *FIJK*, as defined in figure 3.7, may also be generated by use of the ideas in [63.1].

Standing at any point on *FG*, we may keep the shear stress unchanged when moving parallel to the σ_x-axis into the area *FKLG*, if we reduce $|\sigma_{sx}|$ while simultaneously keeping σ_{sy} and the concrete stresses unchanged. Thus, by changing σ_{sx} from $-f_y$ to f_y, a cylindrical yield surface is generated for the area *FKLG*, the direction of generatrix being *FK* parallel to *GL*. In the same way a cylindrical yield surface for the area *FDHI* can be obtained when only σ_{sy}

changes from $-f_y$ to f_y. Here the direction of generatrix is *FI* parallel to *DH*. Lastly, standing at the point *F*, we may move into the area *FIJK* by keeping the concrete stresses unchanged while numerically reducing both σ_{sx} and σ_{sy}. The yield surface in this area is thus a plane parallel to the (σ_x, σ_y)-plane. Within this area none of the reinforcements are yielding. The concrete stresses will correspond to those at point *F* ; namely $\sigma_{c2} = -f_c$, $\sigma_{c1} = -0.125f_c$ and $\theta = 45^\circ$. Thus, we are in this area able to carry the shear stress $|\tau_{cx}| = 0.5|\sigma_{c1} - \sigma_{c2}| = 7/16f_c$.

The remaining parts of the yield condition are slightly more complicated to construct.

Let us consider an arbitrary point *N* on the line *BC*. Along this line, we know that the concrete is in uniaxial compression with $\sigma_{c2} = -0.5f_c$ under varying angles θ and the reinforcement is stressed to tensile yielding in both directions. From point *N* we have the following two options of moving downward parallel to the σ_y - axis.

1) We may keep the concrete stresses unchanged and simultaneously reduce σ_{sy}.

2) We may keep the reinforcement stresses unchanged and instead change the state of stresses in the concrete from uniaxial to biaxial compression.

In both cases the stress component σ_{cx} stays unchanged as we are moving parallel to the σ_y - axis.

Which option to choose must depend upon the magnitude of τ_{xy} that can be carried. Looking at the yield condition for concrete in the (σ,τ)-system, see figure 3.8a, it is clear that if *N* corresponds to a point where $\sigma_{cx} \geq -0.1f_c$, then concrete under uniaxial compression with $\sigma_{c2} = -0.5f_c$ will yield the maximum possible τ_{xy}. On the other hand, if *N* corresponds to a point with $\sigma_{cx} < -0.1f_c$, then τ_{xy} may be increased when we move downward according to option 2).

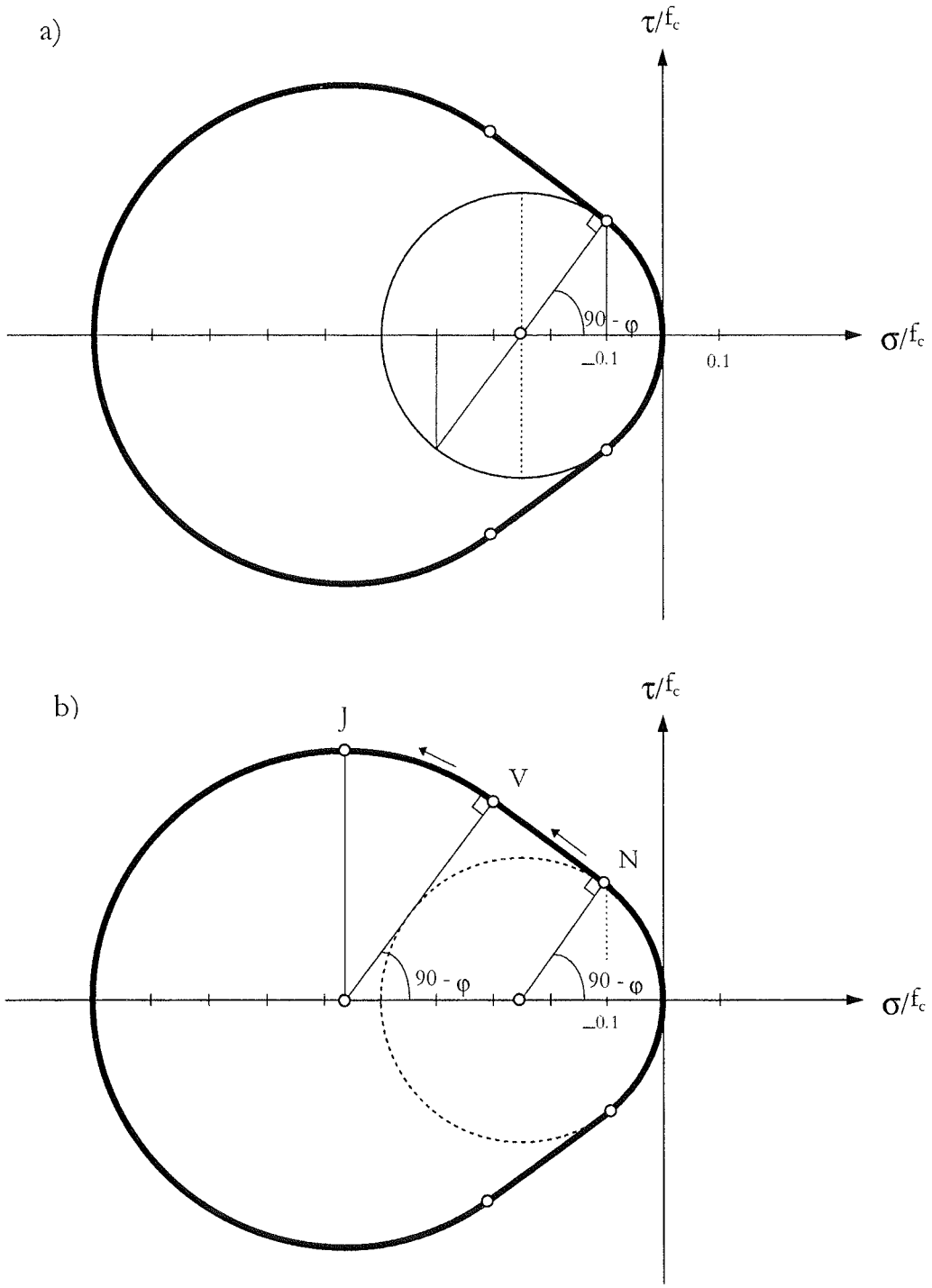

Figure 3.8 *Yield condition for isotropicly cracked concrete in the* (σ,τ)*-system, see also figure 2.8.*

The considerations above lead us to the result that from point *C*, see figure 3.7, to the point *N* corresponding to $(\sigma_x , \sigma_y) = (-0.1+\Phi,-0.4+\Phi)f_c$ [6], we should move downward according to option 1). Thus, in the area *NCRQ* we have a cylindrical yield surface, the direction of generatrix being *CR* parallel to *NQ*.

Similarly, we may obtain a cylindrical yield surface in the area *MAOP* with *MP* as the direction of generatrix. Here point *M* corresponds to $(\sigma_x, \sigma_y) = (-0.4+\Phi, -0.1+\Phi)f_c$ and σ_{sx} is changed from f_y to $-f_y$.

Now, in order to generate the remaining part of the yield condition, we know that concrete stresses corresponding to the cone ③, see figure 3.3, must somehow be mobilized. The yield condition will therefore be described by (3.23) where $(\rho\sigma_{sx}, \rho\sigma_{sy})$ will vary depending on the point in question.

We pose the question : In the remaining area, where shall we put $(\rho\sigma_{sx}, \rho\sigma_{sy}) = (\Phi f_c, \Phi f_c)$? Let us again look at point *N* with $(\sigma_{cx} , \sigma_{cy}) = (-0.1,-0.4)f_c$ and $\theta = 45^o - \varphi/2$, see figure 3.8b. Maintaining the reinforcement stresses $\sigma_{sx} = \sigma_{sy} = f_y$, we may increase τ_{xy} in the most optimal way by moving along the yield envelope. This is illustrated in figure 3.8b by the path *N-V-J*. From *N* to *V* the angle θ is kept constant equal to $45^o - \varphi/2$. From *V* to *J* θ is increased to the value 45^o. Along the path *N-V-J*, we have the stresses $\sigma_{c2} = 4\sigma_{c1} - 0.5f_c$ and $-0.125f_c \leq \sigma_{c1} \leq 0$.

The projection of the path *N-V-J* on the (σ_x,σ_y)-plane is shown in figure 3.7. By symmetry considerations, the path *M-U-J* as shown in figure 3.7 may also be found.

Thus, what we have obtained is the area *NVUM* within which the yield condition is described by (3.23) with $(\rho\sigma_{sx}, \rho\sigma_{sy}) = (\Phi f_c, \Phi f_c)$. Geometrically speaking, the yield condition in this area corresponds to the conical surface ③a, which we have defined in figure 3.3b. Naturally ③a is shifted by Φf_c in the σ_x– and σ_y direction, see figure 3.9.

---

[6] The point N may alternatively be found as follows: $(\sigma_{sx}, \sigma_{sy}) = (\Phi f_c, \Phi f_c)$ is inserted into (3.23) and $\partial\tau_{xy}/\partial\sigma_y$ is determined. Hereafter $\sigma_y = -\sigma_x - 0{,}5fc + 2\Phi f_c$ is inserted and the equation $\partial\tau_{xy}/\partial\sigma_y = 0$ is solved with respect to σ_x.

It is now easy to see where in the yield condition the remainder parts of the cone ③, namely ③b and ③c should be utilized. As shown in figure 3.9, part ③b is shifted to fit with the border *QRL* and part ③c is shifted to fit with the border *POH*. Thus, the yield condition in the areas *QRLT* and *POHS* is described by (3.23) with $(\rho\sigma_{sx}, \rho\sigma_{sy}) = (\Phi f_c, -\Phi f_c)$ and $(\rho\sigma_{sx}, \rho\sigma_{sy}) = (-\Phi f_c, \Phi f_c)$ respectively.

At any points along *N-V-J* we can now move downward by changing σ_{sy} from f_y to $-f_y$ and thus obtaining the cylindrical surfaces *NQTV* and *JVTK*. Similarly, we can from *M-U-J* move toward *P-S-I* by changing σ_{sx} from f_y to $-f_y$.

The complete yield condition has now been established. We make the following remarks:

In the regions where the yield condition is described by a conical surface, the reinforcement is yielding in both directions. In the regions where the yield condition is described by a cylindrical surface the reinforcement is not yielding in one or both direction (the last mentioned case applies to the region *FIJK*). For any given set of stresses $(\sigma_x, \sigma_y, \tau_{xy})$ it is possible to determine the reinforcement stresses. The formulas (3.19) and (3.20) together with (3.2) and (3.4) can therefore be used to determine the stresses in the concrete.

The analytical expressions for the yield condition and the boundaries of the different regions are given in the following. The legends refer to those used in figure 3.9.

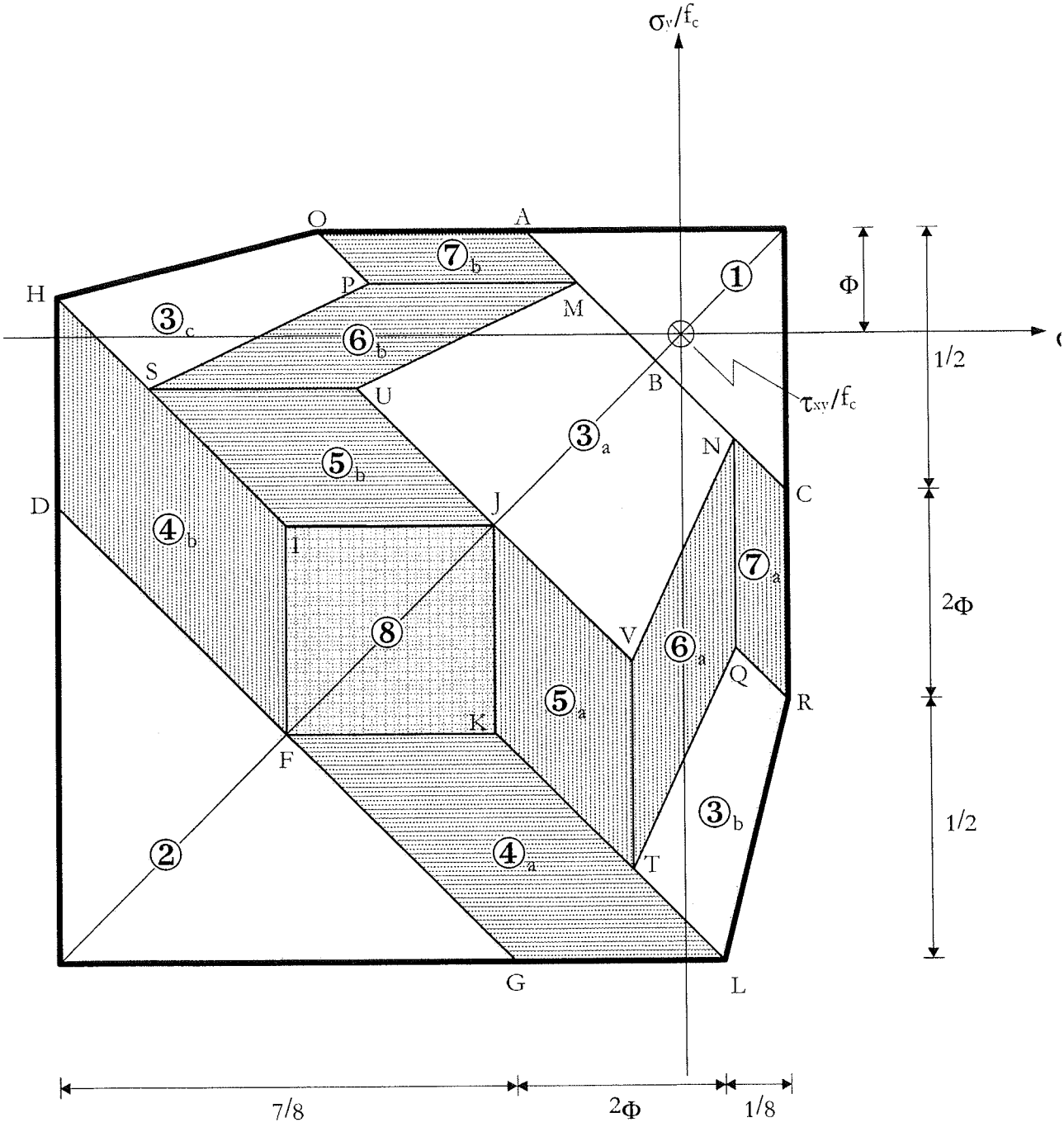

Figure 3.9 *Construction of the yield condition, isotropic reinforcement.*

Yield condition:

$$① : \tau_{xy}^2 - \left(\Phi f_c - \sigma_x\right)\left(\Phi f_c - \sigma_y\right) = 0 \tag{3.24}$$

$$② : \tau_{xy}^2 - \left[\left(1+\Phi\right)f_c + \sigma_x\right]\left[\left(1+\Phi\right)f_c + \sigma_y\right] = 0 \tag{3.25}$$

$$③a: \tau_{xy}^2 - \frac{1}{100}\left[(1+6\Phi)f_c + 2\sigma_x - 8\sigma_y\right]\left[(1+6\Phi)f_c + 2\sigma_y - 8\sigma_x\right] = 0 \quad (3.26)$$

$$③b: \tau_{xy}^2 - \frac{1}{100}\left[(1-10\Phi)f_c + 2\sigma_x - 8\sigma_y\right]\left[(1+10\Phi)f_c + 2\sigma_y - 8\sigma_x\right] = 0 \quad (3.27)$$

$$③c: \tau_{xy}^2 - \frac{1}{100}\left[(1+10\Phi)f_c + 2\sigma_x - 8\sigma_y\right]\left[(1-10\Phi)f_c + 2\sigma_y - 8\sigma_x\right] = 0 \quad (3.28)$$

$$④a: \tau_{xy}^2 + \left[(1+\Phi)f_c + \sigma_y\right]\left[(1/8+\Phi)f_c + \sigma_y\right] = 0 \quad (3.29)$$

$$④b: \tau_{xy}^2 + \left[(1+\Phi)f_c + \sigma_x\right]\left[(1/8+\Phi)f_c + \sigma_x\right] = 0 \quad (3.30)$$

$$⑤a: \tau_{xy}^2 + \left[(\Phi-1/8)f_c - \sigma_x\right]\left[(\Phi-1)f_c - \sigma_x\right] = 0 \quad (3.31)$$

$$⑤b: \tau_{xy}^2 + \left[(\Phi-1/8)f_c - \sigma_y\right]\left[(\Phi-1)f_c - \sigma_y\right] = 0 \quad (3.32)$$

$$⑥a: \tau_{xy}^2 - \frac{1}{400}\left[(5/2+15\Phi)f_c - 15\sigma_x\right]^2 = 0 \quad (3.33)$$

$$⑥b: \tau_{xy}^2 - \frac{1}{400}\left[(5/2+15\Phi)f_c - 15\sigma_y\right]^2 = 0 \quad (3.34)$$

$$⑦a: \tau_{xy}^2 - \left[\Phi f_c - \sigma_x\right]\left[(1/2-\Phi)f_c + \sigma_x\right] = 0 \quad (3.35)$$

$$⑦b: \tau_{xy}^2 - \left[\Phi f_c - \sigma_y\right]\left[(1/2-\Phi)f_c + \sigma_y\right] = 0 \quad (3.36)$$

$$⑧: \tau_{xy}^2 - \left(\frac{7}{16}\right)^2 = 0 \quad (3.37)$$

Boundaries of the different regions:

$$①: \begin{cases} \sigma_x \le \Phi f_c \quad , \quad \sigma_y \le \Phi f_c \\ \sigma_x + \sigma_y \ge 2\Phi f_c - \frac{1}{2} f_c \end{cases} \quad (3.38)$$

$$②: \begin{cases} \sigma_x \ge -(1+\Phi)f_c \quad , \quad \sigma_y \ge -(1+\Phi)f_c \\ \sigma_x + \sigma_y \le -(9/8+2\Phi)f_c \end{cases} \quad (3.39)$$

$$③a:\begin{cases}\sigma_x \ge \frac{1}{16}[34\sigma_y-(18\Phi+3)f_c]\\ \sigma_y \ge \frac{1}{16}[34\sigma_x-(18\Phi+3)f_c]\\ (2\Phi-9/8)f_c \le \sigma_x+\sigma_y \le (2\Phi-1/2)f_c\end{cases} \quad (3.40)$$

$$③b:\begin{cases}\sigma_x \ge \frac{1}{34}[16\sigma_y+(50\Phi+3)f_c]\\ \sigma_y \ge 4\sigma_x-(5\Phi+1/2)f_c\\ -9/8f_c \le \sigma_x+\sigma_y \le -1/2f_c\end{cases} \quad (3.41)$$

$$③c:\begin{cases}\sigma_x \ge 4\sigma_y-(5\Phi+1/2)f_c\\ \sigma_y \ge \frac{1}{34}[16\sigma_x+(50\Phi+3)f_c]\\ -9/8f_c \le \sigma_x+\sigma_y \le -1/2f_c\end{cases} \quad (3.42)$$

$$④a:\begin{cases}-(1+\Phi)f_c \le \sigma_y \le -(9/16+\Phi)f_c\\ -(9/8+2\Phi)f_c \le \sigma_x+\sigma_y \le -9/8f_c\end{cases} \quad (3.43)$$

$$④b:\begin{cases}-(1+\Phi)f_c \le \sigma_x \le -(9/16+\Phi)f_c\\ -(9/8+2\Phi)f_c \le \sigma_x+\sigma_y \le -9/8f_c\end{cases} \quad (3.44)$$

$$⑤a:\begin{cases}(\Phi-9/16)f_c \le \sigma_x \le (\Phi-3/10)f_c\\ -9/8f_c \le \sigma_x+\sigma_y \le (2\Phi-9/8)f_c\end{cases} \quad (3.45)$$

$$⑤b:\begin{cases}(\Phi-9/16)f_c \le \sigma_y \le (\Phi-3/10)f_c\\ -9/8f_c \le \sigma_x+\sigma_y \le (2\Phi-9/8)f_c\end{cases} \quad (3.46)$$

$$⑥a:\begin{cases}\sigma_y \le \frac{1}{16}[34\sigma_x-(3+18\Phi)f_c]\\ \sigma_y \ge \frac{1}{16}[34\sigma_x-(3+50\Phi)f_c]\\ (\Phi-3/10)f_c \le \sigma_x \le (\Phi-1/10)f_c\end{cases} \quad (3.47)$$

$$\text{⑥b}: \begin{cases} \sigma_x \le \frac{1}{16}\left[34\sigma_y - (3+18\Phi)f_c\right] \\ \sigma_x \ge \frac{1}{16}\left[34\sigma_y - (3+50\Phi)f_c\right] \\ (\Phi - 3/10)f_c \le \sigma_y \le (\Phi - 1/10)f_c \end{cases} \tag{3.48}$$

$$\text{⑦a}: \begin{cases} (\Phi - 1/10)f_c \le \sigma_x \le \Phi f_c \\ -1/2f_c \le \sigma_x + \sigma_y \le (2\Phi - 1/2)f_c \end{cases} \tag{3.49}$$

$$\text{⑦b}: \begin{cases} (\Phi - 1/10)f_c \le \sigma_y \le \Phi f_c \\ -1/2f_c \le \sigma_x + \sigma_y \le (2\Phi - 1/2)f_c \end{cases} \tag{3.50}$$

$$\text{⑧}: \begin{cases} -(\Phi + 9/16)f_c \le \sigma_x \le (\Phi - 9/16)f_c \\ -(\Phi + 9/16)f_c \le \sigma_y \le (\Phi - 9/16)f_c \end{cases} \tag{3.51}$$

The plastic strains (or actually strain rates) may, according to the normality condition, be derived from (3.24) - (3.37). When doing so, it can be shown that the yield condition is exact in all regions as the strains correspond to the stresses at all points.

Let us as an example examine the plastic strains corresponding to the yield condition ⑥a. From (2.4) and (3.33) we find :

$$\left.\begin{aligned} \varepsilon_x &= \lambda\frac{\partial f}{\partial \sigma_x} = \lambda\frac{3}{40}\left[(5/2+15\Phi)f_c - 15\sigma_x\right] \\ \varepsilon_y &= \lambda\frac{\partial f}{\partial \sigma_y} = 0 \\ \gamma_{xy} &= 2\varepsilon_{xy} = \lambda\frac{\partial f}{\partial \tau_{xy}} = \frac{4}{3}\varepsilon_x \end{aligned}\right\} \tag{3.52}$$

It can be seen immediately that the strain $\varepsilon_y = 0$ is in agreement with the fact that we within this region have $-f_y < \sigma_{sy} < f_y$. Further, for any value of σ_x in this region we have $\varepsilon_x > 0$ corresponding to tensile yielding in the "x- reinforcement". Inserting (3.52) into the transformation formulas

$$\left.\begin{matrix}\varepsilon_1\\ \varepsilon_2\end{matrix}\right\} = \frac{1}{2}(\varepsilon_x + \varepsilon_y) \pm \sqrt{\frac{1}{4}(\varepsilon_x - \varepsilon_y)^2 + \varepsilon_{xy}^2} \tag{3.53}$$

we find the principal strains to be

$$\left.\begin{matrix}\varepsilon_1\\ \varepsilon_2\end{matrix}\right\} = \begin{cases}\frac{4}{3}\varepsilon_x\\ -\frac{1}{3}\varepsilon_x\end{cases} \tag{3.54}$$

which gives the ratio $\varepsilon_1/\varepsilon_2 = -4$. We notice that this value corresponds to the only possible ratio within region ⑥a, since it may be shown that the principal concrete stresses here vary along the line *BC* in figure 2.7.

The direction between the first principal strain and the ε_x-direction is found by

$$\tan 2\theta = \frac{2\varepsilon_{xy}}{\varepsilon_x - \varepsilon_y} \tag{3.55}$$

which leads to

$$\theta = 45^\circ - \frac{1}{2}\varphi \tag{3.56}$$

We notice, that this direction may be shown to coincide with that of the principal concrete stresses.

The yield surface and it's contour lines are shown in figure 3.10 and 3.11 for the case $\Phi = 0.2$.

In figure 3.12, the curves of intersection between the yield surface with $\Phi = 0.2$ and the planes $\sigma_x + \sigma_y = -0.5f_c$ and $\sigma_x + \sigma_y = -0.725f_c$ are shown. To assess the strength reduction due to isotropical cracking, the corresponding curves for the yield condition of Nielsen [63.1] are also shown in the same figure.

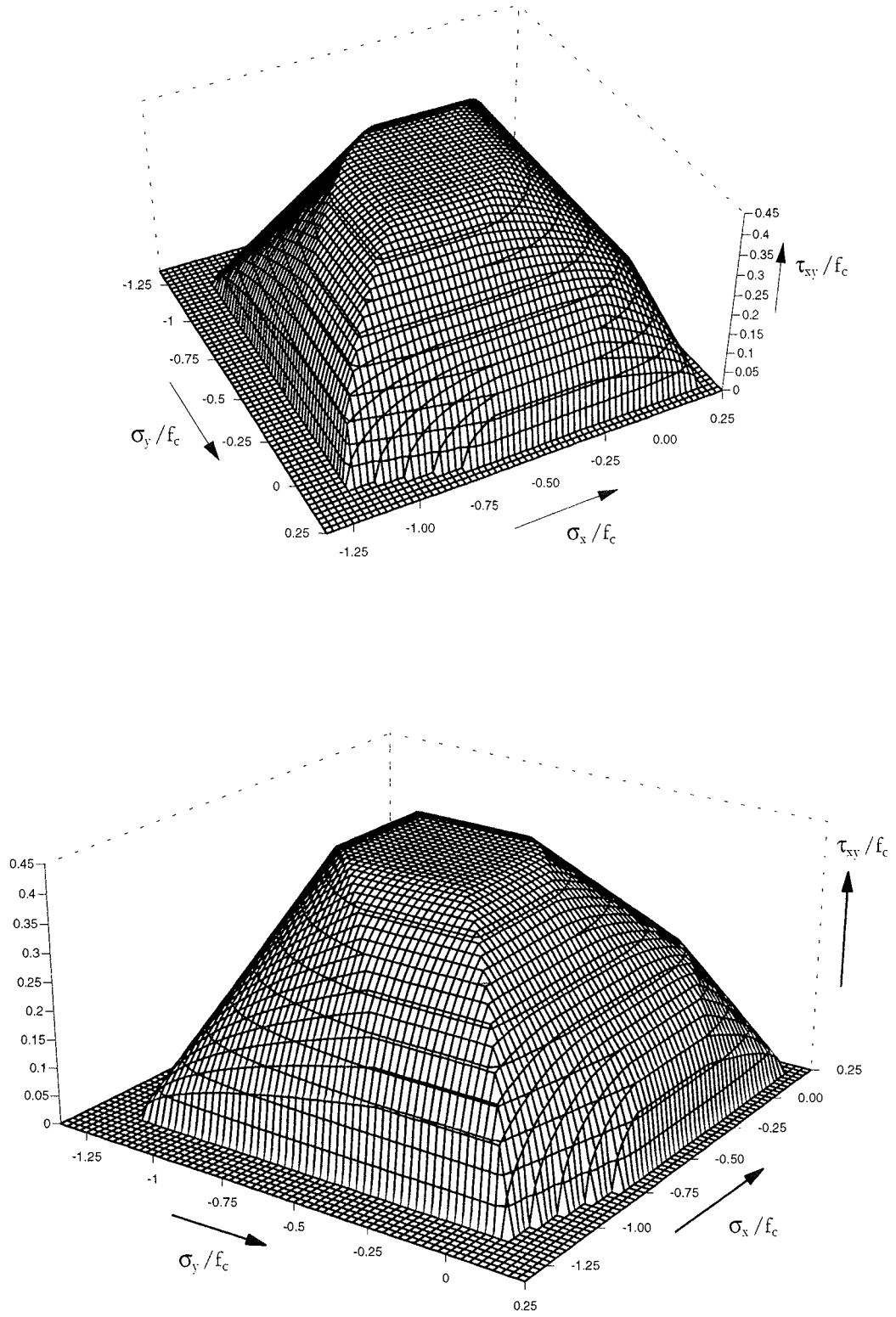

Figure 3.10 *Appearance of the yield surface for an isotropicly cracked disk with* Φ *=0,20.*

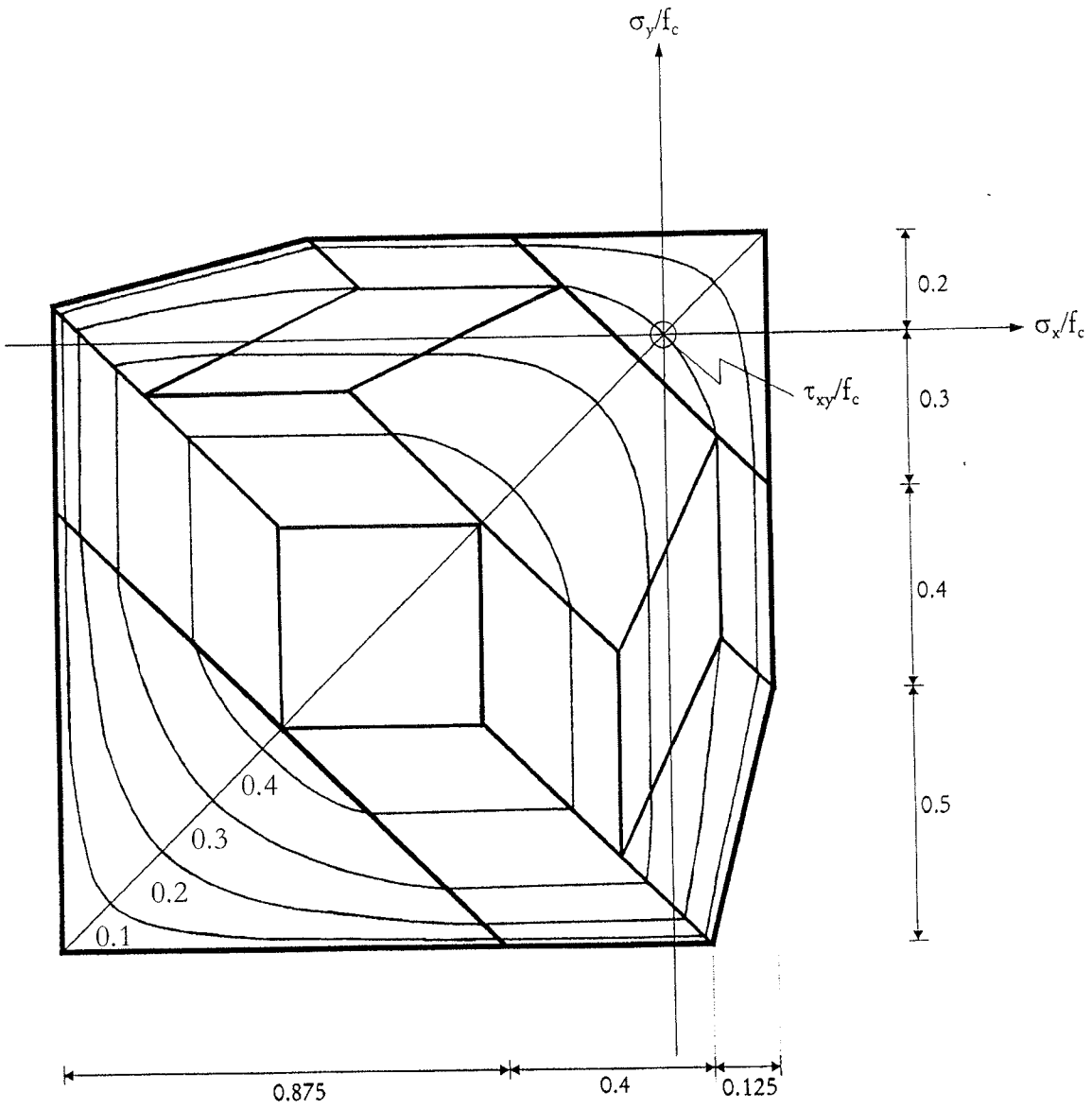

Figure 3.11 *Shear stress contour lines for an isotropicly cracked disk with* $\Phi = 0.20$.

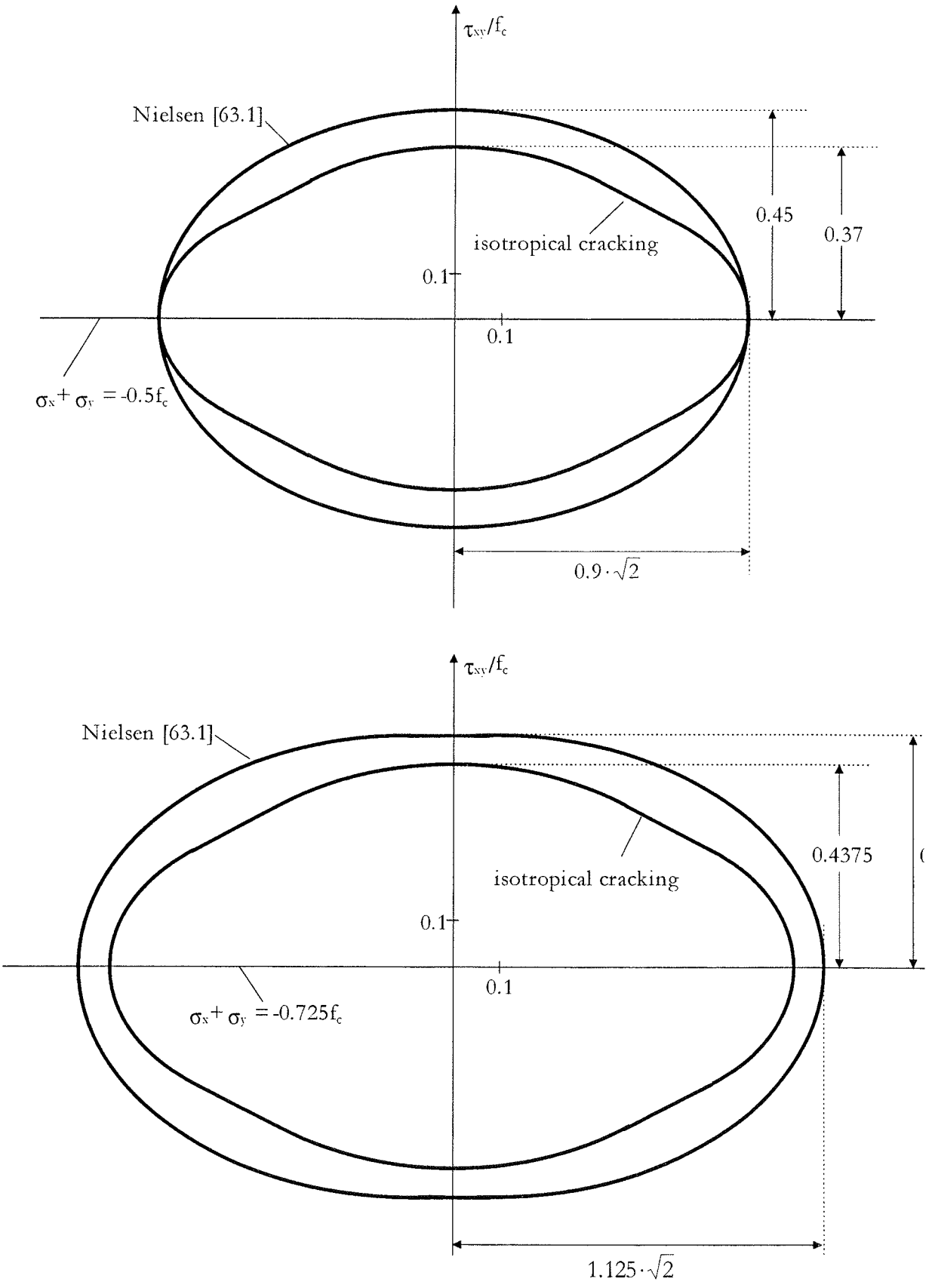

Figure 3.12 *Curves of intersection between the yield surface with* $\Phi = 0.2$ *and the planes* $\sigma_x + \sigma_y = -0.5f_c$ *and* $\sigma_x + \sigma_y = -0.725f_c$.

3.4 Yield condition for orthotropicly reinforced disks

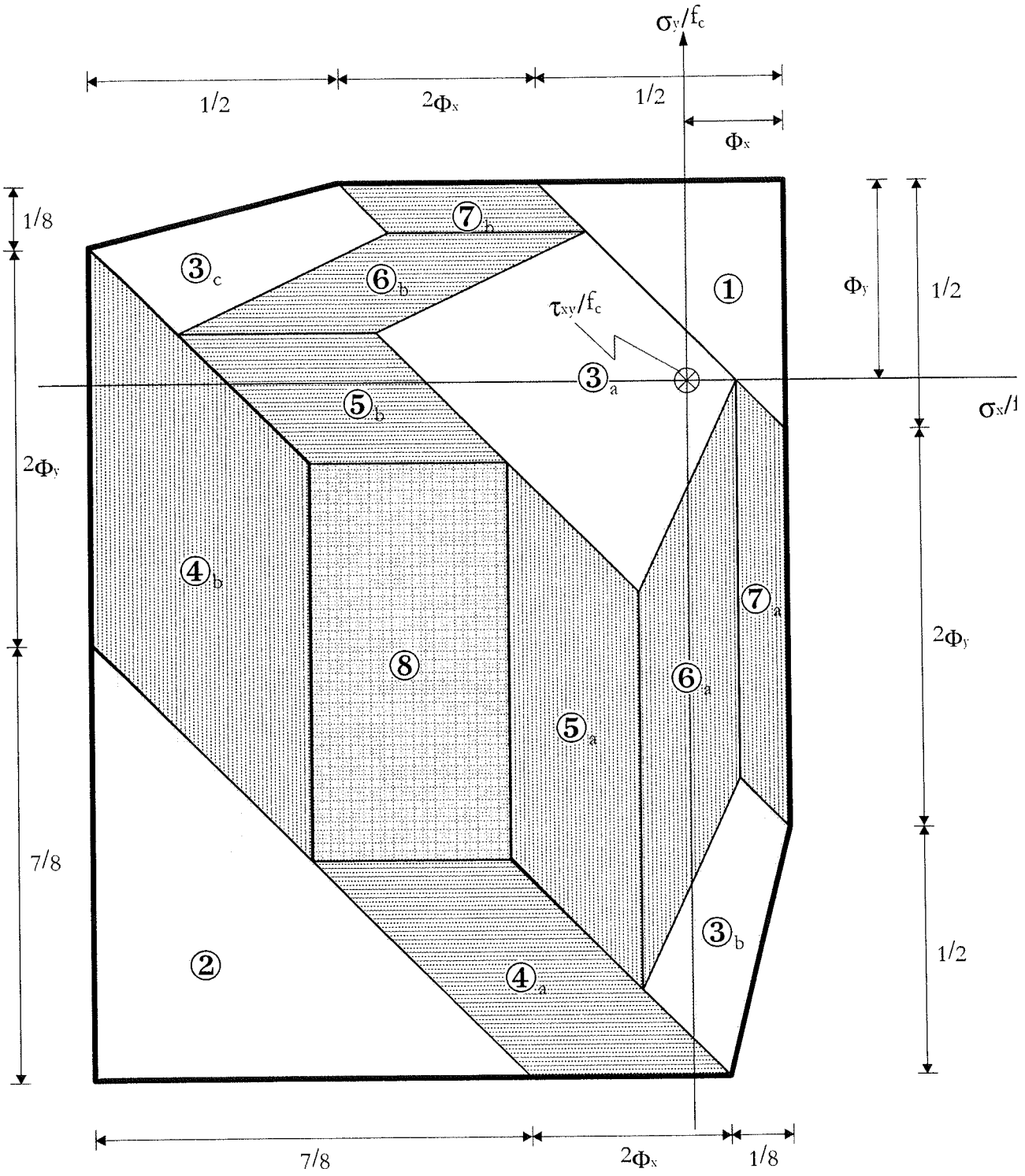

Figure 3.1 *Yield condition for orthotropicly reinforced disks (here* $\Phi_y = 2\,\Phi_x$*).*

A disk is called orthotropicly reinforced when the reinforcement degree Φ_x differs from Φ_y. The yield condition for such disks may be derived in the same way as shown in the previous section. For example, concrete stresses belonging to the cones ① and ② shown in figure 3.3 are combined with the reinforcement stresses ($\Phi_x f_c$, $\Phi_y f_c$) and ($-\Phi_x f_c$, $-\Phi_y f_c$), respectively. Further, the cone ③ is also subdivided into three parts as shown in figure 3.3. Concrete stresses described by the part ③a are combined with the reinforcement stresses ($\Phi_x f_c$, $\Phi_y f_c$) whereas parts ③b and ③c go along with ($\Phi_x f_c$, $-\Phi_y f_c$) and ($-\Phi_x f_c$, $\Phi_y f_c$), respectively.

The yield condition, as it appears for the case $\Phi_y = 2\Phi_x$, is shown in figure 3.13. To identify the different regions we use the same legends as those used in previous section.

The analytical expressions for the yield condition and the boundaries of the different regions are given below.

Yield condition:

$$① : \tau_{xy}^2 - (\Phi_x f_c - \sigma_x)(\Phi_y f_c - \sigma_y) = 0 \tag{3.57}$$

$$② : \tau_{xy}^2 - [(1+\Phi_x) f_c + \sigma_x][(1+\Phi_y) f_c + \sigma_y] = 0 \tag{3.58}$$

$$③a : \tau_{xy}^2 - \frac{1}{100}[(1-2\Phi_x+6\Phi_y) f_c + 2\sigma_x - 8\sigma_y] \cdot [(1-2\Phi_y+6\Phi_x) f_c + 2\sigma_y - 8\sigma_x] = 0 \tag{3.59}$$

$$③b : \tau_{xy}^2 - \frac{1}{100}[(1-2\Phi_x-8\Phi_y) f_c + 2\sigma_x - 8\sigma_y] \cdot [(1+2\Phi_x+8\Phi_y) f_c + 2\sigma_y - 8\sigma_x] = 0 \tag{3.60}$$

$$③c : \tau_{xy}^2 - \frac{1}{100}[(1+2\Phi_x+8\Phi_y) f_c + 2\sigma_x - 8\sigma_y] \cdot [(1-2\Phi_x-8\Phi_y) f_c + 2\sigma_y - 8\sigma_x] = 0 \tag{3.61}$$

$$④a : \tau_{xy}^2 + [(1+\Phi_y) f_c + \sigma_y][(1/8+\Phi_y) f_c + \sigma_y] = 0 \tag{3.62}$$

$$④b:\ \tau_{xy}^2+\left[(1+\Phi_x)f_c+\sigma_x\right]\left[(1/8+\Phi_x)f_c+\sigma_x\right]=0 \tag{3.63}$$

$$⑤a:\ \tau_{xy}^2+\left[(\Phi_x-1/8)f_c-\sigma_x\right]\left[(\Phi_x-1)f_c-\sigma_x\right]=0 \tag{3.64}$$

$$⑤b:\ \tau_{xy}^2+\left[(\Phi_y-1/8)f_c-\sigma_y\right]\left[(\Phi_y-1)f_c-\sigma_y\right]=0 \tag{3.65}$$

$$⑥a:\ \tau_{xy}^2-\frac{1}{400}\left[(5/2+15\Phi_x)f_c-15\sigma_x\right]^2=0 \tag{3.66}$$

$$⑥b:\ \tau_{xy}^2-\frac{1}{400}\left[(5/2+15\Phi_y)f_c-15\sigma_y\right]^2=0 \tag{3.67}$$

$$⑦a:\ \tau_{xy}^2-\left[\Phi_x f_c-\sigma_x\right]\left[(1/2-\Phi_x)f_c+\sigma_x\right]=0 \tag{3.68}$$

$$⑦b:\ \tau_{xy}^2-\left[\Phi_y f_c-\sigma_y\right]\left[(1/2-\Phi_y)f_c+\sigma_y\right]=0 \tag{3.69}$$

$$⑧:\ \tau_{xy}^2-\left(\frac{7}{16}\right)^2=0 \tag{3.70}$$

Boundaries of different regions:

$$①:\begin{cases}\sigma_x\le\Phi_x f_c\ ,\ \ \sigma_y\le\Phi_y f_c\\ \sigma_x+\sigma_y\ge(\Phi_x+\Phi_y-1/2)f_c\end{cases} \tag{3.71}$$

$$②:\begin{cases}\sigma_x\ge-(1+\Phi_x)f_c\ ,\ \ \sigma_y\ge-(1+\Phi_y)f_c\\ \sigma_x+\sigma_y\le-(9/8+\Phi_x+\Phi_y)f_c\end{cases} \tag{3.72}$$

$$③a:\begin{cases}\sigma_x\ge\frac{1}{16}\left[34\sigma_y-(34\Phi_y-16\Phi_x+3)f_c\right]\\ \sigma_y\ge\frac{1}{16}\left[34\sigma_x-(34\Phi_x-16\Phi_y+3)f_c\right]\\ (\Phi_x+\Phi_y-9/8)f_c\le\sigma_x+\sigma_y\le(\Phi_x+\Phi_y-1/2)f_c\end{cases} \tag{3.73}$$

$$③b:\begin{cases}\sigma_x \ge \dfrac{1}{34}\left[16\sigma_y + (16\Phi_y + 34\Phi_x + 3)f_c\right] \\ \sigma_y \ge 4\sigma_x - (4\Phi_x + \Phi_y + 1/2)f_c \\ (\Phi_x - \Phi_y - 9/8)f_c \le \sigma_x + \sigma_y \le (\Phi_x - \Phi_y - 1/2)f_c\end{cases} \tag{3.74}$$

$$③c:\begin{cases}\sigma_x \ge 4\sigma_y - (\Phi_x + 4\Phi_y + 1/2)f_c \\ \sigma_y \ge \dfrac{1}{34}\left[16\sigma_x + (16\Phi_x + 34\Phi_y + 3)f_c\right] \\ (\Phi_y - \Phi_x - 9/8)f_c \le \sigma_x + \sigma_y \le (\Phi_y - \Phi_x - 1/2)f_c\end{cases} \tag{3.75}$$

$$④a:\begin{cases}-(1 + \Phi_y)f_c \le \sigma_y \le -(9/16 + \Phi_y)f_c \\ -(9/8 + \Phi_x + \Phi_y)f_c \le \sigma_x + \sigma_y \le (\Phi_x - \Phi_y - 9/8)f_c\end{cases} \tag{3.76}$$

$$④b:\begin{cases}-(1 + \Phi_x)f_c \le \sigma_x \le -(9/16 + \Phi_x)f_c \\ -(9/8 + \Phi_x + \Phi_y)f_c \le \sigma_x + \sigma_y \le (\Phi_y - \Phi_x - 9/8)f_c\end{cases} \tag{3.77}$$

$$⑤a:\begin{cases}(\Phi_x - 9/16)f_c \le \sigma_x \le (\Phi_x - 3/10)f_c \\ (\Phi_x - \Phi_y - 9/8)f_c \le \sigma_x + \sigma_y \le (\Phi_x + \Phi_y - 9/8)f_c\end{cases} \tag{3.78}$$

$$⑤b:\begin{cases}(\Phi_y - 9/16)f_c \le \sigma_y \le (\Phi_y - 3/10)f_c \\ (\Phi_y - \Phi_x - 9/8)f_c \le \sigma_x + \sigma_y \le (\Phi_x + \Phi_y - 9/8)f_c\end{cases} \tag{3.79}$$

$$⑥a:\begin{cases}\sigma_y \le \dfrac{1}{16}\left[34\sigma_x - (3 + 34\Phi_x - 16\Phi_y)f_c\right] \\ \sigma_y \ge \dfrac{1}{16}\left[34\sigma_x - (3 + 34\Phi_x + 16\Phi_y)f_c\right] \\ (\Phi_x - 3/10)f_c \le \sigma_x \le (\Phi_x - 1/10)f_c\end{cases} \tag{3.80}$$

$$⑥b:\begin{cases}\sigma_x \le \dfrac{1}{16}\left[34\sigma_y - (3 + 34\Phi_y - 16\Phi_x)f_c\right] \\ \sigma_x \ge \dfrac{1}{16}\left[34\sigma_y - (3 + 34\Phi_y + 16\Phi_x)f_c\right] \\ (\Phi_y - 3/10)f_c \le \sigma_y \le (\Phi_y - 1/10)f_c\end{cases} \tag{3.81}$$

$$⑦a: \begin{cases} (\Phi_x - 1/10)f_c \le \sigma_x \le \Phi_x f_c \\ (\Phi_x - \Phi_y - 1/2)f_c \le \sigma_x + \sigma_y \le (\Phi_x + \Phi_y - 1/2)f_c \end{cases} \tag{3.82}$$

$$⑦b: \begin{cases} (\Phi_y - 1/10)f_c \le \sigma_y \le \Phi_y f_c \\ (\Phi_y - \Phi_x - 1/2)f_c \le \sigma_x + \sigma_y \le (\Phi_x + \Phi_y - 1/2)f_c \end{cases} \tag{3.83}$$

$$⑧: \begin{cases} -(\Phi_x + 9/16)f_c \le \sigma_x \le (\Phi_x - 9/16)f_c \\ -(\Phi_y + 9/16)f_c \le \sigma_y \le (\Phi_y - 9/16)f_c \end{cases} \tag{3.84}$$

3.5 Disks subjected to pure shear

The case of disks stressed in pure shear is of great practical importance. This case is met in webs in beams and when disks are designed by the stringer method. Hence, in this section, we shall derive the solutions for the shear strength of isotropicly cracked disks. In order to evaluate the strength reduction due to cracking, the results will be compared with the original plastic solutions.

Having found the general yield condition, it is rather straight forward to treat the special case of pure shear. What we have to do is simply to insert $(\sigma_x,\sigma_y) = (0,0)$ into the expressions for the yield condition, since a disk subjected to pure shear in the (x,y)-system, see figure 3.14, requires

$$\left.\begin{aligned} \sigma_x &= \sigma_{cx} + \sigma_{sx} = 0 \\ \sigma_y &= \sigma_{cy} + \sigma_{sy} = 0 \end{aligned}\right\} \tag{3.85}$$

Obviously (3.85) can only be fulfilled when the reinforcement is stressed in tension. Thus, looking at the yield condition in figure 3.13, it is clear that the point $(\sigma_x,\sigma_y) = (0,0)$ can only be localized within the regions ① and ③a or within the parts of the regions ⑤a, ⑤b, ⑥a, ⑥b, ⑦a, ⑦b and ⑧, where the non yielding reinforcement is still in tension.

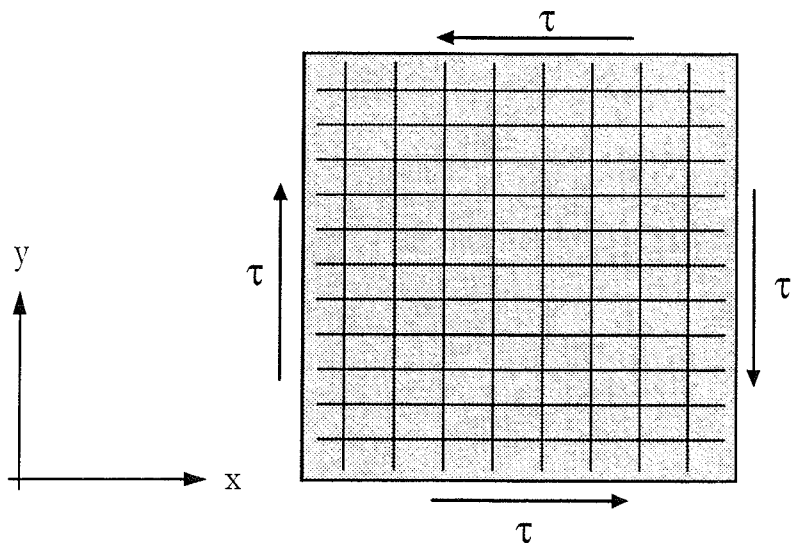

Figure 3.2 *Disk subjected to pure shear.*

3.5.1 Normally reinforced disks. Let us begin with the case of normally reinforced disks; that is disks where the shear strength is governed by yielding of the reinforcement in both directions. In this case, the point $(\sigma_x,\sigma_y) = (0,0)$ can either be found in region ① or in region ③a. Consider first region ①. Here the shear strength is found by inserting $(\sigma_x,\sigma_y) = (0,0)$ into (3.57) which leads to

$$\frac{\tau}{f_c} = \sqrt{\Phi_x \Phi_y} \tag{3.86}$$

From (3.71) we see that the point $(\sigma_x,\sigma_y) = (0,0)$ is localized in region ① when the condition

$$\Phi_x + \Phi_y \leq 1/2 \tag{3.87}$$

is fulfilled. Thus, (3.86) is a valid solution when the amount of reinforcement satisfies (3.87).

We now proceed on to consider the case where $(\sigma_x,\sigma_y) = (0,0)$ lies in region ③a. From (3.59) we find the solution

$$\frac{\tau}{f_c} = \frac{1}{10}\sqrt{(1-2\Phi_x+8\Phi_y)(1-2\Phi_y+8\Phi_x)} \tag{3.88}$$

which, according to (3.73), is valid under the following conditions

$$\left.\begin{aligned} &1/2 \le \Phi_x + \Phi_y \le 9/8 \\ &16\Phi_x - 34\Phi_y \le 3 \\ &16\Phi_y - 34\Phi_x \le 3 \end{aligned}\right\} \qquad (3.89)$$

We notice that the first condition in (3.89) refers to the total amount of reinforcement whereas the last two conditions are requirements on how orthotropicly reinforced the disk may be.

3.5.2 Partially overreinforced disks. We now pass on to the case of partially overreinforced disks, i.e. disks where the shear strength is governed by concrete failure and reinforcement yielding in only one direction. This case is met when all the conditions in (3.89) are not fulfilled at the same time.

Only the regions ⑤b, ⑥b, and ⑦b need to be considered if we assume that the disk is overreinforced with respect to the x-direction, i.e. $\Phi_x > \Phi_y$.

First, if $(\sigma_x,\sigma_y) = (0,0)$ is localized within region ⑦b, we find from (3.69) the following solution

$$\frac{\tau}{f_c} = \sqrt{\Phi_y(1/2 - \Phi_y)} \qquad (3.90)$$

which, according to (3.83), is valid under the following conditions

$$\left.\begin{aligned} &\Phi_x + \Phi_y \ge 1/2 \\ &\Phi_y \le 1/10 \end{aligned}\right\} \qquad (3.91)$$

Next, we find from (3.67) the following solution when $(\sigma_x,\sigma_y) = (0,0)$ is lying in region ⑥b

$$\frac{\tau}{f_c} = \frac{1}{8} + \frac{3}{4}\Phi_y \qquad (3.92)$$

According to (3.81) this solution is valid when

$$\left.\begin{aligned} &16\Phi_x - 34\Phi_y \ge 3 \\ &1/10 \le \Phi_y \le 3/10 \end{aligned}\right\} \qquad (3.93)$$

Finally, when the point $(\sigma_x,\sigma_y) = (0,0)$ is localized in region ⑤b, we find from (3.67) and (3.79) the solution

$$\frac{\tau}{f_c} = \sqrt{(1-\Phi_y)(\Phi_y - 1/8)} \tag{3.94}$$

which is valid under the conditions

$$\left.\begin{aligned} &\Phi_x + \Phi_y \geq 9/8 \\ &3/10 \leq \Phi_y \leq 9/16 \end{aligned}\right\} \tag{3.95}$$

Notice that the case $\Phi_y > \Phi_x$ can be covered by (3.90) - (3.95) if subscript *x* in these formulas is replaced by *y* and vice versa.

3.5.3 Overreinforced disks. When the shear strength is governed by concrete failure without yielding of the reinforcement, we have an overreinforced disk. In this case, the point $(\sigma_x,\sigma_y) = (0,0)$ will be found in region ⑧. According to (3.70) the maximum shear stress which can be carried is

$$\frac{\tau}{f_c} = \frac{7}{16} \tag{3.96}$$

This is valid when

$$\left.\begin{aligned} &\Phi_x \geq 9/16 \\ &\Phi_y \geq 9/16 \end{aligned}\right\} \tag{3.97}$$

The complete solution for the shear strength of an isotropicly cracked disks has now been established. We can immediately conclude that the solutions are exact plastic solutions since they are derived from an exact yield condition.

The solutions are summarized in figure 3.15. The figure shows the different domains of reinforcement amounts (Φ_x,Φ_y), within which each of the derived solutions applies.

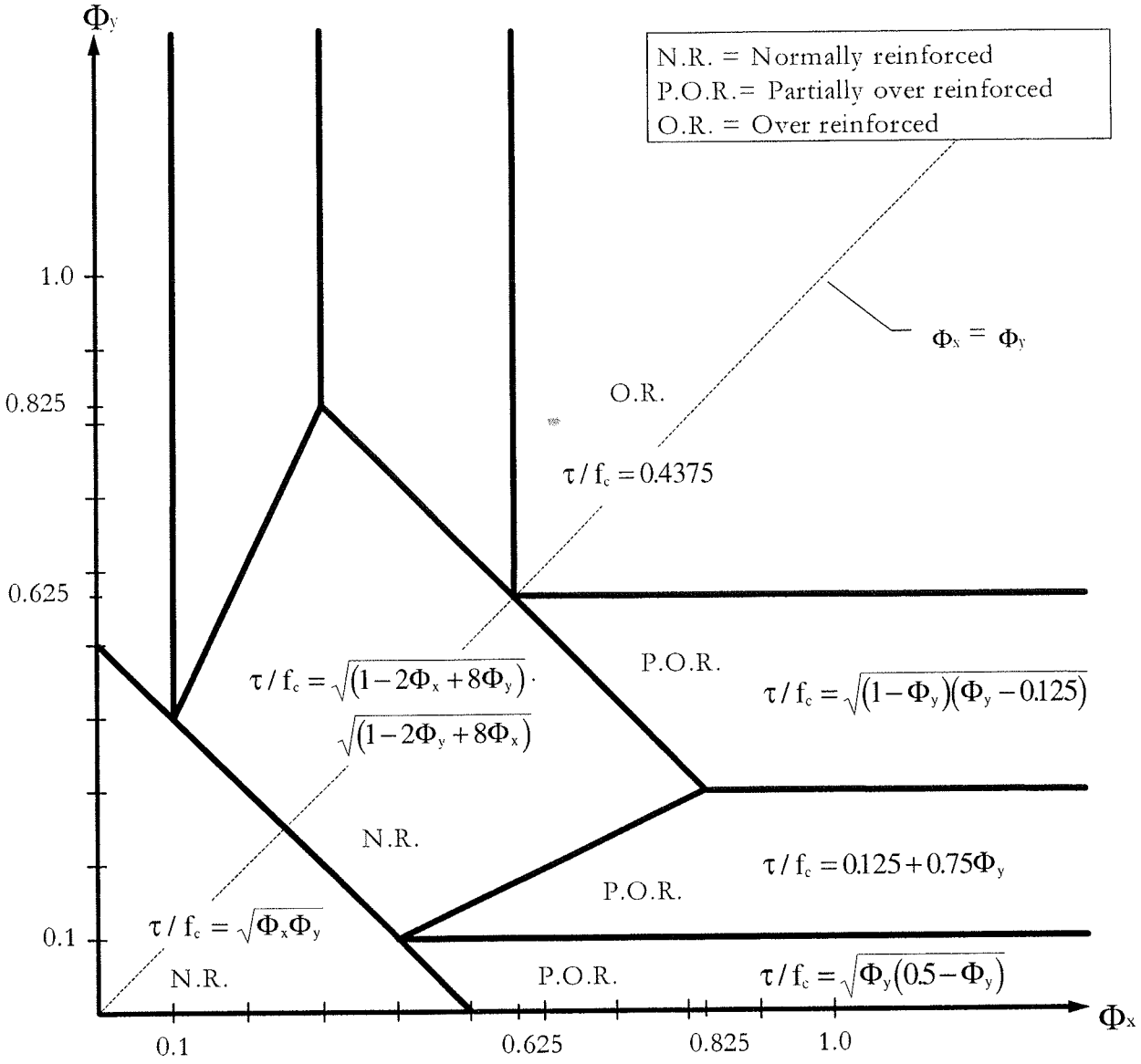

Figure 3.3 *Solutions for the shear strength of isotropicly cracked disks.*

Figure 3.15 is rather illustrative. For example in the case of an isotropicly reinforced disk, we see that the shear strength is either given by solution (3.85), (3.88) or (3.96). These solutions are depicted as a function of Φ in figure 3.16 where the original solution, see [69.1], also has been drawn. The strength reduction for $\Phi > 0.25$ is due to the fact, that a confining stress σ_{con} must be applied in order to increase the largest compression stress σ_c beyond $0.5f_c$. The concrete stresses belonging to the different solutions are illustrated in the same figure.

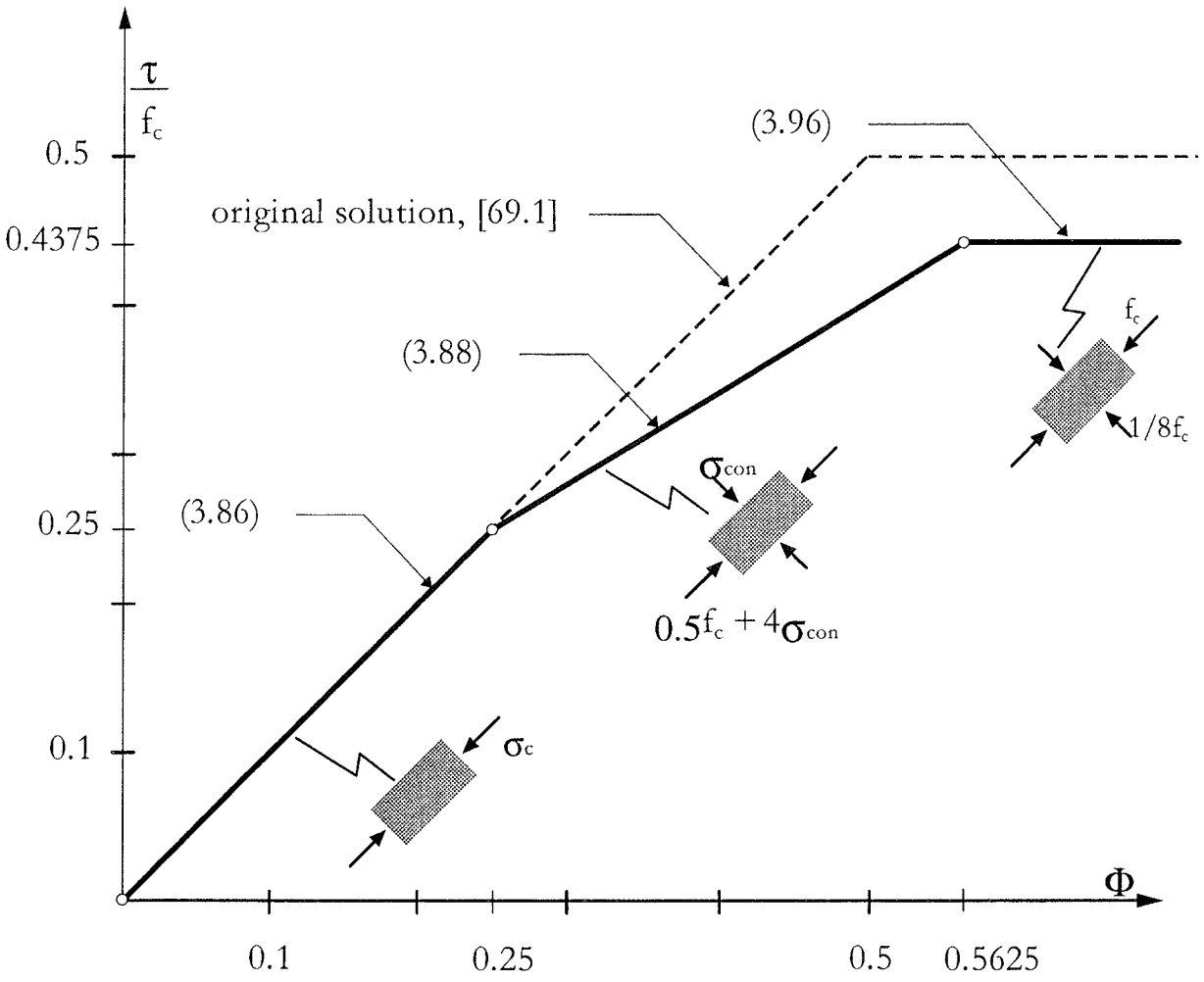

Figure 3.4 *Shear strength of isotropicly cracked disks which are isotropicly reinforced.*

Returning to figure 3.15, wee see that when the reinforcement in the x-direction is sufficiently strong (for example $\Phi_x > 0.825$), only reinforcement yielding in the y-direction can take place and the shear strength is, depending on the magnitude of Φ_y, given by either (3.90), (3.92), (3.94) or (3.96). Figure 3.17 shows these solutions. It can be seen that (3.90) and (3.94) represent two circles (actually Mohr's circles for uniaxial and biaxial compression, respectively) and (3.92) constitutes the tangent to (3.90) and (3.94) at $\Phi_y = 0.1$ and 0.3.

For comparison, the original solution[7] has also been depicted. The maximum relative strength reduction due to cracking is 34% and occurs at $\Phi_y = 0.125$.

---

[7] Applied to beam shear, this solution is well-known as the *web crushing criterion*, see for example [78.1][84.1].

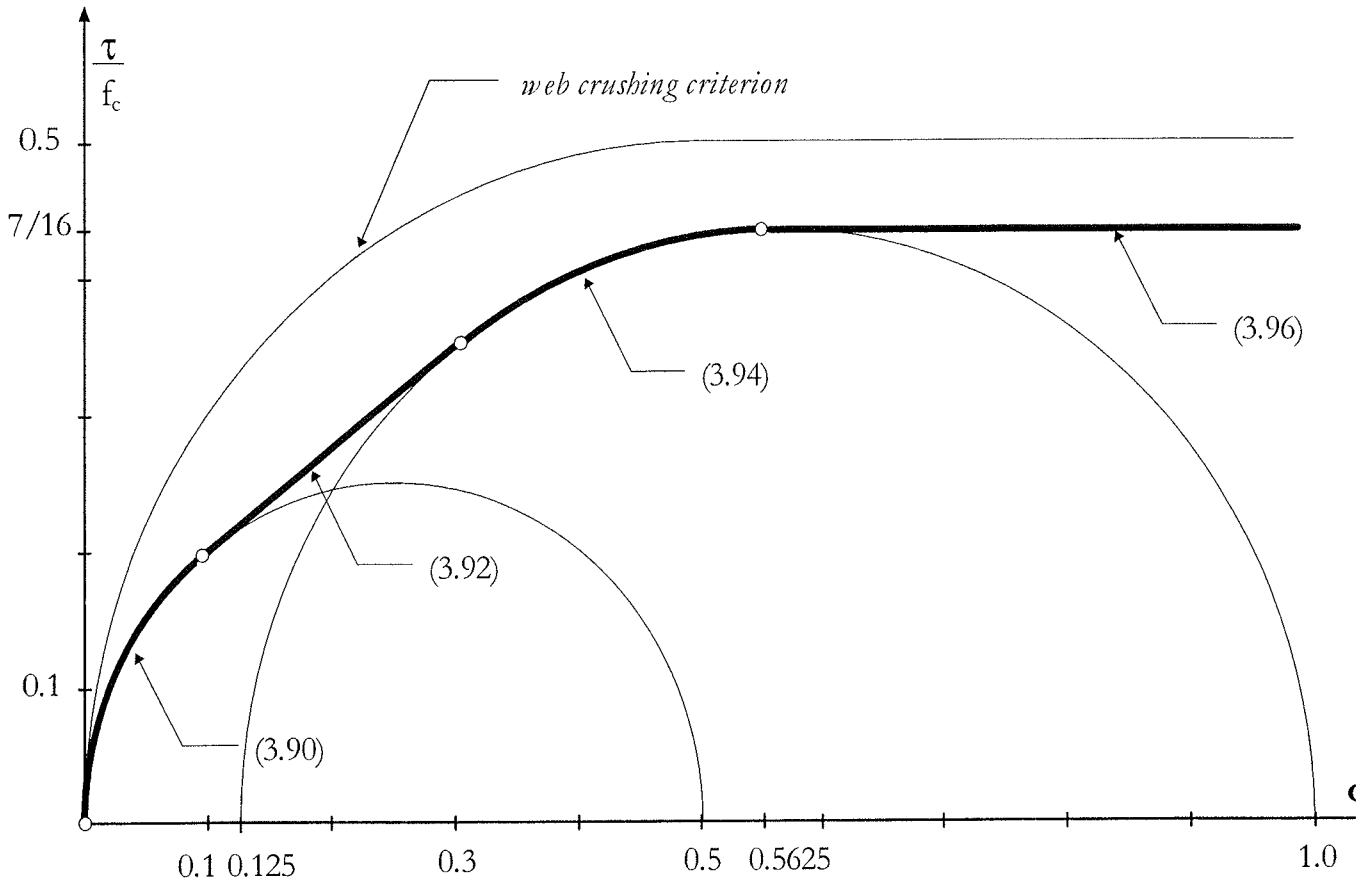

Figure 3.5 *Shear strength of isotropicly cracked disks which are partially overreinforced,* $\Phi_x > \Phi_y$.

The solutions given above may naturally also be derived explicitly without any reference to the general yield condition. In order to demonstrate this, we will close this section by showing how the solutions for isotropicly reinforced disks and for partially overreinforced disks alternatively may be found by applying the upper bound technique.

3.5.4 Upper bound solutions for isotropicly reinforced disks. An isotropicly reinforced disk, $\Phi_x = \Phi_y = \Phi$, as shown in figure 3.18a, is considered. All geometrical quantities of the disk are assumed to be unity. The reinforcement directions (x,y) are rotated by the angle 45° with the directions (1) and (2), which are parallel to the sides of the disk. The disk is loaded with a tensile normal stress equal to τ in the direction (1) and with a compression normal stress τ in the direction (2). Thus, described in the (x,y)-system, the disk is loaded in pure shear with the shear stress τ, see figure 3.18b.

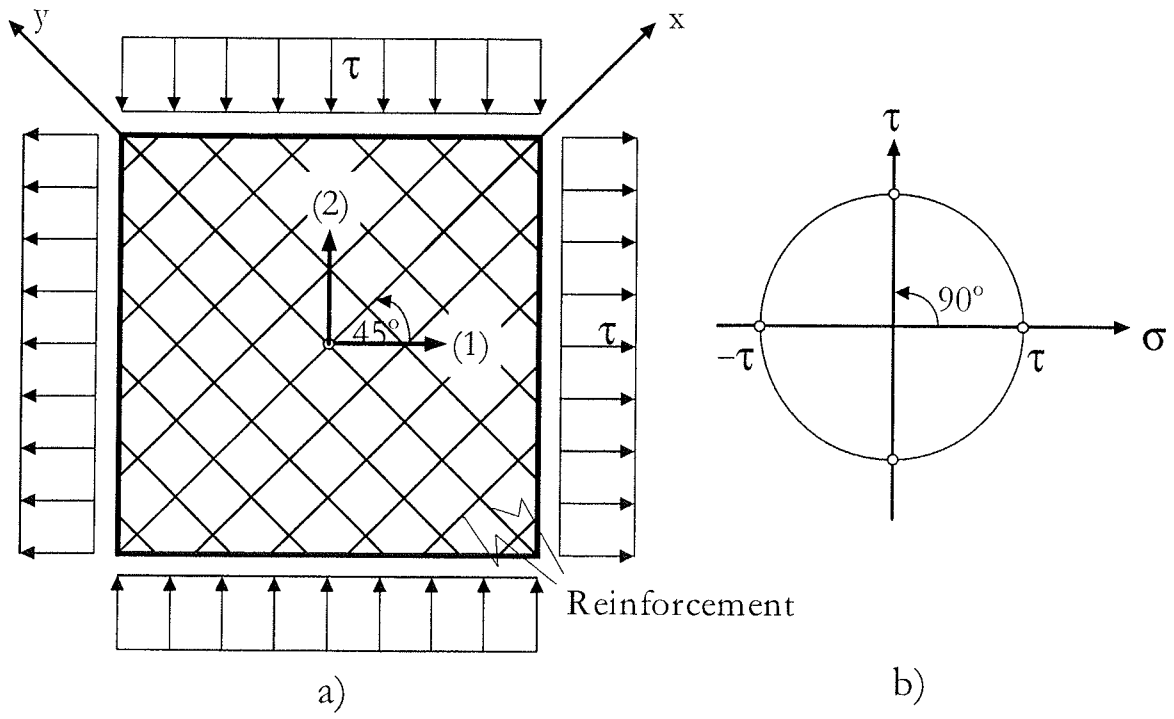

Figure 3.6 *Isotropicly reinforced disk subjected to pure shear in the (x,y)-system.*

The disk is now subjected to three different states of homogeneous strain, see figure 3.19. The directions (1) and (2) are taken as the directions of principal strains.

- Strain field a)

First, we consider the strain field shown in figure 3.19a characterized by the principal strains

$$(\varepsilon_1,\varepsilon_2) = (\lambda,0) \tag{3.98}$$

λ being an arbitrary positive constant.

The normal strains in the x- and y-directions are easily found, e.g. by drawing the corresponding Mohr's circle, see figure 3.19a,

$$(\varepsilon_x,\varepsilon_y) = (\frac{1}{2}\lambda,\frac{1}{2}\lambda) \tag{3.99}$$

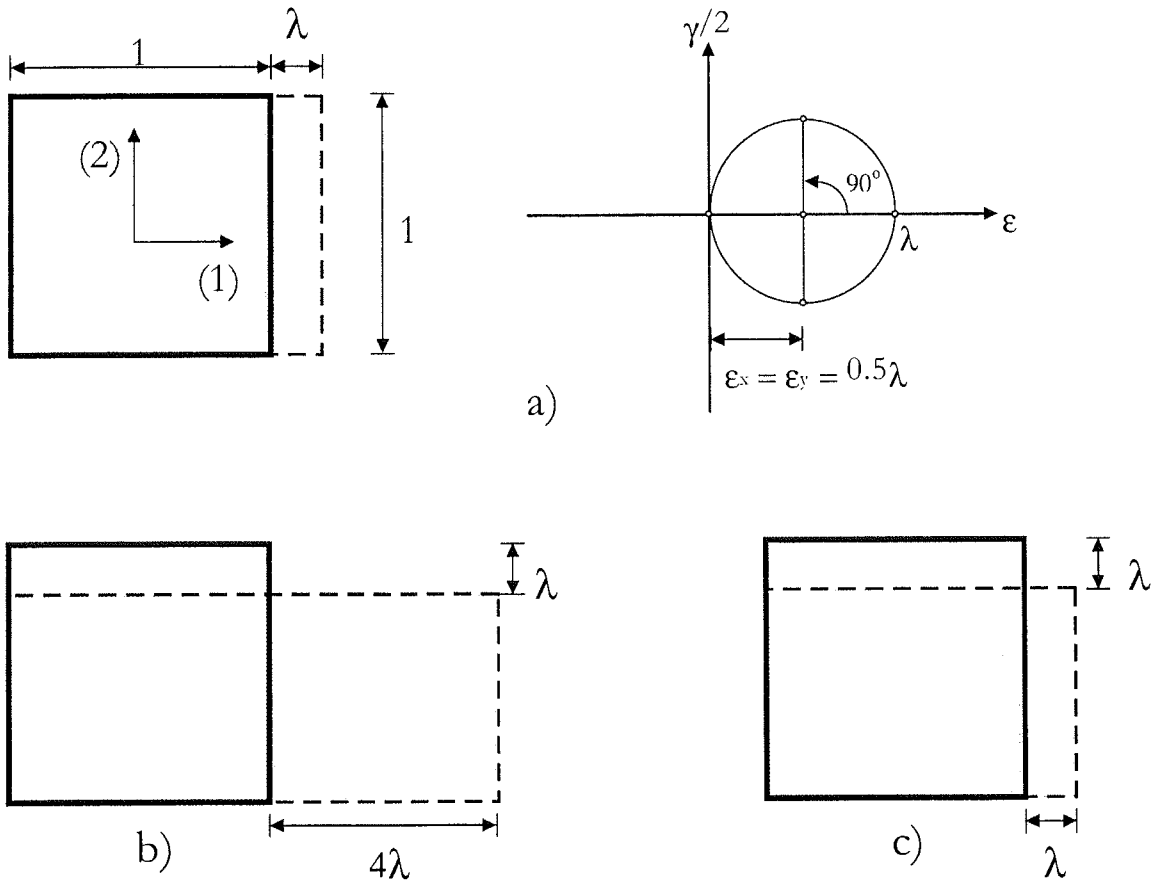

Figure 3.7 *Homogeneous strain fields in isotropicly reinforced disk element.*

For this imposed strain field, we see that the concrete stress vector must, according to the yield condition for concrete shown in figure 2.7, be perpendicular to the strain vector in order to satisfy the normality condition. Thus, only the reinforcement will contribute to the internal work[8], which is found by integration of $f_y\varepsilon_x + f_y\varepsilon_y$ over the reinforcement volume V_{sx} and V_{sy}

---

[8] It is here assumed, that the strains in the reinforcement material can be taken from (3.99). This implies that no premature bond failure is occurring. The fact that we have assumed isotropicly cracked concrete throughout and still insist on an intact bond strength may seem rather contradictory. It must, however, be borne in mind that the assumption of isotropical cracking throughout is an ideal state introduced as a simple and general material model.

Local loss of bond strength due to cracking is, although conflicting with the theoretical assumptions, probably not crucial to the overall strength in practice as long as good a n-chorage arrangements are provided. The latter condition ensures that the reinforcement must be stressed to yielding before unlimited crack sliding can take place.

$$W_I = W_{Is} = \int_{V_{sx}} f_y \varepsilon_x dV + \int_{V_{sy}} f_y \varepsilon_y dV$$
$$= 2\frac{1}{2}\lambda\Phi f_c = \lambda\Phi f_c \tag{3.100}$$

The external work is

$$W_E = \lambda\tau \tag{3.101}$$

By inserting into the work equation, $W_E = W_I$, we find the following solution

$$\tau = \Phi f_c \tag{3.102}$$

which is seen to be identical with (3.86) when $\Phi_x = \Phi_y$.

- Strain field b)

Next, we impose a strain field (figure 3.19b) characterized by the principal strains

$$(\varepsilon_1, \varepsilon_2) = \lambda(4, -1) \tag{3.103}$$

which transformed into the (x,y)-system gives rise to

$$(\varepsilon_x, \varepsilon_y) = \lambda(\frac{3}{2}, \frac{3}{2}) \tag{3.104}$$

According to the normality condition, any stress combination along the line BC in figure 2.7 is capable of producing the given strain field. Hence, we may choose the stress vector corresponding to the apex B:

$$(\sigma_{c1}, \sigma_{c2}) = (0, -\frac{1}{2} f_c) \tag{3.105}$$

The internal works W_{Is} and W_{Ic}, done in the reinforcement and in the concrete respectively, are

$$W_{Is} = 2\frac{3}{2}\lambda\Phi f_c = 3\lambda\Phi f_c \tag{3.106}$$

$$W_{Ic} = \left(0, -\frac{1}{2} f_c\right) \cdot (4\lambda, -1\lambda) = \frac{1}{2}\lambda f_c \tag{3.107}$$

The external work is

$$W_E = 4\lambda\tau + \lambda\tau = 5\lambda\tau \tag{3.108}$$

Inserting into the work equation, we obtain the solution

$$\tau = \left(\frac{6}{10}\Phi + \frac{1}{10}\right) f_c \tag{3.109}$$

which is seen to be identical with (3.88) when $\Phi_x = \Phi_y$.

- Strain field c)

Lastly we consider the following strain field (figure 3.19c)

$$(\varepsilon_1, \varepsilon_2) = \lambda(1, -1) \tag{3.110}$$

In this case we find

$$(\varepsilon_x, \varepsilon_y) = (0, 0) \tag{3.111}$$

Thus, the reinforcement will not contribute to the internal work. Regarding the concrete material, we find from figure 2.7 that only the stress vector corresponding to point C is capable of producing the given strain field. Therefore,

$$(\sigma_{c1}, \sigma_{c2}) = (-\frac{1}{8} f_c, -f_c) \tag{3.112}$$

In this case the work equation leading to the solution reads

$$\begin{aligned} W_E &= W_{Ic} \quad \Rightarrow \\ -\frac{1}{8} f_c \lambda + \lambda f_c &= 2\lambda\tau \quad \Rightarrow \\ \tau &= \frac{7}{16} f_c \end{aligned} \tag{3.113}$$

The solution is seen to be identical to (3.96) when $\Phi_x = \Phi_y$.

Solutions for orthotropicly reinforced disks with reinforcement yielding in both directions may also be reproduced by considering strain fields similar to those shown in figure 3.19. The direction of the principal strains will in this

case form an angle with the sides of the disk. The angle and the solutions are found by minimization according to the upper bound theorem.

3.5.5 Upper bound solutions for partially overreinforced disks. To make use of the dissipation formulas provided in chapter 2, we will hereafter reproduce the solutions for partially overreinforced disks by considering a failure mechanism with plastic strains concentrated in a yield line.

The failure mechanism considered is shown in figure 3.20 where the yield line forms an angle α with the displacement vector. We will assume that the reinforcement in the x-direction is not yielding at failure which means that the relative displacement u must be perpendicular to the x-axis. This mechanism is identical to that developed by Nielsen & Bræstrup for beam shear, see [78.1] and [98.4]. For simplicity the disk considered is assumed to have depth and thickness equal to unity whereas the length is unspecified.

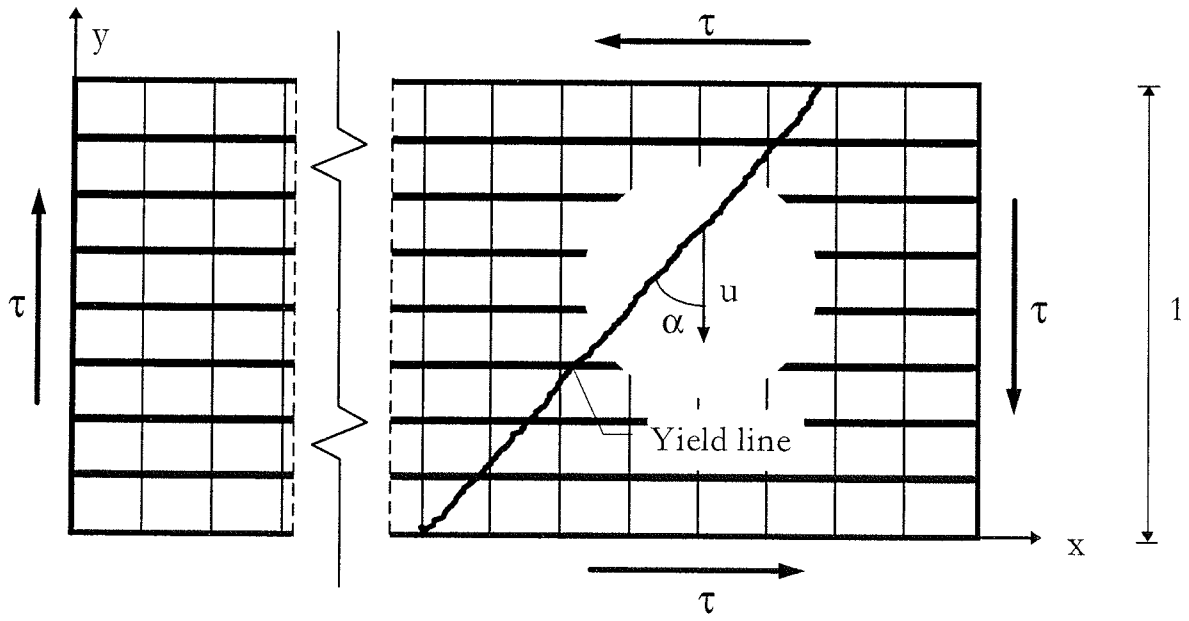

Figure 3.8 *Failure mechanism in a isotropicly cracked disk with yielding in the vertical reinforcement.*

Three upper bound solutions may be derived when the angle α runs through all possible values.

- $\varphi < \alpha \leq \pi/2$:

If the part of the disk to the right of the yield line moves *u* downward, the resultant of the shear stresses does the following work

$$W_E = \tau \cdot u \tag{3.114}$$

The internal work done by the concrete may be found using the dissipation formula (2.22) :

$$W_{Ic} = \frac{1}{4} f_c (1 - \sin\alpha) \frac{1}{\cos\alpha} \cdot u \tag{3.115}$$

where $1/\cos\alpha$ is the total length of the yield line.

The internal work done by the reinforcement is

$$W_{Is} = \Phi_y f_c \tan\alpha \cdot u \tag{3.116}$$

By inserting into the work equation, the following is obtained

$$\frac{\tau}{f_c} = \frac{\left(\Phi_y - \frac{1}{4}\right)\sin\alpha + \frac{1}{4}}{\cos\alpha} \tag{3.117}$$

Minimizing (3.117) with respect to α renders the solution

$$\frac{\tau}{f_c} = \sqrt{\Phi_y \left(\frac{1}{2} - \Phi_y\right)} \tag{3.118}$$

which is identical to (3.90). The angle α is given by

$$\sin\alpha = 1 - 4\Phi_y \tag{3.119}$$

It can be seen that α approaches $\pi/2$ for $\Phi_y \rightarrow 0$. When α approaches φ we have $\Phi_y \rightarrow 0.1$, which thus is the upper limit for the validity of solution (3.118). This limit corresponds to the last condition in (3.91).

- **$\alpha = \varphi$:**

In this case, the external work is the same as (3.114) and the total internal work is found by adding (3.115) and (3.116), where α is replaced by the angle of friction φ. By utilizing that $\sin\varphi = 0.6$, the following solution is found

$$\frac{\tau}{f_c} = \frac{1}{8} + \frac{3}{4}\Phi_y \tag{3.120}$$

which is identical (3.92).

- $0 \leq \alpha < \varphi$:

The contributions to the work equation are

$$W_E = \tau \cdot u \tag{3.121}$$

$$W_{Is} = \Phi_y f_c \tan\alpha \cdot u \tag{3.122}$$

$$W_{Ic} = \frac{1}{16} f_c (7 - 9\sin\alpha) \frac{1}{\cos\alpha} \cdot u \tag{3.123}$$

where the dissipation formula (2.23) has been used to calculate W_{Ic}.

By inserting (3.121) - (3.123) into the work equation and minimizing τ with respect to α, we find the solution

$$\frac{\tau}{f_c} = \sqrt{\left(\Phi_y - \frac{1}{8}\right)(1 - \Phi_y)} \tag{3.124}$$

which is seen to be identical to (3.94). The angle α is given by

$$\sin\alpha = \frac{1}{7}(9 - 16\Phi_y) \tag{3.125}$$

By inserting the upper and lower limit of α into (3.125), we find that the solution (3.124) is valid for

$$\frac{3}{10} < \Phi_y \leq \frac{9}{16} \tag{3.126}$$

When $\Phi_y = 9/16$, we have $\alpha = 0$ meaning that only the concrete is contributing to the internal work,. Hence, reinforcement degrees beyond this value will not increase the shear strength. Inserting $\Phi_y = 9/16$ into (3.124), the maximum possible shear strength is found to be $\tau = 7/16 f_c$.

3.6 Out of plane crack sliding failure

Until now, we have only been dealing with disks, where it has been assumed that the crack planes are perpendicular to the plane of the disk. This assumption ensures, that any sliding failure out of plane will go through uncracked concrete.

However, if the disk is suffering from cracking in all directions, for example due to alkali-silica reactions where the crack planes may be arbitrarily orientated, crack sliding out of plane takes place once the numerically largest principal concrete stress reaches the value $0.5f_c$. This is due to the fact that we do not have any confining stress perpendicular to the disk plane. Thus, for such disks, the yield condition must be derived by use of a square yield condition for concrete, see figure 3.21.

When such reinforced disks are examined, the original yield condition given by Nielsen [63.1] may be used if f_c is replaced by $0.5f_c$ everywhere.

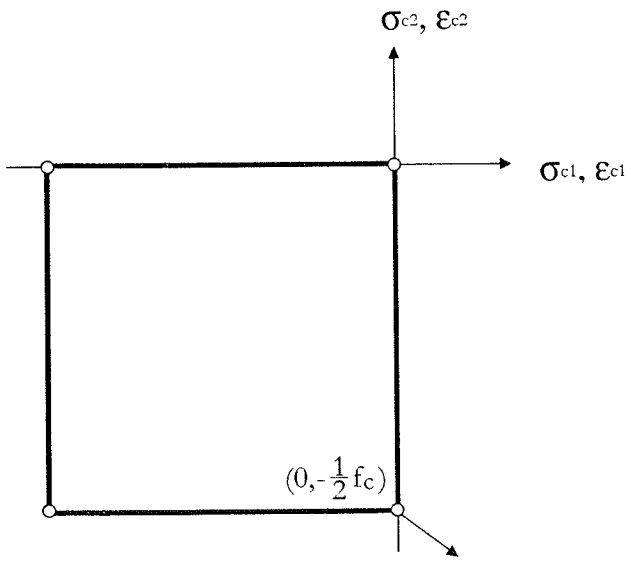

Figure 3.9 *Yield condition for cracked concrete with arbitrarily orientated crack planes.*

3.7 The effectiveness factor

In our derivation of the yield conditions as well as in our treatment of disks in pure shear, the effective strength of concrete has, for convenience, been set equal to f_c.

It is however an established fact that f_c must be multiplied with a so-called *effectiveness factor* ν, less than or equal to unity, in order to obtain good agreement with experiments, see for example [98.4]. A summary of the proposed ν-formulas may be found in [98.3].

The experimentally determined effectiveness factors are necessary for one main reason, that is: concrete is not a *rigid* nor a *perfectly plastic* material. Due to this discrepancy, many effects can not be dealt with theoretically.

It is important to realize that if the effectiveness factor should be correctly introduced into the yield condition, it's magnitude must be a function of the stress field in question. For instance, in the case of uniaxial compression in the x- or y-direction, we have $\nu = 1$. On the other hand, if we have $\tau_{xy} = 0$, $\sigma_x < 0$ and $\sigma_y > 0$, the effectiveness factor will be less than unity due to the bursting stresses transferred from the stressed reinforcement bars to the concrete. This causes local damage of the concrete, see [97.2]. A more thorough discussion on the effects which influence the effectiveness factors may be found in [98.2]

Regarding the effectiveness factor related to shear loading, it is believed that the value to be used for isotropicly cracked concrete will not deviate much from those used in other shear problems.

We must however be aware of the fact, that some of the proposed ν-formulas may already partly include the effect of crack sliding, if they are based on tests, in which changes in the direction of the principal concrete stresses have taken place during loading[9]. Further discussion on this point will be given in the next chapter.

So, since the effect of crack sliding has been theoretically included in the present study, it must not once again be reflected in the effectiveness factor. A ν-formula satisfying this requirement is quoted below, see [97.2],

---

[9] As an example, we mention the case of non shear reinforced beams, for which the effe c-tiveness factor was found to be depending on the shear span ratio a/h, see [79.1]. It has turned out that this dependency was due to the effect of crack sliding. The matters were clarified by J. P. Zhang [94.2][97.3], who introduced the effect of crack sliding in the plastic solutions for beams. The work of Jin Ping Zhang will be touched upon in chapter 4.

$$\nu = \frac{1.9}{f_c^{0.34}} \geq 1, \qquad (f_c \text{ in MPa}) \qquad (3.127)$$

This formula has been extracted from the empirical formula for the ultimate shear strength of isotropicly reinforced disks proposed by Takeda et al. [91.2][10]. The variation of ν as a function of f_c is shown in figure 3.22.

When using the pure shear strength solutions, f_c must be replaced by νf_c whereas Φ_x and Φ_y must be replaced by Φ_x/ν and Φ_y/ν.

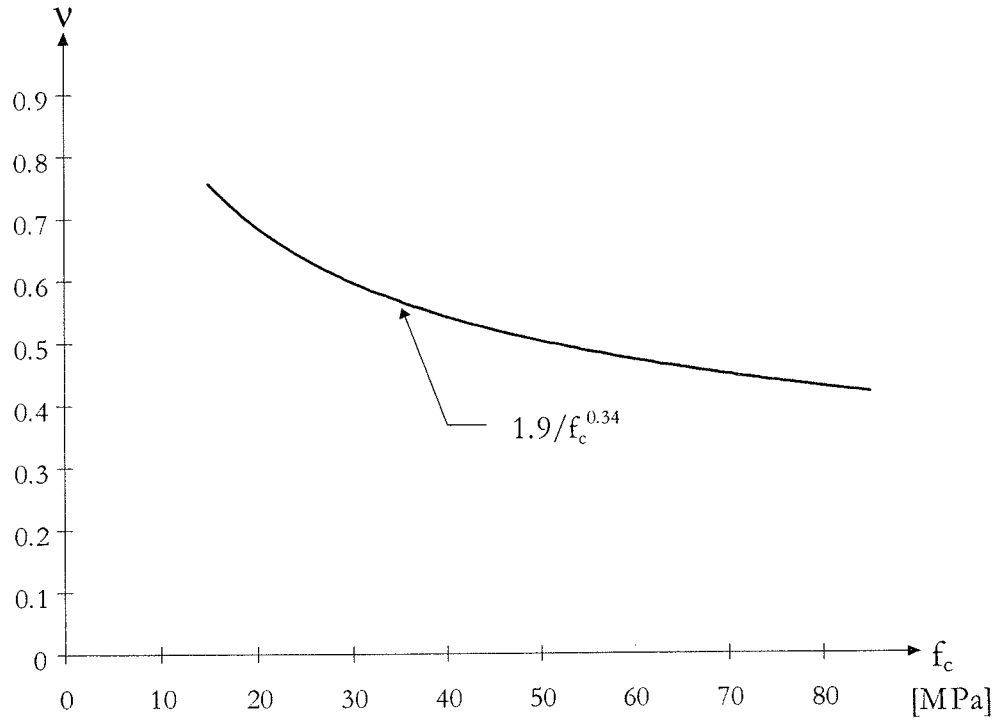

Figure 3.10 *Variation of the effectiveness factor with f_c*

3.8 Concluding remarks

The results obtained in this chapter deal with the strength of isotropicly cracked disks failing by sliding in cracks and/or by yielding of the reinforce-

---

[10] The formula proposed by Takeda et al. is based on test results of isotropicly, overrei n-forced disks. For such disks, the direction of the compression concrete stress does not change during loading. Thus, the possibility of crack sliding is excluded. The tests me n-tioned are due to Yamaguchi & Naganuma [91.1].

ment. Other type of failure may of course be crucial, for example stability failure or anchorage failure.

Stability failure can naturally not be dealt with by the theory of perfectly plastic bodies.

As for the anchorage failure mode, it is to be expected that the bond strength between the concrete and the reinforcement bars to some extent is reduced, and in some locations even may be totally lost, due to cracking thus making the disk more vulnerable to anchorage failure. So, in order to apply the results presented, it is of great importance that the reinforcement is well anchored at the boundaries, for instance as shown see figure 3.23a. The assumption of well anchored reinforcement bars is probably more important here than in the original plastic solutions because we are utilizing a biaxial state of stress in the concrete and therefore need the confining effect from the reinforcement. An optimal utilization of this effect may be obtained if the reinforcement is designed as closed stirrups, which are "self anchored", see figure 3.23b. In this case, we may even to a large extent accept loss of bond strength meaning that the reinforcement is acting more or less as unbonded reinforcement[11].

[11] Unbonded reinforcement, in the form of external reinforcement, is often used to strengthen cracked concrete members.

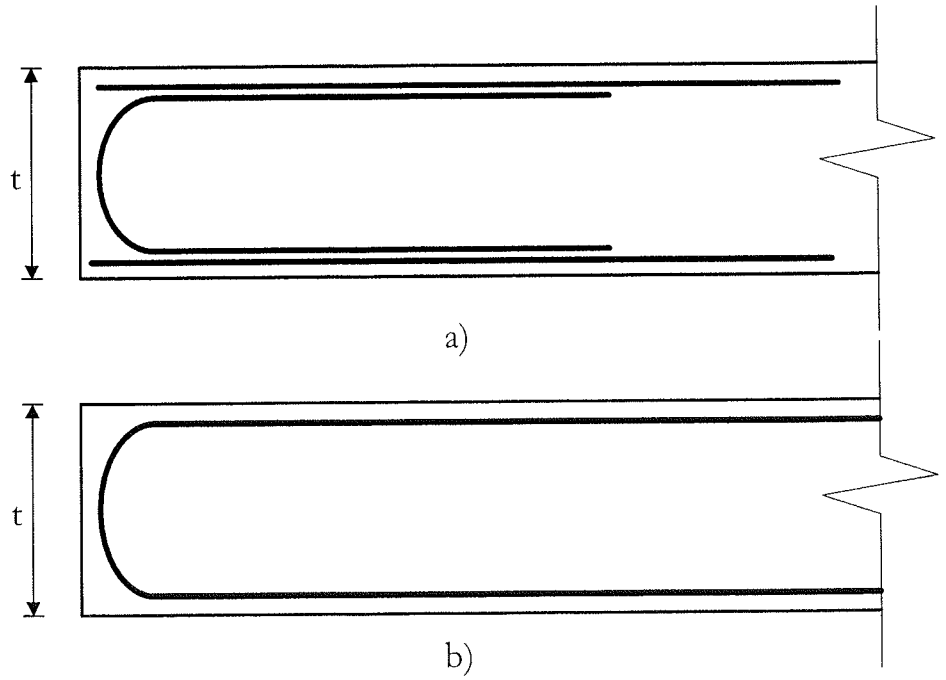

Figure 3.11 *Reinforcement anchorage arrangements.*

Chapter 4
Anisotropicly Cracked Disks

4.1 Introductory remarks

In this chapter, we shall deal with disks, which suffer from cracking in only one direction or in two directions at right angles to each other. Our aim is to investigate how sliding failure through these cracks will affect the strength of the disks.

Figure 4.1 shows two examples on such crack systems. As visualized in the figure we define the orientations of cracks by the (n,t)- coordinate system, which is rotated the angle β relative to the (x,y)-system. Disks cracked as described may be called *anisotropicly cracked.* The crack system in question may arise from different circumstances, for instance from loading or from temperature differences.

For disks subjected to proportional loading, the crack system in question could be the *initial crack system.* These cracks are formed at a lower load level when the maximum principal stress reaches the tensile strength of concrete. The orientation of the initial cracks is in some cases relatively easy to determine, for instance in cases of homogenous stress fields. For complicated load combinations the orientation may be determined approximately by a linear elastic calculation of the stress trajectories.

If the direction of the principal concrete stresses remain unchanged up till failure, then sliding failure in the initial cracks can not take place as these will not be transferring shear stresses [12].

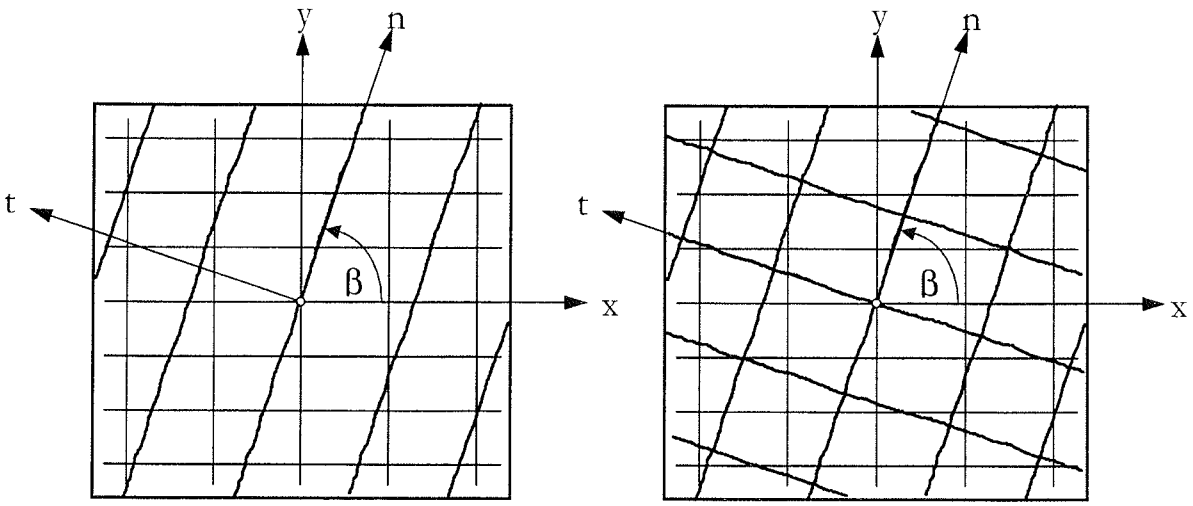

Figure 4.1 *Examples of anisotropicly cracked disks.*

However, if the principal directions are changing due to stress redistribution, the possibility of sliding in initial cracks must be taken seriously.

Besides of the initial cracks, the disk may on the way up to the ultimate load naturally suffer from cracking in many other directions, which also may be vulnerable to sliding failure. The latter developed crack systems are not easy to determine. In such cases, the disk may be considered as isotropicly cracked.

A general derivation of the yield condition for anisotropicly cracked disks is a complicated and tedious task. The reason for this is that the cracked concrete material here, contrary to isotropicly cracked concrete, will display different strength properties depending on the angle between the principal directions and the directions of the cracks. Only in the case of isotropicly reinforced disks with low reinforcement degrees, a relatively simple yield condition can be formulated. More about this in section 4.3.

---

[12] Naturally, the initial crack system may cause other kinds of strength reduction, see [97.2].

First let us study in details the influence of initial cracks on the strength of disks subjected to pure shear.

4.2 Disks in pure shear with sliding in initial cracks

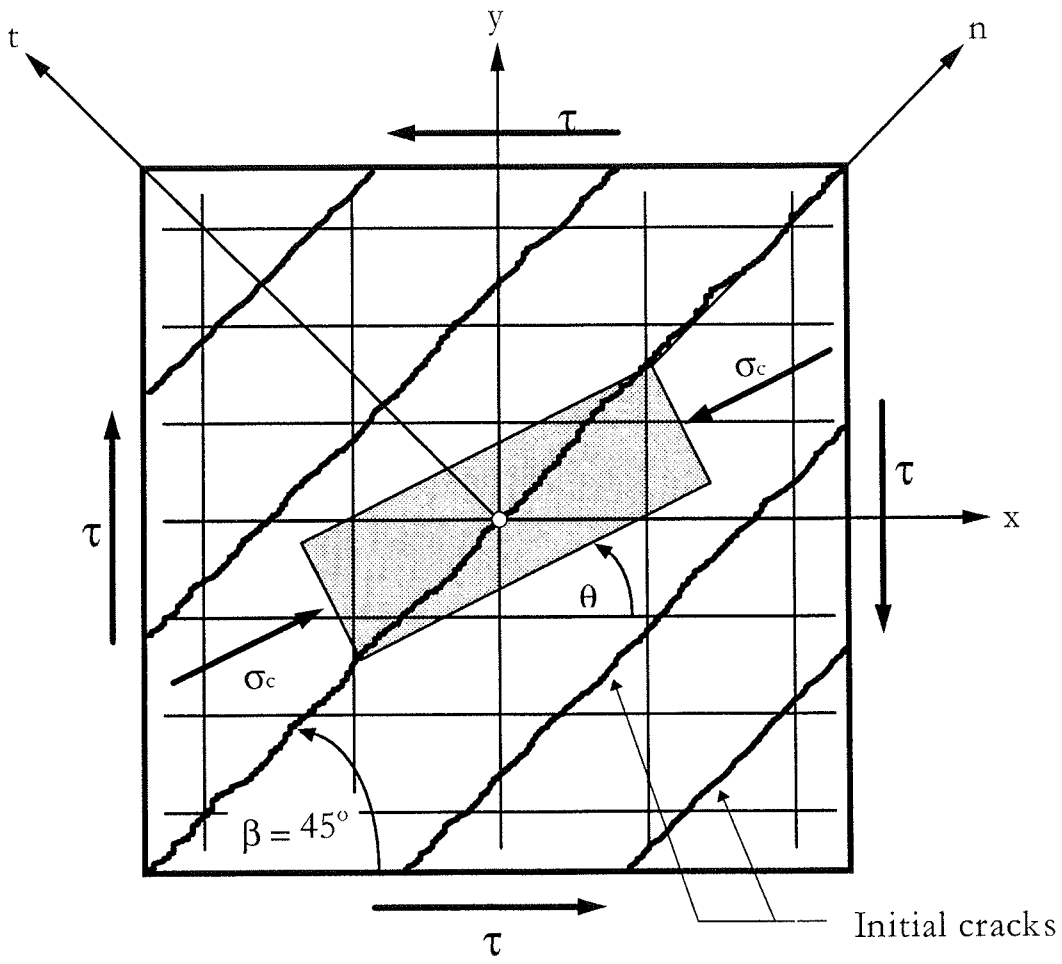

Figure 4.2 *Disk, with initial cracks, subjected to pure shear.*

The effect of sliding in initial cracks in the case of disks subjected to pure shear has been studied by J. P. Zhang [97.2], who calculated upper and lower bounds to the shear strength by means of numerical optimizations. Here, we will contribute to the results in [97.2] by deriving the solutions in an explicit form.

Consider a reinforced disk, which is uncracked before loading. When pure shear is applied as shown in figure 4.2, we will have initial cracks inclined at

(approximately) $\beta = 45^{\circ}$. These cracks are developed when the disk is entering the elastic cracked state.

4.2.1 Original solution. In the well-known original plastic solution, see for example [69.1], the concrete is assumed to be in a state of plane stress and subjected to uniaxial compression with the compressive stress σ_c at an angle θ with the *x*-axis, see figure 4.2. Assuming yielding of the reinforcement in both directions, the solution for the shear strength becomes

$$\frac{\tau}{f_c} = \sqrt{\Phi_x \Phi_y} \tag{4.1}$$

which is valid when

$$\frac{\sigma_c}{f_c} = \Phi_x + \Phi_y \leq 1 \tag{4.2}$$

The angle θ is determined by

$$\tan\theta = \sqrt{\frac{\Phi_y}{\Phi_x}} \tag{4.3}$$

If the condition (4.2) is not satisfied, the shear strength will be given by the *web crushing criterion* ($\sigma_c = f_c$), which in the case of $\Phi_x > \Phi_y$ appears as follows

$$\frac{\tau}{f_c} = \begin{cases} \sqrt{\Phi_y(1-\Phi_y)} & \text{, for } \Phi_y \leq 0.5 \\ 0.5 & \text{, for } \Phi_y > 0.5 \end{cases} \tag{4.4}$$

and

$$\tan\theta = \begin{cases} \sqrt{\dfrac{\Phi_y}{(1-\Phi_y)}} & \text{, for } \Phi_y \leq 0.5 \\ 1 & \text{, for } \Phi_y > 0.5 \end{cases} \tag{4.5}$$

Naturally (4.4) and (4.5) may also cover the case $\Phi_x < \Phi_y$ if subscript *y* is replaced by *x*.

When using (4.1) - (4.5) in practice, we must as discussed in section 3.7 multiply f_c by ν and divide Φ_x and Φ_y by ν.

4.2.2 Modified solution, normally reinforced disks. To take into account the possibility of sliding in initial cracks, the original solution quoted must be modified in such a way, that the crack sliding criterion is included. Thus, besides the requirement (4.2), the magnitude of σ_c must not violate the following condition, see also (2.11),

$$\tau_{cnt} \leq c' - \tan\varphi \cdot \sigma_{ct} \tag{4.6}$$

where τ_{cnt} and σ_{ct} are the concrete stresses on the initial crack surfaces, see figure 4.3.

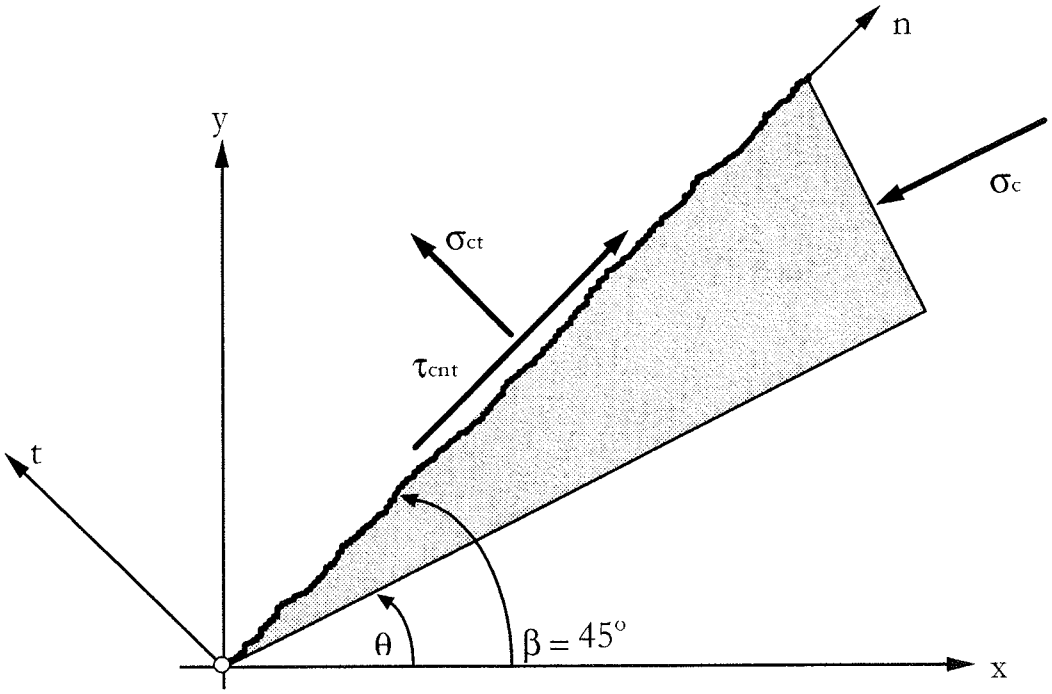

Figure 4.3 *State of stress in concrete.*

Expressing τ_{cnt} and σ_{ct} by means of σ_c, the condition (4.6) turns into :

$$\frac{\sigma_c}{f_c} \leq \frac{1}{8\left[\left|\cos(\beta-\theta)\right|\sin(\beta-\theta) - 0.75\sin^2(\beta-\theta)\right]} \quad \geq 1.0 \tag{4.7}$$

where $\tan\varphi = 0.75$ and $c' = 0.5c = f_c/8$ have been inserted. This expression is actually nothing else but a rewriting of the B.C. Jensen's solution for the strength of plain concrete joints, see [76.1]. Figure 4.4 depicts the maximum

allowable σ_c according to (4.7) as a function of θ. We see that vulnerability to crack sliding is present within a large range of θ.

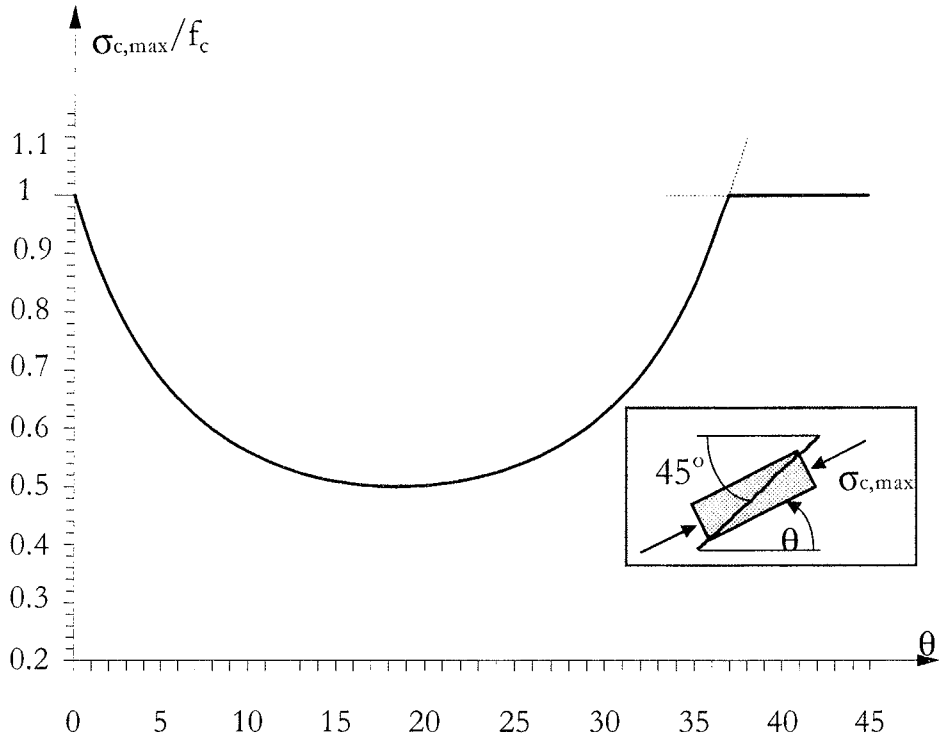

Figure 4.4 *Maximum allowable uniaxial compression stress in concrete with initial cracks,* $\beta = 45^o$.

The condition for the validity of solution (4.1) is now modified to :

$$\frac{\sigma_c}{f_c} = \Phi_x + \Phi_y \leq \min\left\{ \frac{1}{\dfrac{1}{8\left[\left|\cos(\beta-\theta)\right|\left|\sin(\beta-\theta)\right| - 0.75\sin^2(\beta-\theta)\right]}} \right. \tag{4.8}$$

The numerical signs in (4.8) may be removed if wee assume $\Phi_x \geq \Phi_y$, meaning that $\theta \leqq 45^o$. Now, by utilizing that θ is given by (4.3), we may establish the following expression[13]

$$\sin\theta = \sin\left(\text{Arc}\tan\sqrt{\frac{\Phi_y}{\Phi_x}} \right) = \sqrt{\frac{\Phi_y}{\Phi_x + \Phi_y}} \tag{4.9}$$

---

[13] $\sin(\text{Arc}\tan x) = \dfrac{x}{\sqrt{1+x^2}}$

which inserted into (4.8) together with $\beta = 45^{o}$ leads to :

$$\frac{\sigma_c}{f_c} = \Phi_x + \Phi_y \le \min\left\{ \begin{array}{c} 1.0 \\ \dfrac{1+\dfrac{\Phi_y}{\Phi_x}}{\left(1-\sqrt{\dfrac{\Phi_y}{\Phi_x}}\right)\left(1+7\sqrt{\dfrac{\Phi_y}{\Phi_x}}\right)} \end{array} \right. \tag{4.10}$$

If the conditions in (4.10) are not satisfied, then solution (4.1) will no longer be valid. (4.10) thus constitutes the modified criterion for disks, which may be called normally reinforced.

4.2.3 Modified solution, partially overreinforced disks. Consider the case where the magnitude of $\Phi_x + \Phi_y$ is violating the second condition in (4.10) and at the same time being less than unity. In this case, the shear strength will be governed by crack sliding. By assuming $\Phi_x > \Phi_y$ yielding will only occur in the vertical reinforcement. From equilibrium considerations of the stress field shown in figure 4.5 we find

$$\left.\begin{array}{ll} \sigma_{cy} = -\sigma_c \sin^2\theta & (a) \\ |\tau| = |\tau_{cxy}| = \sigma_c \cos\theta \sin\theta & (b) \\ \Phi_y f_c + \sigma_{cy} = 0 & (c) \end{array}\right\} \tag{4.11}$$

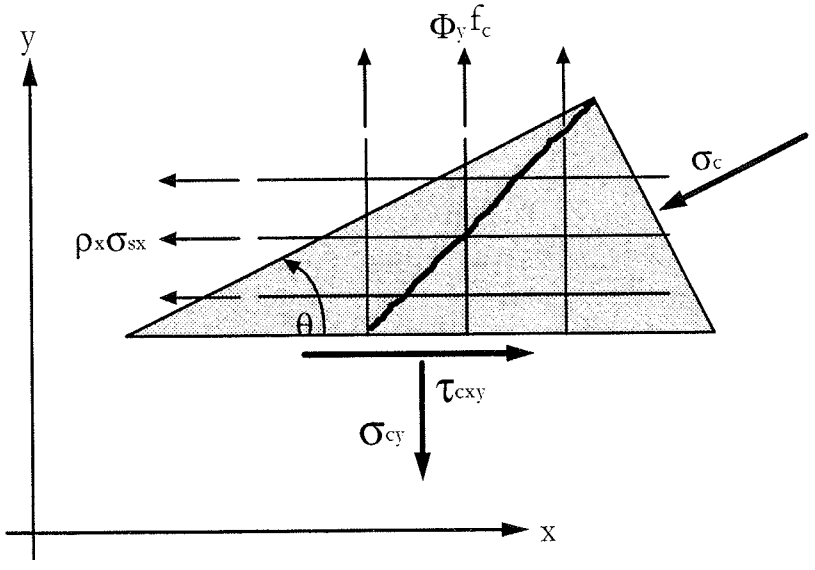

Figure 4.5 *Stress field in concrete and reinforcement in a partially overreinforced disk subjected to pure shear.*

The expressions in (4.11) lead to

$$\Phi_y = \frac{\sigma_c}{f_c}\sin^2\theta \tag{4.12}$$

and

$$\frac{\tau}{f_c} = \Phi_y \cot\theta \tag{4.13}$$

Putting σ_c equal to the maximum allowable according to (4.7), the expression (4.12) turns into

$$\Phi_y = \frac{\sin^2\theta}{8\left[\cos(45^\circ-\theta)\sin(45^\circ-\theta) - 0.75\sin^2(45^\circ-\theta)\right]} \tag{4.14}$$

Here the numerical signs are not necessary since $\theta<45^\circ$ when $\Phi_x > \Phi_y$. By rearranging (4.14) we arrive at the following quadratic equation in $\cot\theta$:

$$\Phi_y \cot^2\theta + 6\Phi_y \cot\theta - (7\Phi_y + 1) = 0 \tag{4.15}$$

which has the following valid solution :

$$\cot\theta = \frac{\sqrt{16\Phi_y + 1} - 3\sqrt{\Phi_y}}{\sqrt{\Phi_y}} \tag{4.16}$$

Now, by inserting (4.16) into (4.13) we finally obtain, what we will term, the *crack sliding solution* :

$$\frac{\tau}{f_c} = \sqrt{\Phi_y(16\Phi_y + 1)} - 3\Phi_y \tag{4.17}$$

This solution is valid as long as the right-hand side of (4.7), with θ defined by (4.16), is less than unity[14]. Thus, we must require

$$\Phi_y \le 9/25 = 0.36 \tag{4.18}$$

---

[14] This is the same as requiring, that the crack sliding solution can not yield larger shear strength than the web crushing criterion.

When Φ_y is larger than 0.36, the shear strength will be given by the web crushing criterion (4.4).

The result is depicted in figure 4.6. Apart from the region with very small degrees of reinforcement Φ_y, we see that the crack sliding solution (4.17) is varying rather linearly. It seems that we by establishing this solution have arrived closely to the many empirically proposed formulas for the shear strength of reinforced beams and disks; namely a constant concrete contribution plus a reinforcement contribution, which varies linearly up to a certain maximum amount of reinforcement.

For comparison the web crushing criterion as well as the solution in the case of isotropical cracking have also been drawn.

The crack sliding solution has been established by use of a uniaxial concrete stress field. It is naturally possible to develop a lower bound solution based on a biaxial stress field by adding a confining stress $\sigma_{con} < \sigma_c$, similar to what was done in the isotropicly cracked case, see figure 4.7.

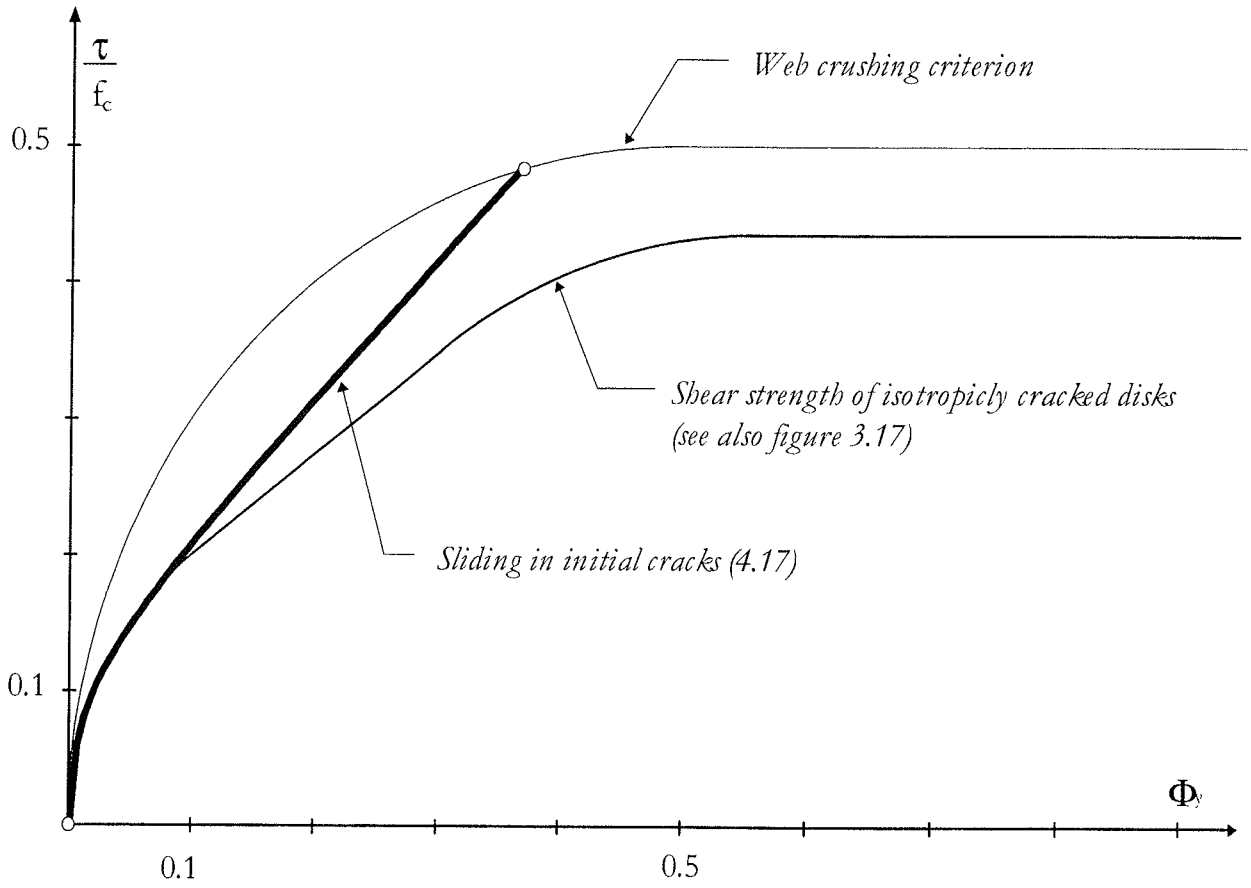

Figure 4.6 *Modified solution for the shear strength of partially overreinforced disks compared with the web crushing criterion and the solution in the case of isotropical cracking.*

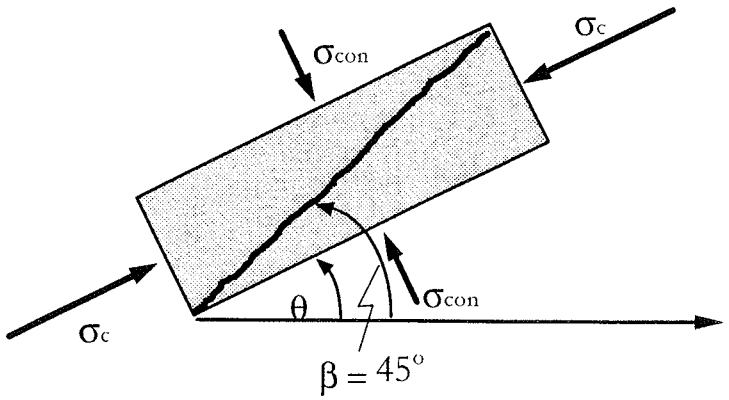

Figure 4.7 *Biaxial stress field in concrete.*

What we obtain is that the magnitude of σ_c increases depending on the chosen value σ_{con}. The crack sliding criterion (4.6), expressed by means of σ_{con} and σ_c, now reads

$$\frac{\sigma_c}{f_c} \le \frac{\frac{1}{8} + \frac{\sigma_{con}}{f_c}\left[\left|\cos(\beta-\theta)\right|\sin(\beta-\theta) + 0.75\cos^2(\beta-\theta)\right]}{\left[\left|\cos(\beta-\theta)\right|\sin(\beta-\theta) - 0.75\sin^2(\beta-\theta)\right]} \quad \geq 1.0 \qquad (4.19)$$

When using this condition instead of (4.7), it may be shown that the optimum lower bound solution is found for $\sigma_{con} = 0$ [15].

Finally, it should be mentioned that the effect of sliding in initial cracks also may be investigated by the upper bound technique, see J. P. Zhang [97.2]. The failure mechanism is simple here because the yield line runs along an initial crack, see figure 4.8a.

Since the crack sliding criterion is only imposed to the state of stresses in one direction, namely the direction of the cracks, we must accordingly derive the dissipation formula directly in the (σ_{cr},τ_{cnt})-system, see figure 4.8b. The dissipation per unit length of the yield line becomes

$$W_l = 0.5c\cos\alpha \cdot u \qquad , \alpha \ge \varphi \qquad (4.20)$$

α being the angle of the relative displacement u to the yield line.

By applying the work equation to the failure mechanism shown in figure 4.8a where the relative displacement is perpendicular to the x-axis, we find the following upper bound solution

$$\frac{\tau}{f_c} = \frac{1}{8} + \Phi_y \qquad (4.21)$$

The upper bound solution is depicted in figure 4.8c. We realize that it is very close to the lower bound solution.

---

[15] If we apply the stress field in figure 4.7 instead of that in figure 4.5, formula (4.11b) changes to: $\tau = (\sigma_c - \sigma_{con})\sin\theta\cos\theta$. We see that although σ_{con} may increase the magnitude of σ_c, it will also cause a decrease in τ. Thus, it is apparently more optimal to increase σ_c by rotating to another angle θ than to confine the concrete.

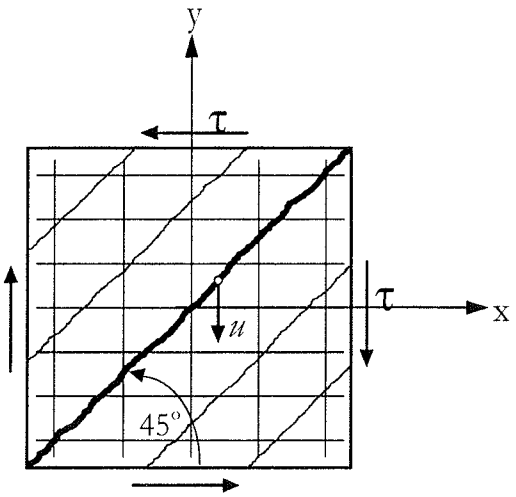

fig. a)

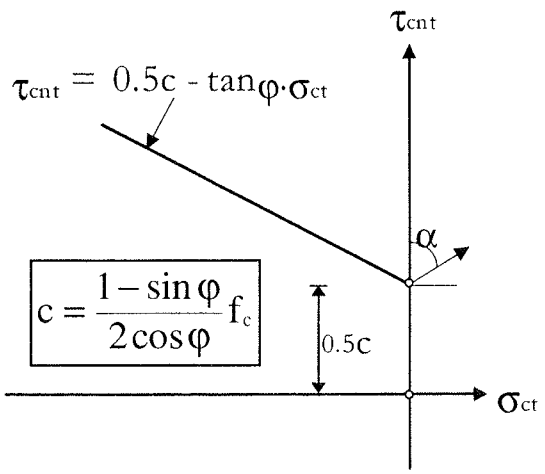

fig. b)

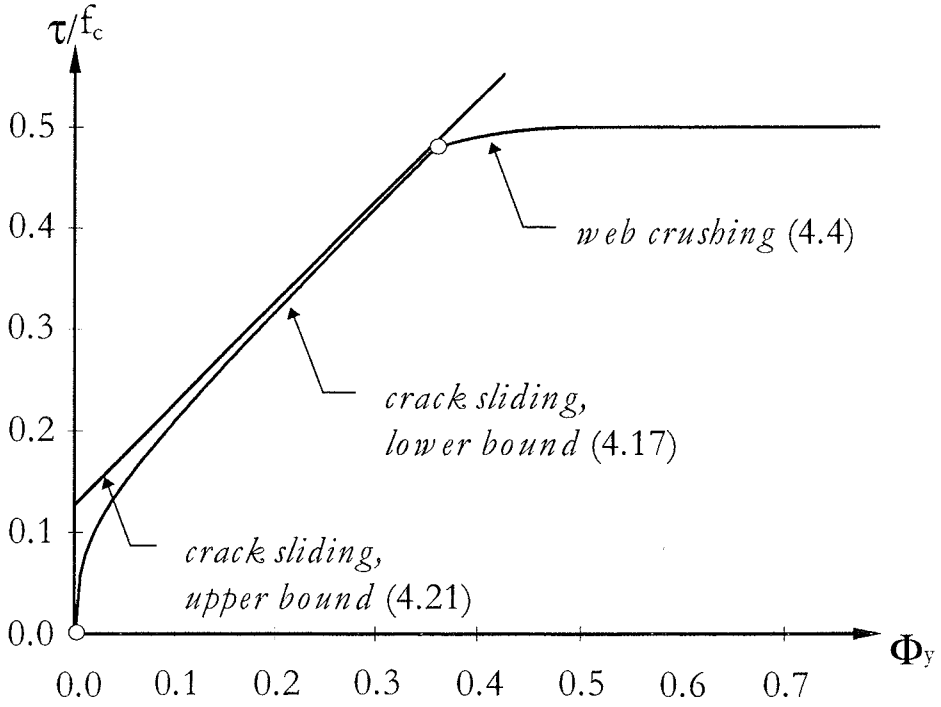

fig. c)

Figure 4.8 *a) failure mechanism with yield line along an initial crack. b) crack sliding criterion. c) comparison of the upper and the lower bound solution.*

Comparison with test results. The results of five test series of reinforced disks have been collected. The tests are reported by Vecchio & Collins [82.1], Yamaguchi & Naganuma [91.1], Vecchio, Collins & Aspiotos [94.1] Pang & Hsu [95.1] and Zhang & Hsu [98.1].

We are in this context only interested in tests, where the shear strength according to the theory is given by (4.4) or (4.17). Therefore, only tests with

$$\frac{\Phi_x}{\nu}+\frac{\Phi_y}{\nu}\geq \min\left\{\frac{1}{\left(1-\sqrt{\frac{\Phi_y}{\Phi_x}}\right)\left(1+7\sqrt{\frac{\Phi_y}{\Phi_x}}\right)}\right. \qquad (4.22)$$

are considered.

The effectiveness factor is taken to be, see (3.127),

$$\nu=\frac{1.9}{f_c^{0.34}} \qquad (f_c \text{ in MPa}) \qquad (4.23)$$

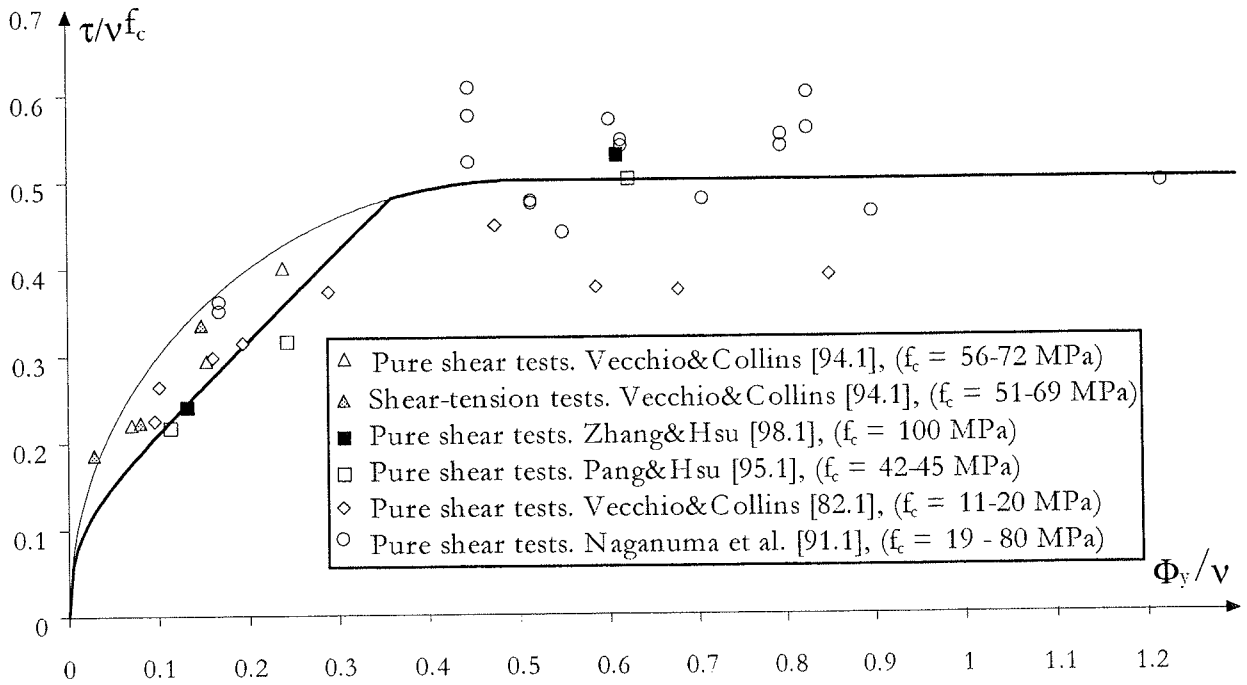

Figure 4.9 *Test results compared with theory.*

The test results are depicted in figure 4.9. The agreement with the present theory is fairly good. It is interesting to notice that within the range of Φ_y, where the theory predicts crack sliding, the test results are lying below the original solution.

Further, we notice that good agreement with theory is also found for disks of high strength concrete (for the tests reported in [94.1] and [98.1] we have $f_c >$ 50MPa and $f_c = 100$ MPa respectively).

As indicated by the legends in figure 4.9, three of the tests reported in [94.1] were combined shear-tension tests. The ratio of loading was $\sigma/\tau = 0.25$, where τ is the applied shear stress and σ is the applied normal stress in the x – and y – direction. For these particular test specimens, the reinforcement degrees have been taken as $\Phi_x = (\rho_x f_y - \sigma_u)/f_c$ and $\Phi_y = (\rho_y f_y - \sigma_u)/f_c$, where σ_u is the normal stress observed at failure.

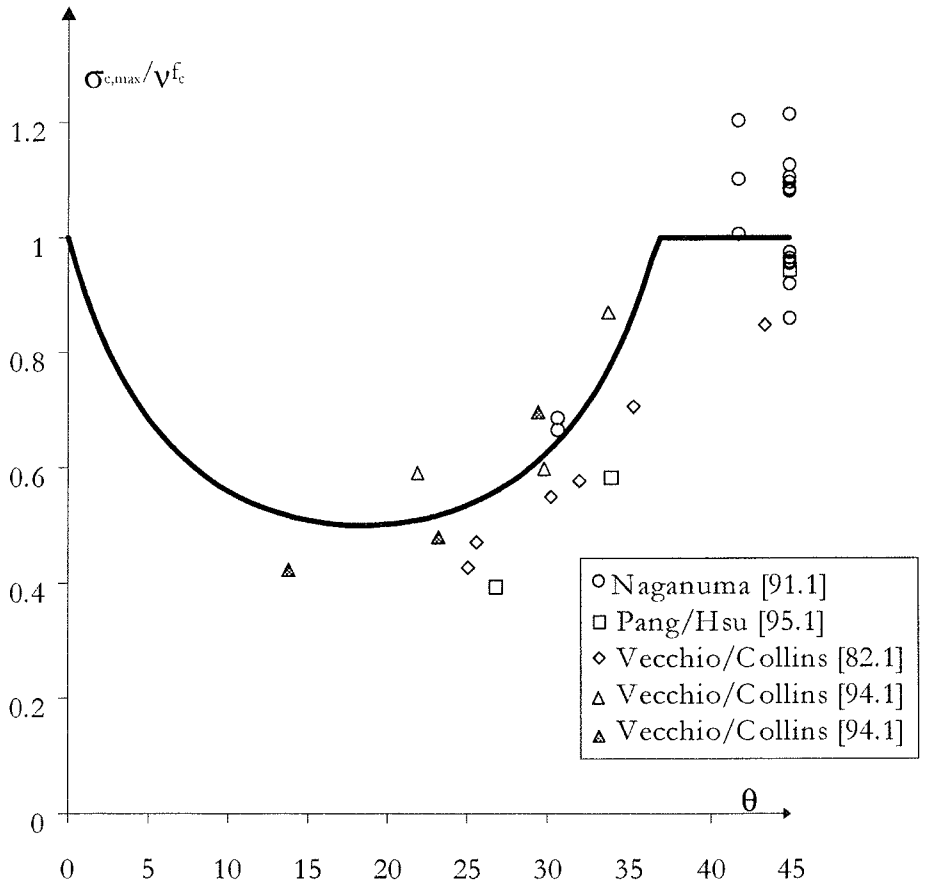

Figure 4.10 *Measured maximum compression stress compared with theory.*

In figure 4.10, we have plotted the measurements of the principal compressive stress at failure. Compared to the $\sigma_{c,max}$ given by formula (4.7), we see that reasonable agreement is obtained. It should be noticed that the angle θ of the test results have been determined by formula (4.16), Φ_y being replaced by Φ_y/ν.

To further explore the influence of initial cracks, we close this section by considering one of the classical problem in concrete mechanics; namely the shear strength of non shear reinforced disks/beams which are over reinforced in the longitudinal direction. It is probably here that the mechanism of crack sliding and its influence on the shear strength appears in its most transparent form. Jin-Ping Zhang [94.2] has dealt with this subject and given a simple and rather accurate upper bound method to calculate the shear strength of such beams.

Here we will approach the problem along the same lines as those previously introduced in this section. Our aim is to investigate whether it is possible to achieve similar results as those in [94.2]. To make the investigation simple, some idealized assumptions will be introduced which render the approach to be of less general character than the method given by Jin-Ping Zhang.

The beam to be considered is simply supported with rectangular cross section and symmetrically loaded with two concentrated forces, see figure A. The loads and the r e-actions are transferred to the beam through rigid plates of the length x_0. The shear span, which is the distance between the outermost edge of the loading plate and the inne r-most edge of the support plate, is a. The longitudinal reinforcement is assumed to be sufficiently strong.

As an idealized assumption we will consider the shear span of the beam to be initially cracked with straight cracks inclined at the angle $\beta = 45^{\circ}$. The cracks, which we may imagine to appear when the beam is entering the cracked elastic range, are indicated in figure A. In real beams, the cracks tend to be curved.

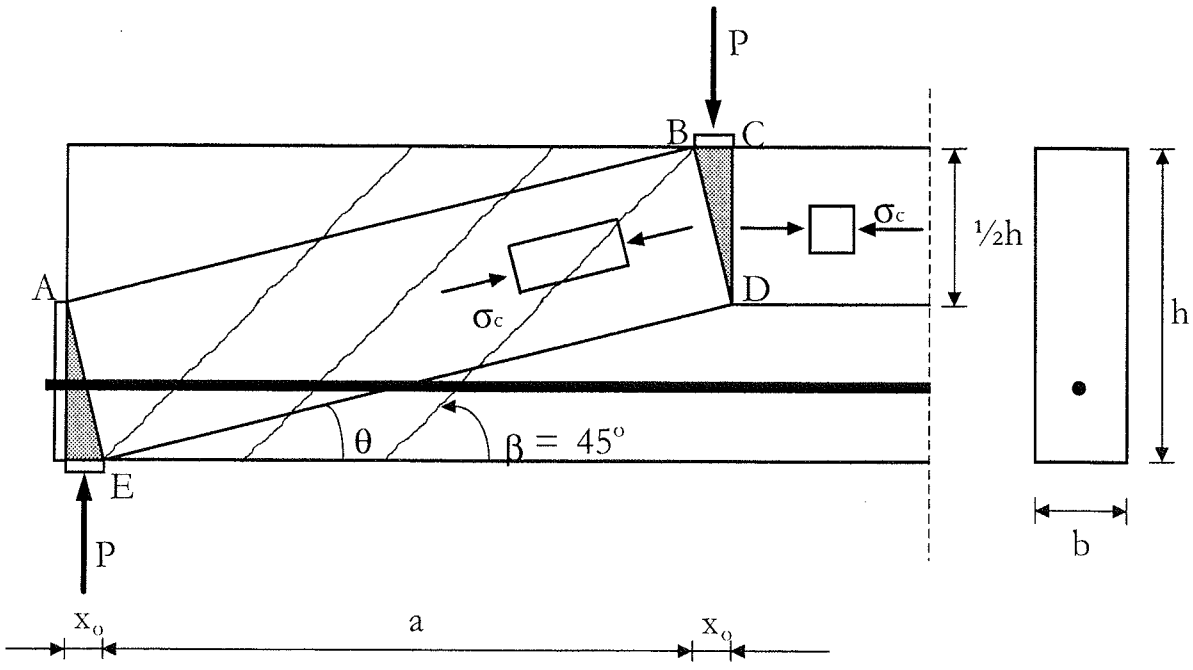

Figure A *Non shear reinforced beam with initial cracks inclined at 45.*

As shown in [84.1] we may construct an optimal lower bound solution by assuming the beam to act as an arch where the rectangular region *ABDE* is subjected to uniaxial compression with the compression stress σ_c at an angle θ with the beam axis. The load and the tensile force in the reinforcement are transferred to the arch through the shaded triangular areas which are in plane hydrostatic pressure with the compression stress σ_c. It appears that the beam, for a given value of σ_c, is able of carrying the load

$$P = \sigma_c b x_o \tag{a}$$

which, as shown in [84.1], will be maximized when *CD* = ½*h* meaning that x_o is given by

$$x_o = \frac{1}{2}\left[\sqrt{a^2 + h^2} - a\right] \tag{b}$$

The inclination of the uniaxial compression stress field becomes

$$\tan\theta = \frac{x_o}{½h} = \left[\sqrt{1 + \left(\frac{a}{h}\right)^2} - \frac{a}{h}\right] \tag{c}$$

If we for the time being disregard the presence of initial cracks, σ_c may be put equal to the uniaxial concrete strength f_c and the following lower bound solution is obtained from (a) and (b):

$$\frac{\tau_o}{f_c} = \frac{P}{bhf_c} = \frac{1}{2}\left[\sqrt{1+\left(\frac{a}{h}\right)^2} - \frac{a}{h}\right] \qquad \text{(d)}$$

This solution, which may be shown to be exact [84.1], will in the following be termed the *original plastic solution.*

Now, due to the presence of the initial cracks, the compression stress σ_c is according to (4.7) restricted to be

$$\frac{\sigma_c}{f_c} = \frac{1}{8\left[\left|\cos(\beta-\theta)\right|\sin(\beta-\theta) - 0.75\sin^2(\beta-\theta)\right]} \not> 1.0 \qquad \text{(e)}$$

By inserting this expression into (a) and utilizing that x_o is given by (b) the following solution, which takes into account the crack sliding criterion, is obtained

$$\frac{\tau}{f_c} = \frac{P}{bhf_c} = \frac{\frac{\tau_o}{f_c}}{8\left[\left|\cos(\beta-\theta)\right|\sin(\beta-\theta) - 0.75\sin^2(\beta-\theta)\right]} \not> \frac{\tau_o}{f_c} \qquad \text{(f)}$$

Here τ_o is the original plastic solution (d) and θ is given by (c). By inserting $\beta = 45^o$ into (f) the solution, after some rearrangements, turns into :

$$\frac{\tau}{f_c} = \frac{\tau_o}{f_c}\frac{\left(1+4\left(\frac{\tau_o}{f_c}\right)^2\right)}{\left(1-28\left(\frac{\tau_o}{f_c}\right)^2+12\frac{\tau_o}{f_c}\right)} \not> \frac{\tau_o}{f_c} \qquad \text{(g)}$$

$$= \frac{\tau_o}{f_c}\frac{\left(1+\left(\sqrt{\left(\frac{a}{h}\right)^2+1}-\frac{a}{h}\right)^2\right)}{\left(1-7\left(\sqrt{\left(\frac{a}{h}\right)^2+1}-\frac{a}{h}\right)^2+6\left(\sqrt{\left(\frac{a}{h}\right)^2+1}-\frac{a}{h}\right)\right)}$$

It should be noticed that for a/h less than unity, only a part of the uniaxial compression field will be crossed by an initial crack if we imagine that the crack with $\beta = 45^o$ originates from the bottom side of the beam, see figure B. The solution is however still a valid lower bound solution for $a/h < 1$.

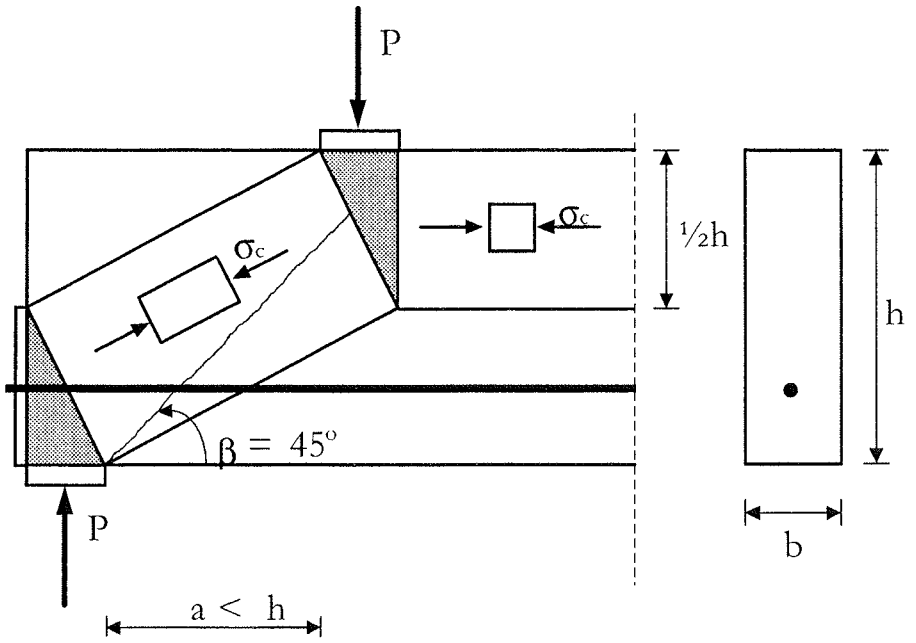

Figure B *Beam with a< h and initial crack at* $\beta = 45^{o}$.

We see that the solution (g) consists of the original plastic solution multiplied by a reduction factor which is a function of the a/h ratio. It is in this connection interesting to notice that the effectiveness factor related to the original solution, besides of depending on f_c, *h* and the amount of longitudinal reinforcement, also implies a function of a/h, see Roikjær et al. [79.1]. The latter dependency has been shown by Jin Ping Zhang to be due to sliding in cracks, [94.2].

From the parameter studies in [94.2], Jin Ping Zhang has proposed an approximate procedure to calculate the shear strength of non shear reinforced beams. The results in [94.2] may be summarized as follows[16]:

$$\frac{\tau}{f_c} = \frac{1}{4}\left[\sqrt{1+\left(\frac{x}{h}\right)^2} - \frac{x}{h}\right] \qquad \text{(h)}$$

and

---

[16] Here, the effectiveness factor to be multiplied on f_c is : $\nu_0 = \frac{0.88}{\sqrt{f_c}}\left(1+\frac{1}{\sqrt{h}}\right)(1+26\rho)$, where f_c is in MPa, *h* is in meter and ρ is the longitudinal reinforcement ratio. This formula is identical to the one proposed by Roikjær et al. [79.1] except that the function depending on a/h has been excluded.

$$\frac{x}{h}=\begin{cases}\frac{a}{h}, & \text{for } \frac{a}{h}\le 2\\ 0.26\frac{a}{h}+1.48, & \text{for } \frac{a}{h}>2\end{cases} \qquad (i)$$

Here τ is the shear strength and x denotes the horizontal projection of the diagonal crack along which sliding takes place. Notice that the model proposed by Jin-Ping Zhang takes into account the fact that the inclination of the cracks, $\tan\beta = h/x$, assumes different values depending on the a/h ratio whereas we in our lower bound solution only deal with one fixed crack inclination.

The original solution, the solution in (g) and the solution by Jin-Ping Zhang have been depicted in figure C as a function of a/h.

It can be seen that within the interval a/h = 1 - 4, the solution for beams with 45 degrees initial cracks is quite similar to the solution by Jin-Ping Zhang. The fact that the first mentioned solution, being a lower bound solution, is lying above the Jin-Ping Zhang solution for a/h < 1 is due to the assumption of fixed crack inclination.

Comparison with test results in [94.2] shows, that the Jin-Ping Zhang solution gives quite good agreement for a/h >2 whereas the test results for a/h < 2 are very scattered and they tend to be lying within the whole area confined by the original solution and the Jin-Ping Zhang solution. Discussion on this point may be found in [94.2].

Naturally, crack inclinations different from 45° can also be considered. When doing so, formulas (f) and (c) may be used directly because an explicit derivation of the solution will be too troublesome. The variation of the shear strength versus a/h for $\beta = 40°$ and $\beta = 50°$, as it has been obtained by use of (f) and (c), can be seen in figure D.

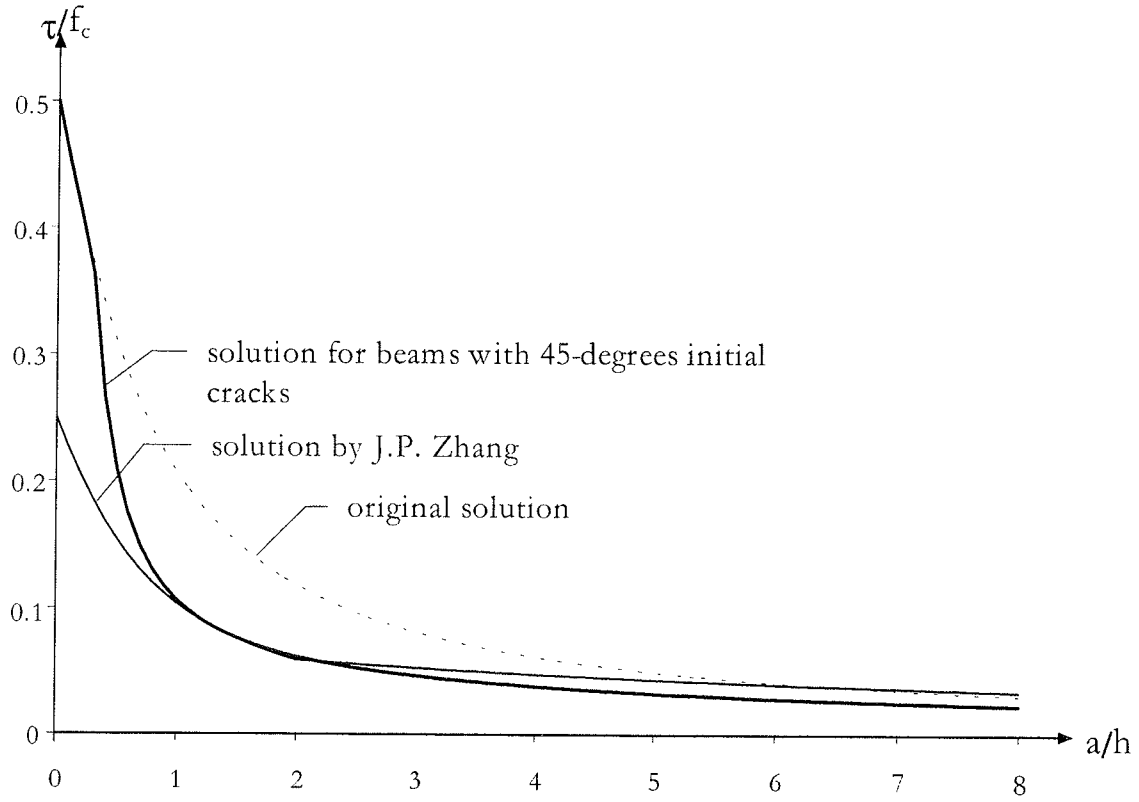

Figure C *Shear strength of non shear reinforced beams versus a/h.*

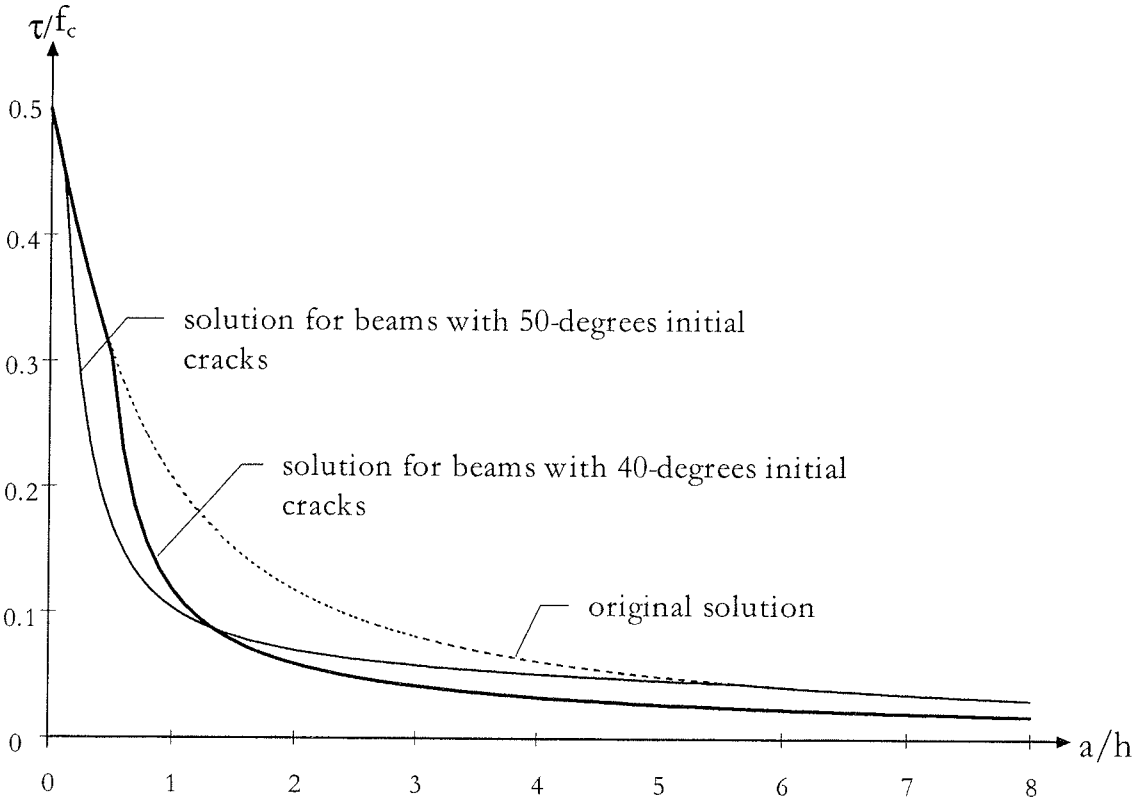

Figure D *Shear strength of non shear reinforced beams with different initial crack systems versus a/h.*

4.3 Yield condition for isotropicly reinforced disks

We will return to our investigation of the strength of anisotropicly cracked disks by considering the case of arbitrary in-plane loading. We restrict ourselves only to treat isotropicly reinforced disks with low degrees of reinforcement.

The aim is to formulate a yield condition which takes into account the crack sliding criterion. Our point of departure will be the *isotropic yield condition* given by Nielsen [69.1], see figure 4.11. This yield condition is an approximation to the original yield condition and applies for low degrees of reinforcement only [17]. The approximations being made imply, that the reinforcement is either unstressed or stressed to tensile yielding. The compressive yield strength of the reinforcement is neglected.

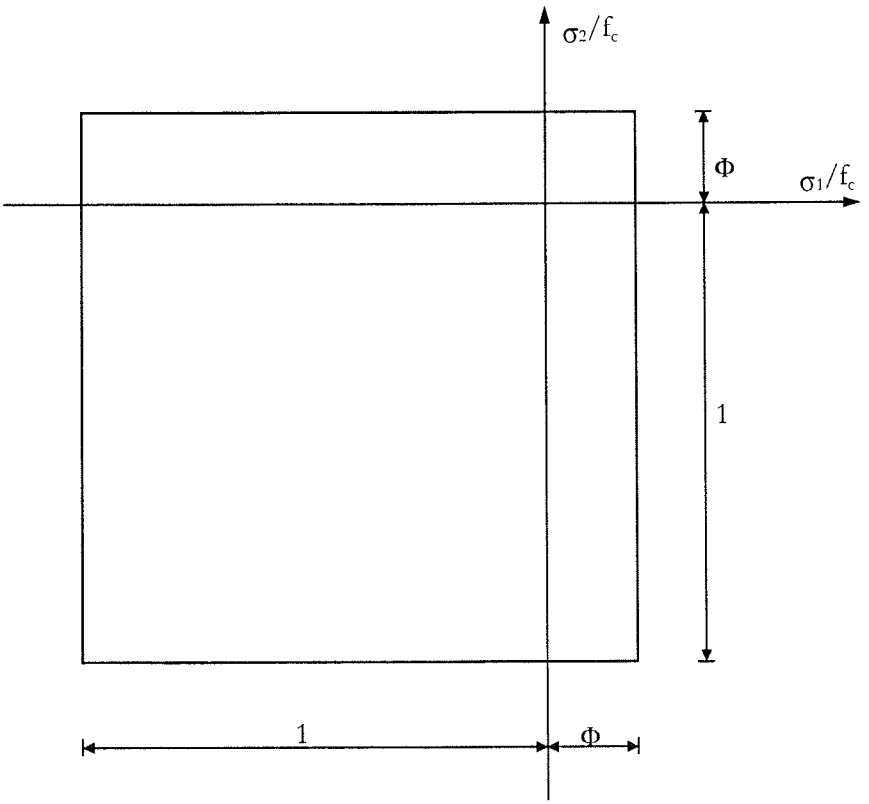

Figure 4.11 *Appearance of the isotropic yield condition, [69.1].*

The isotropic yield condition states that the stresses which can be carried are independent of the directions of the principal sections. Thus, in any arbitrary

---

[17] With low degrees of reinforcement we mean Φ less than about 0.1.

rectangular (σ_n, σ_t, τ_{nt})-system of coordinates, the yield condition appears identically as two conical surfaces defined as follows :

$$\tau_{nt}^2 - (\Phi f_c - \sigma_n)(\Phi f_c - \sigma_t) \le 0 \qquad \text{for} \begin{cases} \sigma_n \le \Phi \\ \sigma_t \le \Phi \\ \sigma_n + \sigma_t \ge -(1-\Phi) f_c \end{cases} \tag{4.24}$$

$$\tau_{nt}^2 - (f_c + \sigma_n)(f_c + \sigma_t) \le 0 \qquad \text{for} \begin{cases} \sigma_n \ge -f_c \\ \sigma_t \ge -f_c \\ \sigma_n + \sigma_t \le -(1-\Phi) f_c \end{cases} \tag{4.25}$$

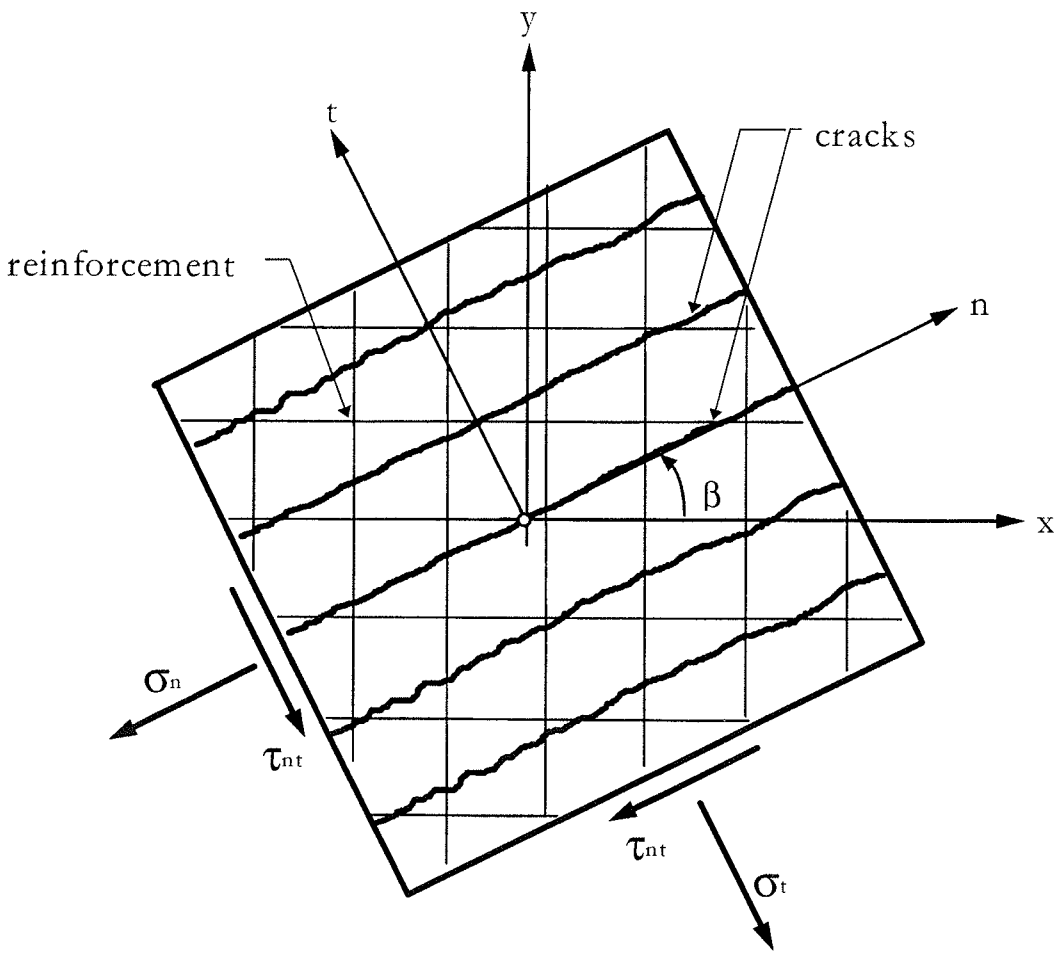

Figure 4.12 *Isotropicly reinforced disk with cracks parallel to the n-axis.*

If the disk considered is suffering from cracking parallel to the n-axis, see figure 4.12, we must additionally impose the crack sliding criterion upon the concrete stresses σ_{ct} and τ_{cnt} in sections normal to the t-axis. Thus besides of (4.24) – (4.25), we require

$$\tau_{cnt}^2 - \left(\frac{1}{8}f_c - \frac{3}{4}\sigma_{ct}\right)^2 \le 0 \qquad (4.26)$$

Here we have $\tau_{cnt} = \tau_{nt}$ due to the above mentioned assumption about the states of stresses in the reinforcement. Assuming further that crack sliding is critical only when the reinforcement is yielding, we may replace σ_{ct} by $\sigma_t - \Phi f_c$, thus turning the condition (4.26) into

$$\tau_{nt}^2 - \left(\frac{1}{8}f_c - \frac{3}{4}(\sigma_t - \Phi f_c)\right)^2 \le 0 \qquad (4.27)$$

Now, to ensure that a given stress field in an isotropicly reinforced disk with cracks parallel to the *n*-axis is admissible, we have the following yield condition :

$$\sigma_n \le \Phi f_c \qquad (4.28a)$$

$$\sigma_t \le \Phi f_c \qquad (4.28b)$$

$$\sigma_n \ge -f_c \qquad (4.28c)$$

$$\sigma_t \ge -f_c \qquad (4.28d)$$

$$\tau_{nt}^2 - (\Phi f_c - \sigma_n)(\Phi f_c - \sigma_t) \le 0 \qquad (4.28e)$$

$$\tau_{nt}^2 - (f_c + \sigma_n)(f_c + \sigma_t) \le 0 \qquad (4.28f)$$

$$\tau_{nt}^2 - \left(\frac{1}{8}f_c - \frac{3}{4}(\sigma_t - \Phi f_c)\right)^2 \le 0 \qquad (4.28g)$$

What we have obtained here for cracked disks with low reinforcement degrees is, that the orientation β of the initial cracks does not enter explicitly as a parameter in the yield condition. This of course is a great help in practice as we need only to transform the applied load into the $(\sigma_n, \sigma_t, \tau_{nt})$-system in order to apply the yield condition. Naturally, the yield condition can no longer be called *isotropic*.

The yield condition described by (4.28) is depicted in figure 4.13 for the case $\Phi = 0.1$. Contour lines for τ_{nt} is shown in figure 4.14 for the special case of $\Phi = 0$.

Finally, if we are dealing with a disk which also suffers from cracking in the θ-direction, the following condition is added to those in (4.28)

$$\tau_{nt}^2 - \left(\frac{1}{8} f_c - \frac{3}{4}(\sigma_n - \Phi f_c)\right)^2 \leq 0 \qquad (4.28h)$$

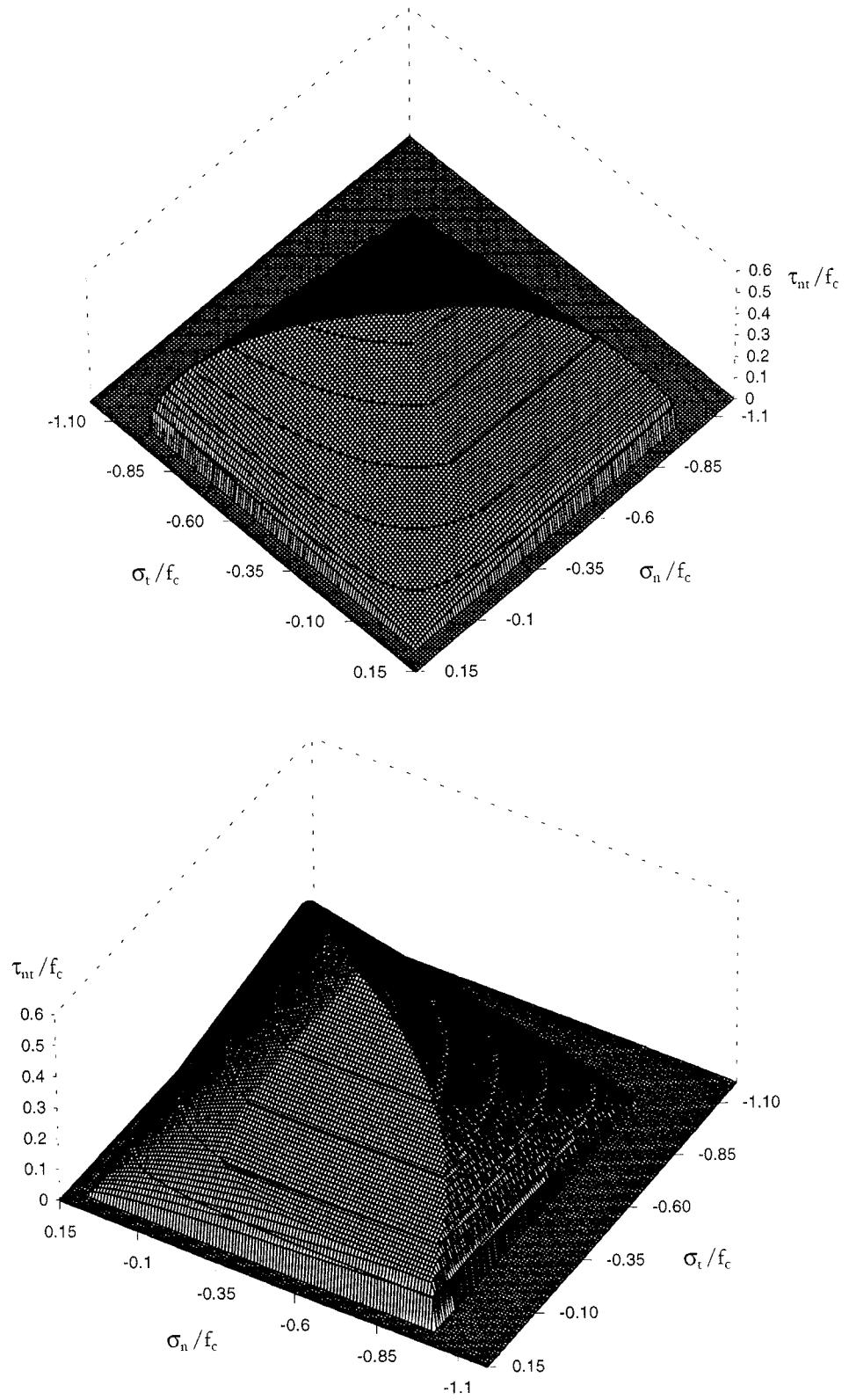

Figure 4.13 *Yield surface for an isotropicly reinforced disk with initial cracks parallel to the n-axis,* $\Phi = 0.1$.

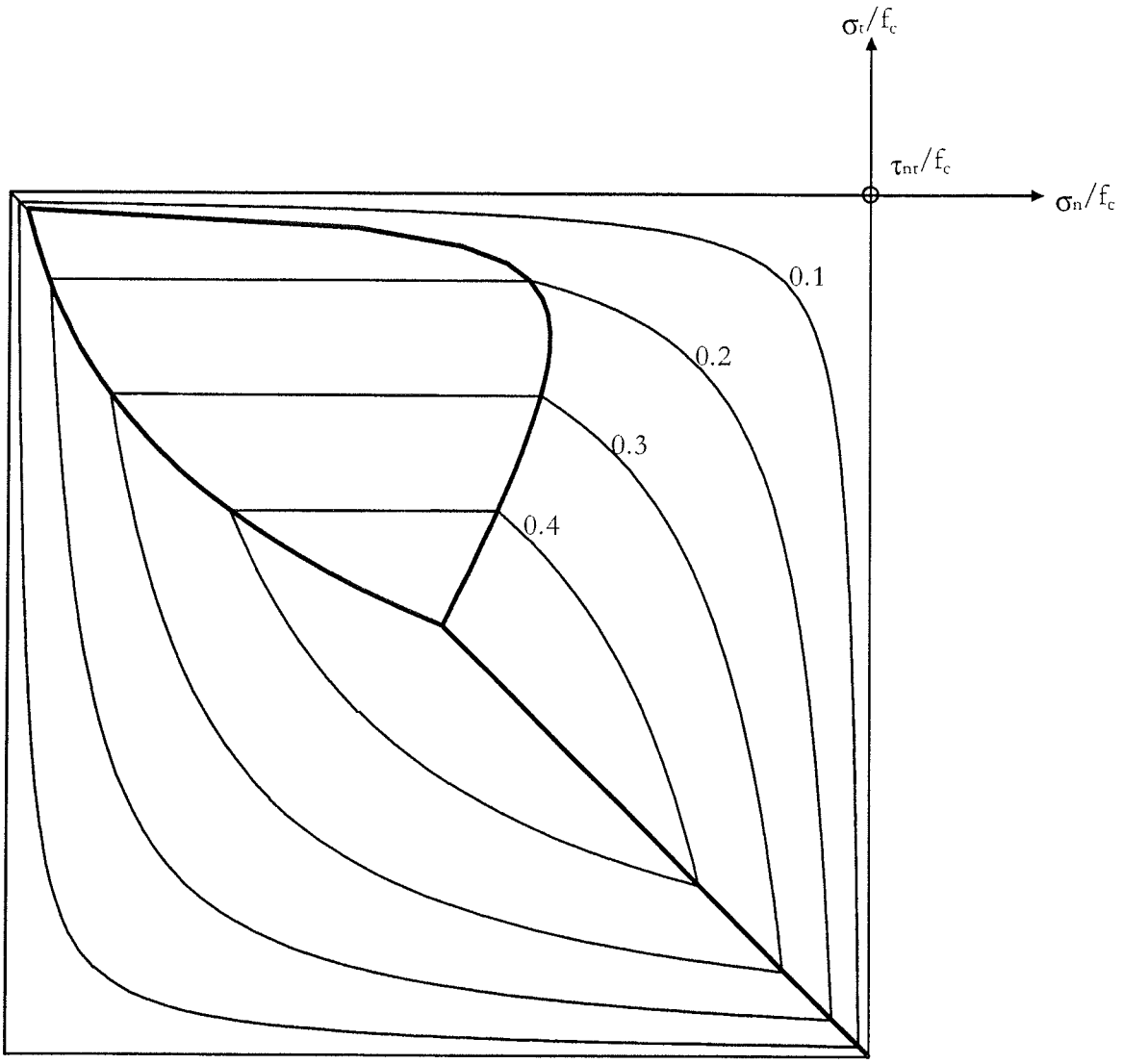

Figure 4.14 *Shear stress (τ_{nt}) contour lines for a disk with initial cracks para llel to the n-axis, $\Phi = 0$.*

Chapter 5
Conclusion

In this report, the strength of cracked reinforced concrete disks has been dealt with by means of the theory of plasticity.

The influence of different types of cracking on the strength has been treated. The basic idea is that the resistance against sliding failure in cracks is smaller than the resistance against sliding failure through uncracked concrete. Thus, two modified Coulomb failure criteria, one for uncracked concrete and one for cracks, are used for the material. The failure criterion for cracks has been taken from [97.1].

Disks suffering from cracking in many directions are assumed to be isotropicly cracked. The assumption implies that in any section perpendicular to the plane of the disk a crack may be found. This means that the cracked concrete material can be treated as an isotropic material. By means of the two above mentioned modified Coulomb failure criteria, a resulting isotropic failure criterion for the cracked concrete material has been formulated. Based on this failure criterion a yield condition for isotropicly cracked reinforced disks has been developed. Comparison of this yield condition with the original yield condition for uncracked concrete, [63.1], shows that isotropical cracking may cause significant strength reductions. Obviously, the state of isotropical cracking is a theoretical abstraction. Nevertheless, this idealized assumption may be useful in practice in two ways . Firstly, it leads to simple solutions as

we are dealing with an isotropic material. Secondly, the results obtained define, together with the original yield condition, the domain within which we may expect to find the real strength of a given cracked disk. So, when a cracked disk in an existing structure is evaluated, one would know that, with respect to sliding failure, the solution obtained from the original yield condition constitutes an upper limit for the strength of the disk whereas the solution obtained under the assumption of isotropical cracking represents a lower limit. The more cracks and the more crack directions, the closer will the strength be to the solution for isotropicly cracked concrete. If the latter solution corresponds to higher stresses than those occurring in the disk, then the disk has sufficient strength to resist sliding failure through cracks.

Although the results obtained for uncracked and isotropicly cracked concrete are based on failure criteria, which individually have proved to agree reasonably well with tests, it should be emphasized that the result of the combined failure criterion do not necessarily agree with tests. The failure criterion for isotropicly cracked concrete as well as the yield condition (or parts of the yield condition) for cracked disks should therefore be experimentally verified.

For disks suffering from cracking in one direction only, a lower bound solution for the special case of pure shear loading has been derived. The cracks considered in this case are the initial cracks, which are formed when the disks enter the cracked elastic state. By taking the reduced sliding resistance of these cracks into consideration, it is found that the maximum allowable concrete stress depends on the direction of the principal concrete stresses. The result shows that concrete crushing ($\sigma_c = \nu f_c$) can only be developed when the smaller one of the two degrees of reinforcement is larger than 0.36. For smaller amounts of reinforcement, failure will be due to crack sliding and the maximum allowable uniaxial concrete stress will be less than νf_c. The predicted maximum allowable concrete stress has been compared with test measurements and good agreement was found.

The consequence of the limited utilization of the web crushing strength is, that the disk might be partially overreinforced (i.e. reinforcement yielding in only one direction) for reinforcement amounts much less than that corresponding to $\Phi_x + \Phi_y = \nu$, which, according to the usual plastic solution, is the upper limit for normally reinforced disks.

For disks suffering from cracking in one direction or in two directions at right angle to each other and subjected to arbitrary in-plane loading, a yield condition, which takes into account the crack sliding criterion, has been given. The yield condition, valid for isotropicly reinforced disks (i.e.$\Phi_x = \Phi_y$) with low degrees of reinforcement, is a modification of the isotropic yield condition developed by Nielsen [69.1]. The yield condition is formulated for stresses referred to a coordinate system defined by the directions of the cracks.

References

[63.1] Nielsen, M.P. : *Yield conditions for reinforced concrete shells in the me m-brane state.* Non-classical Shell Problems (ed. Olszak & Sawczuk), Proc. IASS Symposium, Warsaw 1963. Amsterdam 1963. pp. 1030 - 1040.

[69.1] Nielsen, M.P. : *Om jernbetonskivers styrke.* Polyteknisk Forlag, København 1969, 254 pp. Doktorafhandling.(English edition :*On the strength of reinforced concrete dics*, Acta Polytech. Scand., Ci-70, Copenhagen, 1971, 261 pp.)

[70.1] Bræstrup, M.W. : *Yield Lines in Discs, Plates and Shells.* Structural Research Laboratory, Technical University of Denmark, Report R No. 14, Copenhagen, 1970.

[75.1] Jensen, B.C. : *Lines of discontinuity for displacements in the theory of plasticity for plain and reinforced concrete.* Magazine of Concrete Research. Vol. 27, No. 92. September 1975. pp 143-150.

[76.1] Jensen, B.C. : *Nogle plasticitetsteoretiske beregninger af beton og jernbeton*. Technical University of Denmark , Institute of Building Design, Report No. 111. Lyngby, 1976. (English edition :*Some applications of plastic analysis to plain and reinforced concrete*. Technical University of Denmark, Institute of Building Design, Report No. 123. Lyngby, 1977.)

[77.1] Marti, P. & Thürlimann, B. : *Fliessbedingung für Stahlbeton mit Berücksichtigung der Betonzugfestigkeit*. Bericht Nr. 67, Institut für Baustatik und Konstruktion, ETH Zürich,Switzerland, 1977.

[78.1] Nielsen, M.P. & Bræstrup, M.W. & Jensen, B.C. & Bach, F. : *Concrete Plasticity----Beam shear-Shear in joints-Punching shear*. Special Publication. Danish Society for Structural Science and Engineering, Structural Research Laboratory, Technical University of Denmark, Lyngby, 1978.

[78.2] Müller, P. : *Plastische Berechnung von Stahlbetonscheiben und -balken*. Bericht Nr. 83, Institut für Baustatik und Konstruktion, ETH Zürich, Switzerland, 1978.

[79.1] Roikjær, M. & Pedersen, C. & Bræstrup, M. W. & Nielsen, M. P. & Bach, F. : *Bestemmelse af ikke-forskydningsarmerede bjælkers fo r-skydningsstyrke (shear capacity of beams without shear reinforcement)*. Technical University of Denmark, Structural Research Laboratory. Report I 62. Copenhagen 1979.

[80.1] Marti, P. : *Zur plastischen Berechnung von Stahlbeton*. Bericht Nr. 104, Institut für Baustatik und Konstruktion, ETH Zürich, Switzerland, 1980.

[82.1] Vecchio, F. J. & Collins, M.P. :*The response of reinforced concrete to in plane shear and normal stresses.* The Department of Civil Engineering, University of Toronto, Canada, 1982.

[84.1] Nielsen, M. P. : *Limit analysis and concrete plasticity.* Prentice-Hall, Inc. Englewood Cliffs, NewJersey, 1984.

[91.1] Yamaguchi, T. & Naganuma, K. : *Experimental study on mechanical characteristics of reinforced concrete panels subjected to in-plane shear force* . Journal of Struct. Constr. Engng., AIJ, No. 419, 1991.

[91.2] Takeda, T. & Yamaguchi, T & Naganuma, K. : *Report on tests of nuclear prestressed containment vessels* . Transactions of the International Workshop on Concrete Shear in Earthquake. University of Houston, Texas, USA, 1991.

[91.3] MacGregor, J. : *Dimensioning and Detailing.* IABSE Colloquium Stuttgart 1991, Structural Concrete. IABSE Report Vol. 62, Stuttgart 1991.

[94.1] Vecchio, F. J. & Collins, M. P. & Aspiotos, J. : *High-Strength Concrete Elements Subjected to Shear.* ACI Structural Journal, Vol. 91, No. 4, July - August 1994. pp. 423-433.

[94.2] Zhang, J. P. : *Strength of cracked concrete. Part 1--- Shear strength of conventional reinforced concrete beams, deep beams, corbels, and prestressed reinforced concrete beams without shear reinforcement.* Technical University of Denmark, Department of Structural Engineering, Report R No. 311, Lyngby, 1994.

[95.1] Pang, X. B. & Hsu, T. T. C. : *Behavior of Reinforced Concrete Membrane Elements in Shear.* ACI Structural Journal, Vol. 92, No. 6, Nov - December 1995. pp. 665-679.

[97.1] Zhang, J. P. : *Strength of cracked concrete. Part 2--- Micromechanical modelling of shear failure in cement paste and in concrete.* Technical University of Denmark, Department of Structural Engineering and Materials, Report R No. 17, Lyngby 1997.

[97.2] Zhang, J. P. : *Strength of cracked concrete. Part 3--- Load carrying capacity of panels subjected to in-plane stresses.* Technical University of Denmark, Department of Structural Engineering and Materials, Report R No. 18, Lyngby 1997.

[97.3] Zhang, J. P. : *Diagonal cracking and shear strength of reinforced concrete beams.* Magazine of Concrete Research, Vol. 49, No 178, March 1997, pp. 55-65.

[97.4] Hoang, L. C. : *Shear strength of non-shear reinforced concrete elements. Part 3- Prestressed hollow-core slabs.* Technical University of Denmark, Department of Structural Engineering and Materials, Report R No. 30, Lyngby 1997.

[98.1] Zhang, L. X. & Hsu, T. T. C. : *Behavior and Analysis of 100 MPa Concrete Membrane Elements.* Journal of Structural Engineering, ASCE, Vol. 124, No. 1, Jan. 1998, pp. 24 - 34.

[98.2] Hoang, L. C. & Nielsen, M. P. : *Plasticity Approach to Shear Design.* Cement and Concrete Composites, Vol. 20, No. 6, 1998, pp. 437-453.

[98.3] Nielsen, M. P. : *Beton 2 del 2. (Concrete Structures 2, Part 3).* Technical University of Denmark, Department of Structural Engineering and Materials (to be published).

[98.4] Nielsen, M. P. : *Limit analysis and concrete plasticity.* Second edition, CRC Press, 1998.

[98.5] Hoang, L. C. : *Shear strength of lightly shear reinforced concrete beams.* Technical University of Denmark, Department of Structural Engineering and Materials (to be published).